CHARACTERISATION AND PURIFICATION OF BACTERIAL LYSATES CONTAINING POLY-γ-GLUTAMIC ACID

Benjamin Pearson

A thesis submitted to the University of Birmingham for the degree of *Master of Research in Biomaterials*

Department of Metallurgy and Materials
University of Birmingham
December 2014

Acknowledgements

I would like to express my sincerest gratitude to the following people

Firstly, thank you to my supervisors, Dr Artemis Stamboulis and Dr Izabela Radecka for allowing me to pursue this project, for welcoming me into your groups and giving me space to make mistakes which helped me grow as a scientist and gain a greater appreciation of experiment design and scientific error.

Dr Artemis Stamboulis, thank you particularly for the time you offered and for being patientwith me when I was ignorant about how to proceed with the project, when I felt frustrated about getting access to equipment and when I felt lost in a sea of seemingly endless and meaningless data.

Dr Izabela Radecka, who provided me with plenty of samples to work with and for sharing your previous data, publications, knowledge and expertise.

Adetoro Ogunleye for preparing samples and discussing how to alterthe culture conditions.

Dr Luke Alderwick, for showing me how to perform the sugar analysis and supporting me in the laboratory.

Dr Eva Hyde, thank you for letting me use and loiter in your laboratory, forthe many hours you shared your wisdom, correcting my uneducated ideas and for helping meshow *how and why* experiments failed. Thank you for taking my samples to the EMBL facility in Hamburg.

Dr Raul Pacheco for assistance with the circular dichroism and fluoroscopy instruments.

Rosemary Parslow, for putting up with me, helping me work safely and showing me how to label and store things properly - skills that are surprisingly useful.

Chi Tsang, for assistance with the HPLC

Neil Spencer, for setting up and running my NMR experiments and offering advice and support.

Abstract

Bacillus spp. and other bacterial species produce poly γ gamma acid (PγGA), a polymer with many applications that are briefly reviewed in this study. As PγGA is produced by biosynthetic methods, the price of the material depends on efficiency of synthesis and extraction; furthermore altering conditions in which the biosynthetic reactions takes place can effect the properties of the produced material. However since there are a large number of variables (species/subspecies used, media composition…etc) it is unclear which variables independently effect PγGA production.

This study altered the broth in cultures of *Bacillus subtillis* natto subspecies to determine whether manganese or NaCl concentration effected the chemical properties or yield of products precipitated and purified from culture. It also compared 2 methods of PγGA purification (using ethanol and copper ions) published for extraction of PγGA from *Bacillus licheniformis*.

NMR spectroscopy showed that the product contained PγGA with a large amount of carbohydrate which couldn't be removed by purification techniques. Analysis of this impurity showed that it was carbohydrate composed of 1,2-linked hexose monosaccharides. And that it was likely a similar size to PγGA. Addition of Mn^{2+} increased the ratio of PγGA to impurity after purification and NaCl likely decreased the size of PγGA.

The findings suggest novel strategies for purification of PγGA and discusses the lack of published evidence that proves the effectiveness of PγGA purification techniques. We suggest that ^{1}H NMR experiments may be an effective method to prove the absence of carbohydrate.

Table of Contents

i List of abbreviations

Abbreviation	Meaning
18C	A chromatography column that uses molecules containing 18 carbon atoms
Ac	Acetyl groups R-CH_2COOH as the stationary phase.
A	Absorbance, A followed by subscript refers to absorption of light at a wavelength in nanometers
ANOVA	Analysis of Variance
ATR	Attenuated Total Reflectance
cap	Genes used by Bacilli to produce encapsulated PγGA
^{13}C	Isotope of carbon that contains 6 protons and 7 neutrons
C	Carbon
Cu	Copper
D	Dextrorotatory – Rotates the plane of polarised light clockwise
D_2O	Deuterium replaced water
Da	Daltons, measure of atomic mass
dd	Doublet of doublets (NMR peak splitting pattern)
DMF	N,N-dimethylformamide
E	Energy of a photon in NMR spectra
EDTA	Ethylenediaminetetracetic acid
EWG	Electron withdrawing group
FDNB	Fluoro-Dinitrobenzene
FTIR	Fourier Transform Infra red spectroscopy
γ	In NMR – Gyromagnetic ratio.
g	gravity equivalent (9.8 m s^{-2})
GC	Gas chromatography
GC-MS	Gas chromatography coupled to mass spectroscopy
Glr	Glutamate racemase – an enzyme that produces D glutamate
h	Planck's constant (6.63 x 10^{-34} m^2 kg s^{-1})
IR	Infrared
J	J-coupling (NMR) signal splitting in NMR spectra, which gives information about adjacent protons
K_a	Acid dissociation constant ($[H^+]+[A^-]/[HA\}$
KBr	Potassium Bromide
L	Levorotatory – Rotates a plane of polarised light counter-clockwise
LD_{50}	Lethal dose required to kill 50% of rats
m/z	mass to charge ratio – units used in mass spectra
MALDI-TOF	Matrix assisted laser desorption ionization – Time of Flight mass spectroscopy. A technique used to measure the mass of large molecules by mass spectroscopy
Me	Methyl groups CH_3
Mg	Magnesium
M_n	Molecular number. The greatest number of chains of a particular length
Mn	Manganese
$MnSO_4$	Manganese sulfate
MS	Mass spectroscopy

- M_w Molecular weight of a polymer. The average chain length of a polymer.
- MWCO Molecular weight cut off – size of pores in dialysis tubing
- ND No data
- NMR Nuclear Magnetic Resonance
- PαGA Poly-α-glutamic acid or poly-α-glutamate
- Pd Palladium
- pH $pH = -\log_{10} [H^+]$, where H^+ are hydrogen ions
- PGA Poly Glutamic Acid – not specified whether α or γ
- PγGA Poly-γ-glutamic acid or poly-γ-glutamate
- *pgsBCA* Poly Gamma Glutamate Synthesizing Gene
- pK_a Acid dissociation constant on a logarithmic scale
- ppm parts per million – units to describe the chemical shift in NMR experiments
- R Rectus –right handed stereoisomer configuration
- s singlet (NMR peak splitting pattern)
- sex sextet (NMR peak splitting pattern)
- S Sinister – left handed stereoisomer configuration
- sp species
- spp. Lat. Species pluralis. I.e. multiple species within a genus.
- t triplet (NMR peak splitting pattern)
  TFA Trifluoroacetic acid
- TSB Tryptone Soy Broth
- XRD X-ray Diffraction
- *YrpC* A gene that catalyses PγGA and may be involved in producing D glutamate
- ZnSe Zinc selenide crystal

1 Introduction

1.1 Chemical Structure of Poly Glutamic Acid

1.1.1 Properties of glutamic acid

Poly γ glutamic acid (PγGA) is a polymer composed of glutamic acid (figures 1, 2)bonded with the carboxyl group attached to the γ carbon and the amino group of the α carbon (figure 2). Glutamic acid, like every other naturally occurring amino acid (except glycine) is chiral; it contains 1 chiral centre (the α-carbon or Cα) and therefore exists in 2 enantiomeric forms. Pure solutions containing only one enantiomer rotate planes of polarised light in opposite directions at angles proportional to their concentration. Rotational deviations of polarised light produced by a racemic mixture,which contains equal amounts of both enantiomer, cancel each other out, therefore the angle of rotation is 0°.

The levorotatory (L) formof amino acids, which rotates polarised lightcounter-clockwise,are common to all living organisms and are used in protein synthesis. Commonly, the stereochemistry of a molecule is referred to using the theoretical Cahn-Ingold-Prelog system, which allows naming of a chiral center theoretically rather than empirically.The Lconfiguration of glutamic acid is referred to as sinister (S), whereasthe dextrorotatory (D) form, which rotates polarised light clockwise, is referred to as rectus (R) (see figure 1). Both enantiomers can be incorporated into poly-γ-glutamic acid (PγGA)(3).

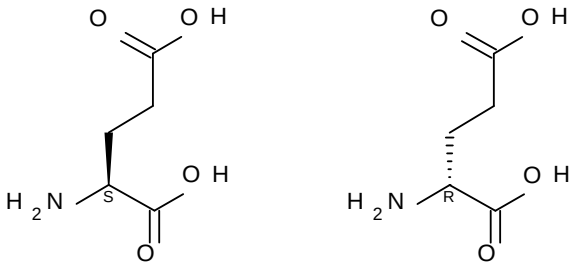

Enantiomer pair of glutamic acid. Chiral carbon are marked R and S.

Figure 1: Optically pure glutamic acid can rotate the plane of polarised light clockwise -the D form (R) or counter clockwise - the L form (S)

The functional groups of glutamic acid make it a weak diprotic acidand a weak base. When glutamic acid loses its proton and becomes negatively charged it is referred to as glutamate. The functional groups of glutamic acid have the following pK_a values[1]:

	α-carboxylic acid	γ-carboxylic acid	α-amine
pK_a	**2.10**	**4.07**	**9.47**

Table 1: pK_a values ($-\log^{10} K_a$) for the three functional groups[i]

Figure 2 shows how the charged species of glutamic acid/glutamate vary with pH based on the pK_a values of glutamate's functional groups. With PγGA, protonation of the α-carboxyl side chains depends on the solution's pH. At a neutral pH, the conjugate base will predominate and the polymer will be a polyelectrolyte stabilised by cations - this form of PγGA is very water soluble. Alternatively, when PγGAis in acidic solutions, the free acid form dominates. The structure of this form is highly coiled and insoluble in water. PγGA can refer to either the protonated form, or the polyanionic form(4).

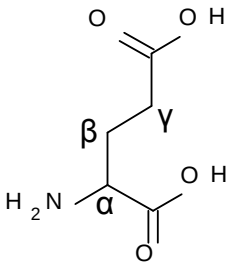

Figure 2Carbons atoms are labelled using the Greek alphabet; α representing the chiral carbon. Carbons within carboxylic acids are referred to by the carbon to which they are attached. Thus glutamic acid can be said to have α and γ carboxylic acid groups.

[1] Data taken from the department of chemistry University of Michigan: http://www.cem.msu.edu/~cem252/sp97/ch24/ch24aa.html (Accessed 17/09/11)

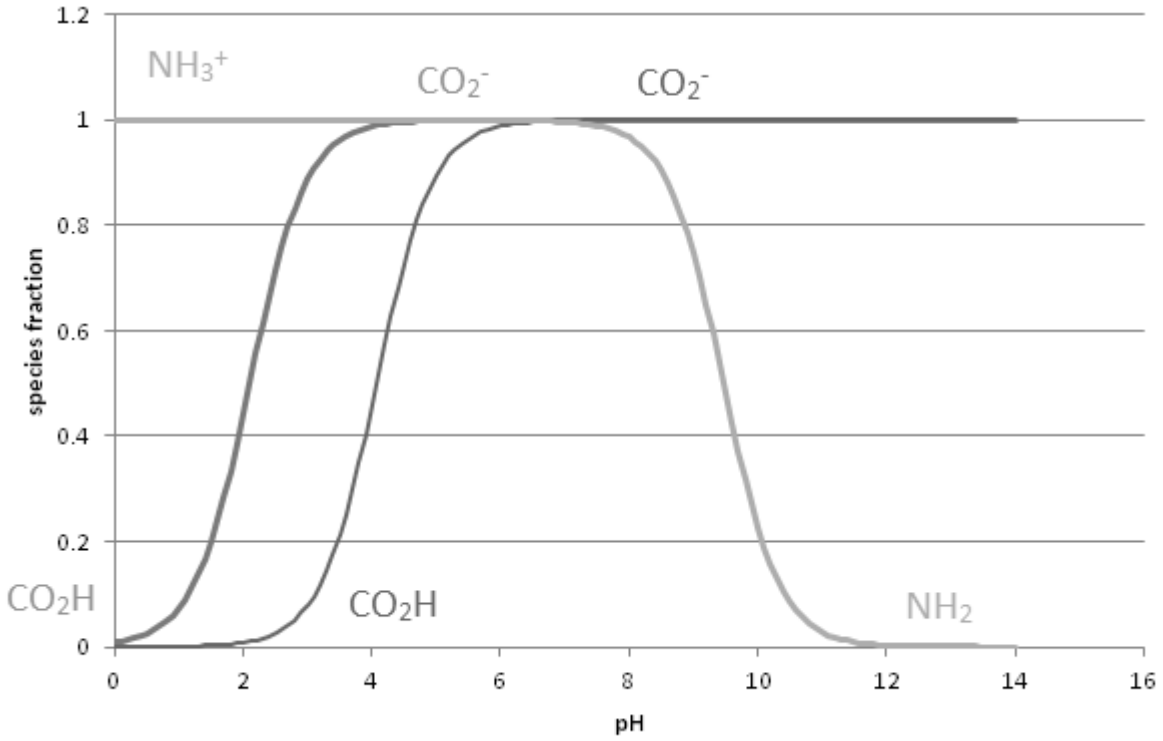

Figure 3: Alpha plot for the deprotonated species with varying pH.

1.1.2 Polymers of glutamic acid

When neutrally charged, each glutamyl unit within the polymer weighs on average 127.11 g mol^{-1} ($C_5H_7NO_3$); when negatively charged, the weight of each unit depends on which element is acting as the counter ion. For example if sodium is acting as the cation, each glutamyl unit would weigh 149 g mol^{-1}. Glutamic acid weighsmore than glutamyl, or 147.13 g mol^{-1}as 1 mol of H_2O is lost from every mole of polymer formed.

The relative reactivity of carboxyl groupsis proportional to the K_a values,therefore the α-COOH is more reactive than the γ-COOH. For this reason P*γ*GA is difficult to synthesise without the assistance

of either biological macromolecules or organisms; crude attempts to polymerise glutamate produce a poly-α glutamic acid.

The alpha form of the polymer is not produced by living organisms and attempts to genetically engineer micro-organisms to produce poly α glutamic acid have failed. This is believed to be because the codons encoding glutamic acid are similar to the Shine-Dalgarno sequence(5). The polymer is prepared chemically(6)and the structure of small length chains have been studied extensively in solution by NMR, ORD and FT-IR in order to gain information about protein folding dynamics.

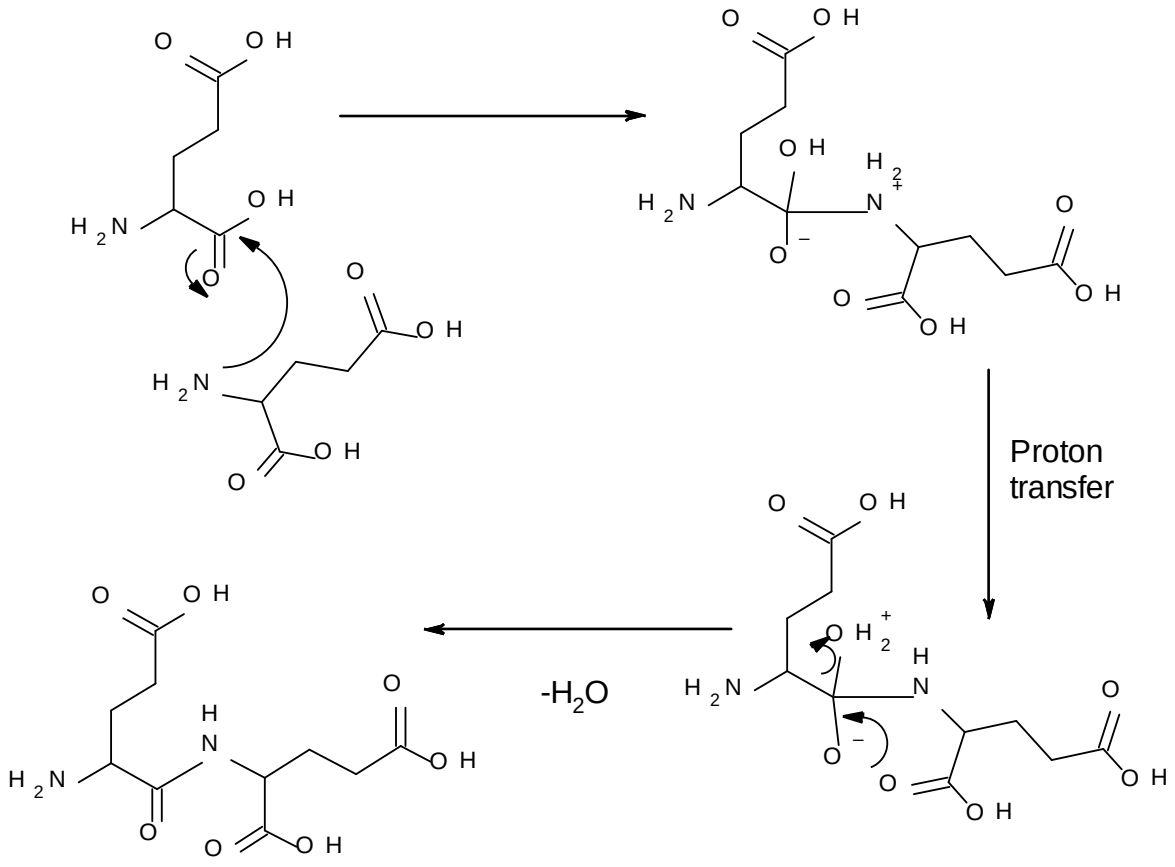

Figure 4: The condensation mechanism for alpha polymerisation of glutamic acid, showing the production of a glutamic acid dimer. The α carboxyl group is likely to be more δ^+ due to the electron withrawing effect of the local amine. This explains why the pK_a of the α-carboxyl group is greater than the γ-carboxyl and also why the α-carboxyl reacts with the nucleophile.

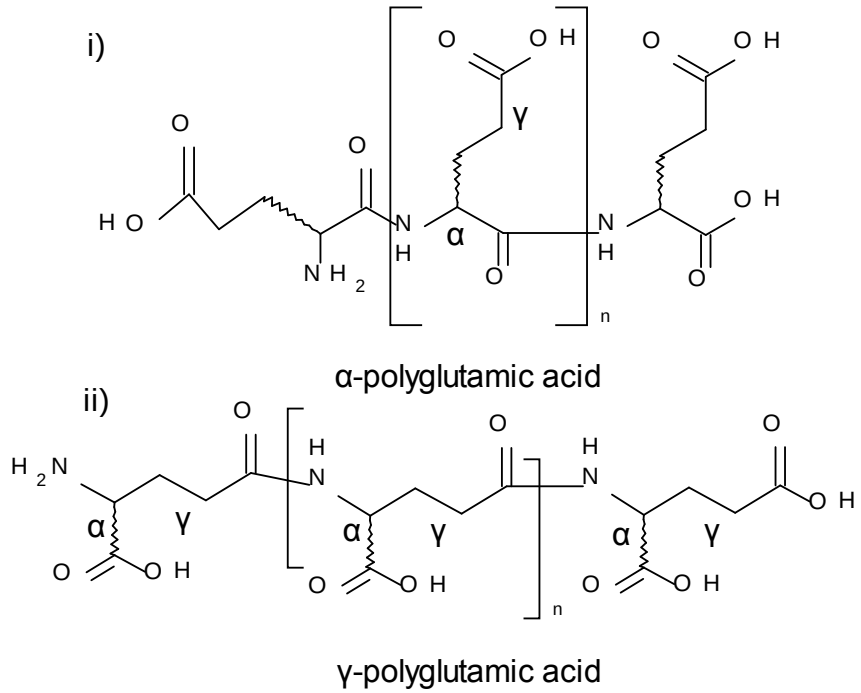

.

Figure 5: Different polymer structures that can arise from the polymerisation of glutamic acid. 5i) The chemically favoured poly-α-glutamic acid. 5ii) Poly-γ-glutamic acid, produced by biosynthesis.

Less is known about the macromolecular structure of PγGA, but it must depend on the proportion and position of each optical isomer within the polypeptide, the size of the molecule and also the degree of (de)protonation/or the particular ionic form. Zanuy has investigated the structure of short chain D-PγGA in detail using a variety of modelling software and experimental techniques such as XRD and electron diffraction (2, 7-10). In small peptides of only 20 residues simulations of the protonated PγGA forms a left handed helix with a helical repeat occurring every 3 residues in the aqueous phase(10).

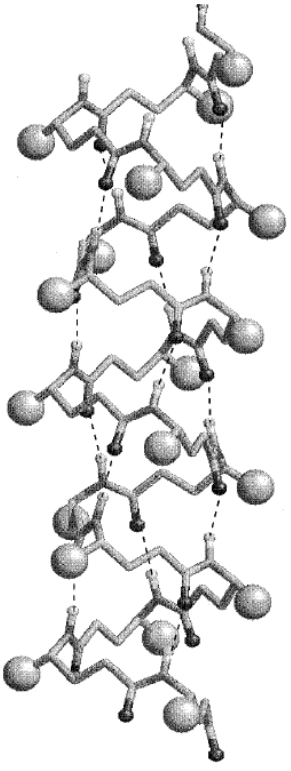

Figure 6: Model of most stable conformation of a 20 residueD - γPGA molecule taken from Zanuy et al. (2)

1.2 History of the Production and Use of Poly γ Glutamic acid.

1.2.1 Medically relevant history

PγGA was first discovered by Ivanovics and Bruckner in 1937 (11) on the surface of *Bacillus anthracis*. Controversially, the polymer was identified as being composed of D glutamate (an enantiomer uncommon to biological processes) and covalently attached to the bacterial capsule. In 2011 an experiment showed PγGA enhanced the potency of the anthrax toxin "Lethal Factor" (12). Other authors hypothesize that PγGA is weakly immunogenic; since its backbone makes it resistant to proteases, antigen presenting cells struggle to digest the molecule and therefore cannot present the molecule to T cells (13). This has led to the investigation of treatments and vaccines which target either the polymer or its method of attachment to the capsule via the protein CapD (14). This strategy is not only useful for anthrax treatments as a number of other pathogens such as *Staphalcoccus aureus* utilize PγGA in a similar way (15).

PγGA was also found to be a useful biomaterial. It is safe to administer orally and intravenously and is today an ingredient in multiple pharmaceutical products currently undergoing clinical trials (16). Doses required to kill 50% of rats (LD_{50}) are 2.05 g kg^{-1} administered intravenously or 6 g kg^{-1} orally.(17)

1.2.2 History of the production of PγGA

The late 80's and early 90's saw increased enthusiasm for production of bacterially synthesized polymers, but due to the toxicity of *B. anthracis* it is an unsuitable organism for large scale production of PγGA. Fortunately, PγGA was known to be produced in much more palatable forms. Five years after Ivonicks' discovery, *Bacillus subtillis* - strain 41259 (generally regarded to be harmless) was found to secrete a similar D-form PγGA freely into solution(18). Other *B. subtillis* strains secrete PγGA containing D and L glutamyl.

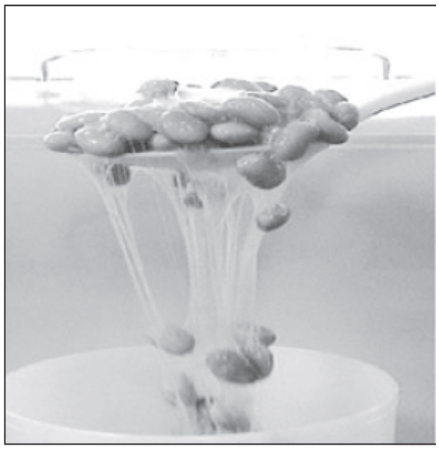

Figure 7: The Japanese food natto produced by fermenting soy beans with B. Subtilliis natto. Image from Sung (1)

Among these subspecies are 'natto' and 'chungkookjang', named respectively after Japanese and Korean traditional fermented foods, which these bacillus species help to produce. Whilst tasteless(4), PγGA gives these food products a gelatinous texture.

The size of PγGA produced varies between species.*B. subtillis chungkookjang* produces very high molecular weight PγGA (19) which allows it to be used for specific medical applications (20).

1.2.3 PγGA Production in Bacillus spp.

To date, *Bacillus spp*. are the most studied bacterial genus known to produce PγGA. At the turn of the millennium Ashiuchi used *B. subtillis* strains to determine the genetic and biochemical mechanisms of PGA synthesis (3). Other than *B. Subtillis,Bacillus licheniformis* is commonly used for investigating PγGA production. Initial experiments with *B. licheniformis ATC9945A* showed PγGA produced was similar to that produced by *B. Anthracis* – i.e. an encapsulated D form of the polymer (21, 22). Other experiments using the same strain produced a DL polymer and two other studies have shown that the ratio both is (23) and isn't altered by the manganese ion Mn^{2+} concentration(24). Many strains of *B. Licheniformis* have been studied in order to find the most effective method for cheap production, and some strains are reported to produce very high yields >59.90 g l^{-1}(25). Many other bacillus species such as *Bacillus halodurans* and *Bacillus megaterium*are known to produce PγGA(1)but few studies were found that examined the effects of culture conditions on the production of PγGA.

1.2.4 PγGA Production in non Bacilli Bacterial

Other morphologically diverse bacteria produce PγGA, however none of these species are used to prepare purified polymers for different applications and the methods of PγGA production has not been reported in current literature. Amongst these are pathogenic (and gram negative) species. A study has shown *Staphylococcus epidermidis* needs this secreted DL- PγGAto resist high salt concentrations and evade the host immune response (15). Complete genome sequencing of the gram-negative L*eptospira interrogans (26)* and *Fursobacterium nucleatum* (27) has shown these

species to contain the genes necessary for PγGA production. No literature was found reportingproperties such as quantities, size, or the DL ratio of polymers produced from these pathogenic species. However, these discoveries illustrate that it is conceivable that an understanding of the function and biochemistry of PγGA might yield novel treatments and targets for a range of infectious diseases.

1.2.5 PγGA Production in Non-Bacterial spp.

Other studies have shown that production of γ-linked glutamate is not exclusively limited to bacteria but also can be produced by Eukaryotes. PγGA is found in the stinging cells of Hydra, it was suggested by the authors that PγGA might be a molecule characteristic of the Cnidarian phyla (28). However PγGA has also been found in mammals; post translation modification of tubulin in murine neurons produces PγGA. Finally, at least 2 halophilic Archaea have been found to produce γPGA, enabling them to survive in extreme habitats. *Natrialba aegyptiaca*producesPγGA and the authors of this discovery predicted PγGA prevents severe dehydration in halophilic conditions (29).Finally the Achaea species*Natronococcus occultus*contains smallPγGA fragments (~8 kDa) in their cell wall for an unknown function. (30)

1.3 Applications of PγGA

Bajaj (25) comprehensively reviewed the variety of applications in 2011 covering: medical, cosmetic, wastewater remediation industries and agriculture. PγGA can be produced over a wide range of molecular weights, is water soluble, non toxic, non-immunogenic (except in rare cases (31)) and biodegradable.

1.3.1 PγGA as a Drug Delivery System

Research into the pharmaceutical applications of PγGA have focused two main areas: drug delivery systems and an immune activating effect of PγGA. The former utilise the α carboxylic acid residues/side chains on the polypeptide to attach pharmaceutical products. Perhaps the most significant finding has been attachment of PGA to paclitaxel. Conjugates with a molecular weight

greater than 30kDa cannot readily diffuse across capillaries or the glomerular endothelium,(25) but if the M_w is less than 50kDa it preferentially diffuses into cancerous tissue and malignant tumour cells; therefore efficacy of this anticancer drug is increased. During transit in the systemic circulation paclitaxel molecules are contained within the polymer, therefore the drugs is less toxic to non cancerous cells and fewer side effects are observed (32). Other PγGA treatments decelerate the release of a drug or growth factor. A dopamine-PγGA conjugate has been studied, which released dopamine slowly and prevented angiogenesis (33). A similar technique was developed by Akagi, who produced PγGA nanoparticles to be used as adjuvants (34). These release and expose delicate immune activating particles such as HIV proteins over long/controlled periods of time. As attachment to PγGA could protect molecule from the environment, it has been proposed that PγGA could be used as a vector for gene therapy (35, 36).

1.3.2 PγGA as an immune modulating drug

The immune activating properties of PγGA have been shown in a variety of papers (37-39). Oral administration of particularly high weight PγGA has been shown to activate natural killer cells and provide mice with an increased survival chance when injected with foreign tumour cells (40). PγGA is being observed in a phase 2 clinical trial to treat cervical intraepithelial neoplasia (41). PγGA is has been shown to have anti-inflammatory properties; which, along with PγGA's water retaining properties has been exploited to promote corneal wound healing (42). Other claimed health benefits gained by eating PγGA are increased calcium absorption in the gut (43, 44) and chelation of toxic heavy metal ion poisoning(45, 46).

1.3.3 PγGA in Tissue Engineering

The biodegradability of PγGA makes it useful in tissue engineering, where it may be employed as a tissue scaffold. Methods to produce scaffolds have used electrospinning on cross-linked PγGA (47) or preparation of hydrogels (48) – the latter was achieved by crosslinking PγGA with polyacrylamide (49), dihalogen alkanes (50), gelatine (51), alginate (52) or without crosslinking – but by exposure to γ radiation (53). PγGA has been used with silica to produce a hybrid replacement for bioactive glasses used for bone grafts (54). At least two PγGA hydrogels have been studied using rats as biodegradable biological adhesives (51, 55).

1.3.4 Other Uses of PγGA

The number of potential and proven non-biomaterial uses for PγGA are many and diverse, but will not be discussed in any detail within the rest of this report. However, these uses include:

- cosmetics – as a humectant
- the food industry – removing bitter tastes of foods
- water treatment – removing heavy metal ions and acting as a flocculant(56)
- Agriculture – various uses(57)
- Cryoprotectant (58)
- biodegradable plastics

Many applications are limited by the high cost of the material, therefore it is not just of academic interest to find methods which increase yields, or produce a low cost, continuous (non-batch) process technique (59). Some studies have focused on fermentation of manure to produce PγGA (60-63).

1.4 Production of Poly Glutamic Acid

1.4.1 Chemical production

Waley (64)was the first to chemically synthesise polymerised D-PγGA. He made two important intuitive observations: that all α-carboxyl groups need to remain protected during polymerisation in order to prevent intramolecular condensation from occurring – producing a five-membered ring now known as “pyroglutamic acid”. The amine group must also be protected, but in a way that it can be removed preferentially over the alpha carboxyl protective group so that polymerisation can subsequently occur. The mechanism prepared alpha methyl N-(alpha methyl gamma-L-glutamyl)-L-glutamate, then polymerised using tetraethyl pyrophosphate, followed by hydrolysis of the methyl ester bonds. The product was contaminated with a phosphorus containing polymer and had a molecular weight of 9 kDa.

Bruckner, who discovered PγGA with Ivanovics, also developed a chemical synthesis of alpha and gamma forms of the polymer (65). This was later developed by Bruckner with Kajitar (66) and Hollosi(67). They also used protective groups attached to the alpha carbonyl to form polymethyl, polybenzyl and poly tert-butyl esters. This mechanism reportedly[2](68) used a polycondensation reaction from glutamyl dipeptides.

No literature on the chemical synthesis of PγGA was found to be published between 1967 and 2001. Sanda reported a synthesis for PγGA using a polymerisation reaction in a range of solvents, finding N,N-dimethylformamide (DMF) to give the most satisfactory yield. The molecular number of the PγGA was effected by the choice of solvent, and length of the reaction, and the enantiomeric form of the polymer was controlled by the reactants. However, DL polymers were much smaller than the isotactic D and L forms(68). A further problem was removal of the methyl ester side chains without fission of the backbone. Later success came from conversion to benzyl esters following removal, using hydrogenation over a Pd/C catalyst. However, this only removed 93% of the benzyl groups. The authors also reported in a later paper that this method was accompanied by pyroglutamate formation, which they assumed to be due to backbiting(69).

At the beginning of the 21st century a method of production for an atactic polymer was not reported, but the following year Sanda published a method for stepwise synthesis of a 16 unit PγGA polypeptide(69). Whether this method is feasible for producing much longer chains similar to those produced by microorganisms was not reported. Furthermore, the authors neglected to publish any chemical data for a purified polymer.

Therefore pyroglutamate formation, the reactivity of the α carboxyl group and removal of protective groups are major challenges involved in designing by a chemical synthesis of pure γPGA. This may be why the use of micro-organisms in the biosynthesis of PγGA is so appealing.

[2] Reference 34 cannot be accessed as papers are only available in German and Hungarian.

1.4.2 Biosynthetic production

Ashiuchi – one of the key researchers in the field of PγGA biosynthesis, has written much to further the understanding of the genetics (3, 70) and enzymatic (71-74) processing of PγGA. In 1999 genes named *pgs*[3]*B, C* and *A* extracted from *Bacillus subtilis* IFO 3336 were incorporated into *Escherichia Coli*, causing the *E. Coli* to produce PγGA (70). These genes resembled*capB*, *C* and *A* genes found in *B. Anthracis,* and encode a membrane complex *pgsBCA* similar to that discovered by Troy. The finding that all three genes (B, C and A) are required for PγGA synthesis is backed up in transgenic studies using the tobacco plant, where all 3 genes were required to produce PγGA (75). However this study was not conclusive, as Urushibata found that PγGA is still produced in *Bacillus subtilis* IFO16449 when *pgsA* is interrupted (76). The gene *capD*, which encodes the membrane protein CapD attaches PγGA to the capsuleof*B. anthracis* and *licheniformis(77)*.

The proteins responsible for PγGA synthesis, associated with the above genes, were isolated by Troy before the genetic material was described (78). Proteins within the cell membrane were isolated as a particulate fraction of the cell envelope of*B. Licheniformis ATCC 9945A* and PγGA production from this fraction was observed. This investigation was sufficient to conclude that PγGA biosynthesis is independent of an RNA template and occurs in a membrane associated protein complex. Furthermore the membrane fraction produced PγGA when glutamate was not present in the growth media, which suggested that (at least some) biosynthetic mechanisms are capable of de novo synthesis of glutamic acid. The findings also suggested that Mg^{2+} ions were needed to initiate the glutamate polymerisation.

These findings were not ubiquitous to all PγGA producing species.Some require glutamate in the growth medium for PγGA production and Mg^{2+} is not required. Despite similarity of the genes

[3]Polygammaglutamic acid Synthesising Gene

responsible for the production of PγGA the products vary. The following table demonstrates product diversity in terms of size.

Producer	Molecular mass (kDa)	Content (%)	
		D-Enantiomer	L-Enantiomer
Bacillus subtilis (*natto*)	10–1000	50–80	20–50
Bacillus subtilis (*chungkookjang*)	>1,000	60–70	30–40
Bacillus licheniformis	10–1000	10–100	0–90
Bacillus anthracis	ND[a]	100	0
Bacillus megaterium	>200	50	50
Bacillus halodurans	10–15	0	100
Natrialba aegyptiaca	>1000	0	100
Hydra	3–25	0	100

Figure 8: From Ashiuchi(3) - size and relative quantities of optical isomers of PGA species in a variety of γPGA-producing species

A study of membrane associated enzymes in *B. Subtillischungkookjang* showed that the enzyme had no preference for either optical isomer of glutamate, and PγGA had the same ratio of glutamyl optical isomers as the substrate. Therefore also suggesting that the enzyme complex did not produce or convert D or L glutamate (73). Racemisation of glutamate has been reported in *B. Subtillis R22* by the intracellular enzyme glutamate racemase (Glr)(79) and also by a second enzyme YrpC to a lesser degree (80). Whilst PγGA production is barely effected when the *YrpC* is inactivated(79)another study using*B. subtillis chungkookjang* transfected withYrpC plasmids showed increasing Zn^{2+} concentration tripled PγGA production. The authors believed that *B. subtillis natto* could be similarly affected by Mn^{2+}(81). The authors predict this because earlier experiments which used *E. Coli* clones containing B. natto PGS genes produced much more PγGA in the presence of Mn^{2+}. In this experiment Mn^{2+} did not affect the optical isomer distribution(70). Therefore it is not clear whether YrpC plays a role in racemisation or increased production of PγGA.

Isomerisation in *B. licheniformis* occurs via a different 'indirect route,' where D glutamate is

converted from D alanine, which is produced by the enzyme alanine racemase. (82)

Alteration of the substrateclearlydemonstrates two groups of PγGA-producing bacterial strains: glutamic acid dependant and independant. The latter are likely to produce glutamic acid from either the citric acid cycle (α-ketoglutaric acid) or glutamine, and hence addition of citric acid increases polymer yields(83). Others studys have linked PγGA production to the concentration of inorganic ions, ammonia, other metabolites and precursors,changing aeration rates, stirring speed, altering membrane permeability, temperature and pH. PγGA fementation can either be achieved using a submerged fermentation or solid state fermentations methods, each technique can pose additional difficulties. (25)

After fermentation PγGA is purified by preparing aqueous solutions followed by filtration and/or centrifugation to remove the cellular material. PγGA is then precipitated from solution by adding either ethanol/methanol or Cu^{2+}(84). Chromatographic methods or dialysis are used to preparea medically pure product(85).

1.4.3 Manipulating PγGA production in the following work

Mn^{2+} concentrations have been shown to dramatically increase the yield of PγGA in E. Coli clones transfected with PGS genetic material from *B. Subtillis natto*. However acellular enzymatic experiments from *B. Subtillis chungkookjang* relied on Mg^{2+} and Zn^{2+} but were not effected by Mn^{2+} concentration(73). Furthermore, experiments with *B. licheniformis*showed that addition of between 61.5 and 615 µmol $MnSO_4$ produced optimal yields of PγGA (23). These concentrations increased the yield of PγGA by more than threefold compared to experiments when no or less than 615 nmol were used. However the yield decreased from the optimal amount when more than 33.8 µmol were used. In this study we decided to test whether $MnSO_4$could affect the PγGA yield with B. subtillis natto, the same subspecies used in the experiment involving the E.Coli clones. Experiments using this same subspecies showed ^{14}C radiolabelled glutamate was incorporated into PγGA(86). This

suggests that this natto subspecies at least prefers glutamate as a substrate if the species is not glutamate dependent for producing PγGA.

B. Subtillis chungkookjang also produces lower molecular weight PγGA at high NaCl concentrations. >2,000kDa when NaCl is <0.5% and 10-200 kDa when NaCl concentration was > 10% (1). Therefore we deicded to see whether addition of NaCl might also alter the molecular weight in B. Subtillis.

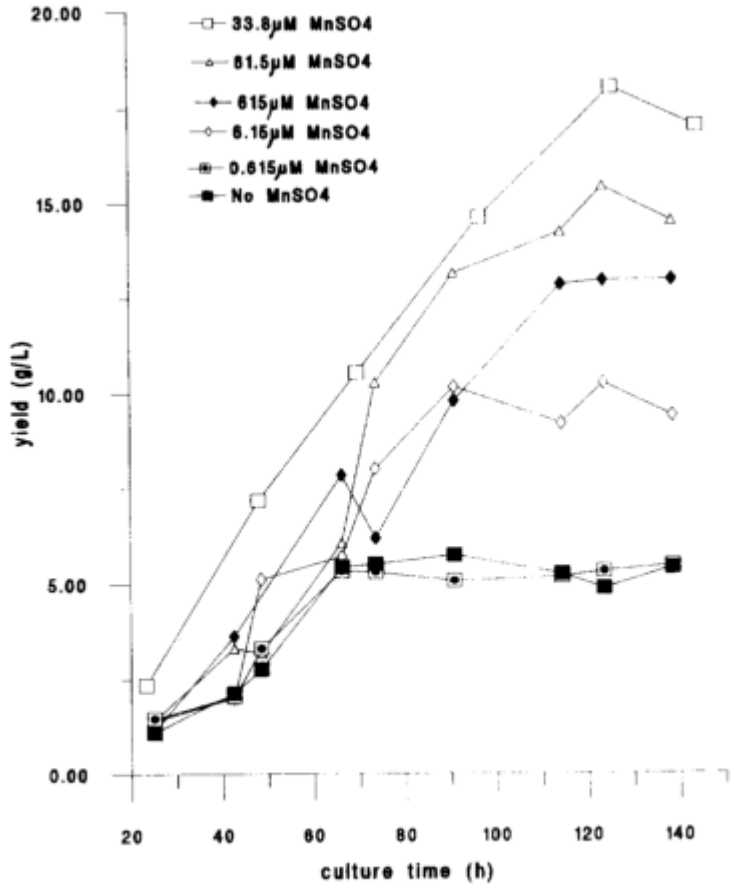

Figure 3 Volumetric γ-PGA yield as a function of $MnSO_4$ concentration in the culture medium

Figure 9: Effect of concentration of $MnSO_4$ on PγGA production over time with B. Licheniformis. Taken from Cromwick et al. (23)

A patent was found to purify PγGA. but it did not specify which species was used. Searching the literature provided no method for purifying PγGA from B. Subtillis. However Manocha published a

comparison of 2 methods used to purify PγGA produced by B. Licheniformis. Therefore we decided to see if either of these two methods were useful for purifying PγGA produced by *B. subtillis*.

1.5 Aims and objectives

The aims of this project are:

1) To analyse the chemical identity of crude precipitates from *B. subtillis*, identifying the presence and quantity of PγGA and any other impurities

2) Compare the effectiveness of methods developed to extract PγGA from B. Iicheniformisto extract PγGA from *B. subtillis*.

3) Using equipment available at Birmingham University, identify methods which can be used to determine the properties of PγGA within these samples, such asthe size (molecular number) and D/L ratio.

4) Alter the culture conditions using the strain Bacillus subtillis natto ATC15245. To test whether [Mn^{2+}] or [NaCl] effects the purity, yield or properties of any PγGA produced.

Chapter 2

Materials and methods

2.1 Preparation of the samples

Two samples were bought from Natto Biosciences, Nanjing shineking Biotechnology Co. Ltd. One was a water soluble Na^+ salt, the other was a free acid (H - form). Both samples were said to be >92% pure and with a molecular weight of> 1,000kDa. The company provided no laboratory evidence with the material. All other samples were prepared at the University of Wolverhampton using their patented method (87). *Bacillus Subtillis* natto ATC15245 was purchased from the national collection of Industrial and Marine Bacteria (NCIMB). The samples are summarised in table 2.

Sample name	Organism	[NaCl]	[Mn^{2+}] g/dm^{-3}	Media	
A	Unknown	0	0	??	
B	Bacilus Subtillis Natto IFO16449 (commercial)	0	0	??	Commercial Na-form
C	Bacilus Subtillis Natto IFO16449 (commercial)	0	0	??	Commercial - H-form
D	*Bacillus Subtillis* Natto ATC15245	0	0	GS	
E	*Bacillus Subtillis* Natto ATC15245	0	0	GS	
F	*Bacillus Subtillis* Natto ATC15245	0	0.05	GS	
G	*Bacillus Subtillis* Natto ATC15245	0	0.5	GS	
H	*Bacillus Subtillis* Natto ATC15245	2.5	0	GS	

Table 2: Growth conditions known for different samples provided

GS media was prepared using deionized water which had been sterilized for 20 minutes at 15 p.s.i. using the ingredients listed in table 3.The pH was altered to 7.2 using 3M NaOH and 1 M HCl.

Samples were inoculated in 250 ml tryptone soy broth (TSB - obtained from Lab M Ltd) at 37°C for 24 hours. 12.5 ml of TSB was then introduced into GS medium and incubated on a rotary shaker (Innova 43)at 150 rpm for 96 hours. Cellular debris was then removed via centrifugation at 17,000 g

for 30 minutes, discarding the sediment. The supernatant was then combined with 4 equal volumes of cold ethanol (90%), which caused a white substance to precipitate. The ethanol-water mixture was allowed to stand for 72 hours before centrifuged again at 17,000 g for 30 minutes. The sediment was dissolved in 10 ml of deionised water and samples were lyophilised to obtain a dry powder. The mass was obtained to determine a crude yield in g (product) / volume (GS medium). Sample D was prepared by Adityah Bhat. Samples E,F, G and H were prepared in triplicate and prepared by Adetoro Ogunleye. Each biological replicate is referred to as E1,E2,E3,F1,F2,F3...etc). Each replicate was grown in separate flasks under identical growth conditions. The additional ingredients were added to the GS media before introduction of inoculated TSB. Sample F contained an additional 1.81 mmol $MnSO_4$, sample G contained 181 µmol of $MnSO_4$ and sample H contained 42 mmol NaCl.

Chemical	Quantity	Source	Notes
L-glutamic acid	20 g dm^{-3}	Sigma Aldrich	
Sucrose	50 g dm^{-3}	Acros Organics	Separately sterilised at 110°C at 5 p.s.i for 30 min
Potassium dihydrogen orthophosphate	2.7 g dm^{-3}	Fischer Scientific	
Anhydrous di-sodium hydrogen phosphate	4.2 g dm^{-3}	AnalaR	
Sodium Chloride	50 g dm^{-3}	Aldrich Chemical Co. Ltd	
Magnesium sulfate heptahydrate	5 g dm^{-3}	AnalaR	
Murashige-Skoog vitamin solution	1 ml dm^{-3}	Sigma Aldrich	Filter sterilised using 0.2 µm Ministart

Table 3: Composition of GS medium

2.2 Purification of crude product

2.2.1 Copper precipitation of PγGA

Manocha et al(84)purified PγGA fromBacillus Licheniformis fermentation broth using $CuSO_4$ to precipitate the polymer and then used $EDTA^{8-}$ to displace the Cu^{2+} from the polymer- these were then dialysed prior to lyophilisation.

Five samples (C, E1, F1, G1, H1), were weighed out and added to 0.1M phosphate buffer to ensure the concentration of sample was 2 g dm^{-3}. $CuSO_4$ was added at a ratio of 60mmol per gram of

sample which the authors quote was sufficient to precipitate >99% PγGA. More than 20 minutes later, the samples were centrifuged at 7,000 g for 10 minutes. The supernatant was extracted and tested for residual polymer by adding a few drops of 1M $CuSO_4$. No additional precipitate formed. The sediment was resolubilised by adding 20 ml of 0.5M EDTA and stirred overnight. The resultant liquid was transferred into dialysis bags with a molecular weight cut off (MWCO) of 20 kDa. Dialysis bags were weighed and left in 500 ml 0.1 M phosphate buffer, which was replaced 3 times over 24 hours. The dialysis tubing was weighed a second time and transferred to pre-weighed round bottom flask and freeze dried. These were left overnight and the new weight of the round bottom flask was used to calculate the yield.

2.2.2 Ethanol precipitation of PγGA

Samples were purified according to the method provided by the same paper (84). Samples were weighed and dissolved in distilled water, 0.2 M $NaCO_3H$,was added to precipitate remaining Mn^{2+}in samples F and G. The solution was centrifuged at 7,000 g and the supernatant was added to 4 volumes of cold ethanol and left overnight. The precipitate was extracted by filtration under suction through a Whatmman cellulose filter with a pore size of 20-25 µm and washed with cold ethanol. The precipitates were dried in a desiccator then dissolved in distilled water and dialysed in tubing with a MWCO of 20kDa. The dialysate was replaced 3 times over 24 hours. The contents of the bag were then precipitated in 4 volumes of cold ethanol and filtered a second time, the product was then dissolved in water then lyophilised in pre-weighed round bottom flasks and the dry weight was used to calculate the yield.

2.2 Characterisation of samples

2.2.1 Fourier Transform Infra Red Spectroscopy

Infrared spectroscopy measures the natural vibrational frequencies that occur between two or more atoms within a molecule when the atoms form a dipole. As a photonmoves,an oscillating electrical field is generated perpendicularly to that direction. This field causes photons of particular

wavelength to be absorbed and causes molecules to vibrate in specific modes. In a simple harmonic oscillator model the natural vibrational frequency of a bond is proportional to the bond's stiffness or strength and inversely proportional to the mass of the nuclei on either side of the bond. Many known substances have been investigated using infrared spectroscopy and expected absorption patterns for particular moieties, functional groups and bonds are known. Spectra obtained from samples with unknown chemical structure show which groups are present in that compound.

The region of the IR spectra between 1500 and 500 cm^{-1} is known as the fingerprint region. Many molecules have unique fingerprint spectra as vibrations caused by photons of this wavelength interact. Individual peaks are difficult to spot, but pure samples can be identified by comparing fingerprint spectra.(88)Erno Pretcsh's tables of spectral data(89)was used as a reference for bond analysis.

Fourier Transform Infrared Spectroscopy uses a non-monochromatic light source which passes through the sample and a Michelson interferometer. The beam detected contains absorption information for a variety of wavelengths, which is interpreted by a computer to give a spectra.

Solutions were analysed by mixing known masses of sample with either fractionally distilled D_2O or distilled H_2O and measured against references (pure D_2O / H_2O respectively) and placed on a ZnSe ATR crystal.

2.2 Nuclear Magnetic Resonance

Nuclear magnetic resonance spectroscopy (NMR) probes the nucleus of any atom which doesn't have a net nuclear spin of 0, i.e. it has a nucleus with at least one unpaired proton or neutron. Such nuclei, when placed in a magnetic field, occupy one of two energy levels, either opposing or aligning with the magnetic vector. The nuclei transition between states by absorbing or emitting a photon with the same amount of energy as the energy gap. This quantity can be expressed as:

$$E = h\gamma B$$

Where E is the energy of the photon, h is Planck's constant, B is the strength of the magnetic field and γ is the gyromagnetic ratio, which is unique for each isotope. E is effected by electrons, which shield the nucleus from the magnet; ΔE is called chemical shift. Electron density is affected by local electron withdrawing and donating groups, therefore NMR spectra which show chemical shifts of a signal suggest which functional groups are in close proximity to the nucleus emitting the signal.

In addition to chemical shift, adjacent nuclei in different spin states affect their neighbours and increase the number of possible energy states the nuclei can occupy. This causes splitting of peaks in a NMR spectra (see figure 7). The number of smaller peaks a signal splits into is always 1 more than the number of nuclei causing this splitting. The distance between peeks (J) is specific for certain stereochemistry and also indicates which nuclei are adjacent.

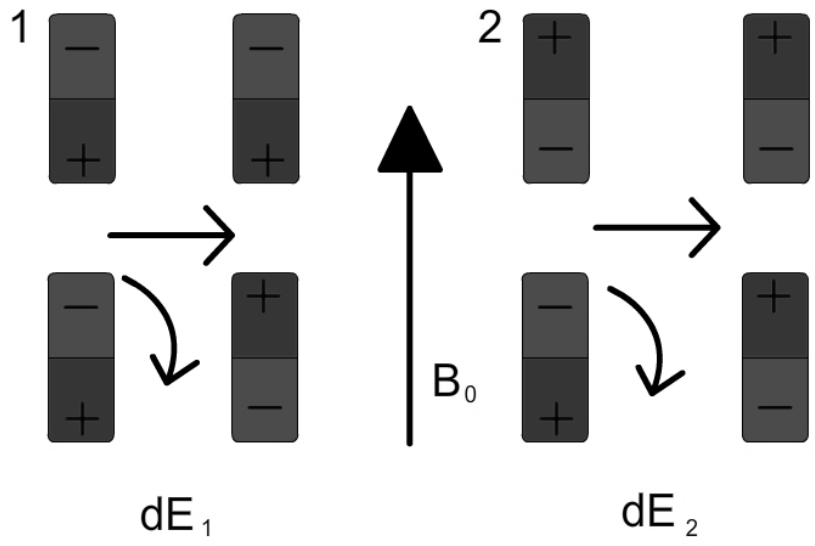

Figure 10: Diagram showing simplest possible spin coupling. In the diagram, the lower nuclei/magnet absorbs a photon to make it change its spin state, whilst its neighbout (upper magnet) remains static. The differences in energy between these two states are not identical ($dE_1 > dE_2$) therefore one transition will show two peaks.

All experiments were performed using an AV400 Bruker instrument in 99.9% D_2O. Peaks were analysed using the Bruker software package 'TOPSPIN'.

2.2.2.1 Proton (^{1}H) NMR

^{1}H is the (>99.98%) abundant isotope and therefore nearly all of the hydrogen within the molecule will have the same gyromagnetic ratio(γ). A strong signal to noise ratio means an integration trace allows a quantification of the number of protons.Furthermore coupling gives information that can link two peaks to identify hydrogen atoms on adjacent carbon atoms. Samples were run using a water suppression method as residual protons in the solvent produced the largestsignal.
Spectra were obtained for samples A, B, D, E1, F1, G1 and H1. After purification using ethanol samples F1, F2, F3, G1, G2, G3, H1, H2 and H3 were obtained.

2.2.2.2 ^{13}C NMR

^{13}C isotope abundance is only 1.1%, more time is required to reduce the signal/noise ratio, andthe probability that two ^{13}C isotopes are neighbours is extremely small ($1/1.21 \times 10^{-6}$). Coupling is only rarely attempted in experiments known as Incredible Natural Abundance Double Quantum Transfer Experiment (INADEQUATE).Some carbon signal frequencies are enhanced by interactions with local protons, therefore ^{13}C spectra cannot give relative quantities of atoms. 13C spectra however can show the number of different chemical environments for carbon atoms in a molecule. For example PγGA has 5 different carbon atoms per monomer unit therefore it would be expected to have a ^{13}C spectra of 5 peaks. Spectra were obtained for samples A, B and D.

2.3 Analysis of impurities using polysaccharide analysis

An impurity from sample D was isolated by dialysis using tubing with an unknown (but presumablylarger than 20 kDa) molecular weight cut off (MWCO) in distilled H_2O. The material was shown using ^{1}H NMR to contain very little PγGA and due to the chemical shifts in the ^{1}H spectra was likely to be mostly carbohydrate. Therefore the unknown material was studied using the following two chemical analytical processes.

Determining the identity of carbohydrate units from alditol acetate derivatives

To determine the identity of any monosaccharide units, 50 mg of sample was hydrolysed in 200 µl of 2 M TFA for 11 hours at 120 °C. Samples were then reduced according to the Abdel method in 260 mM $NaBH_4$ with 0.5 M aqueous ammonia and 50% ethanol and left overnight. Samples were then acetylated by adding 3 drops of glacial acetic acid and then dried. Two further steps of adding 10% acetic acid in methanol and drying followed by 3 repeats of wetting in 3 drops of methanol followed by drying in warm air were performed. 100 µl of acetic anhydride were then added and the samples were incubated at 110 °C for 1 hour. 100 µl of toluene were then added and the sample dried. The sample was then extracted in chloroform using a chloroform water mixture and analysed using gas chromatography. Theexperiment was performed in duplicate and the overall strategy used is shown in figure 11. The chromatograph was compared to a control sample that contained alditol acetates derivatives of known sugars.

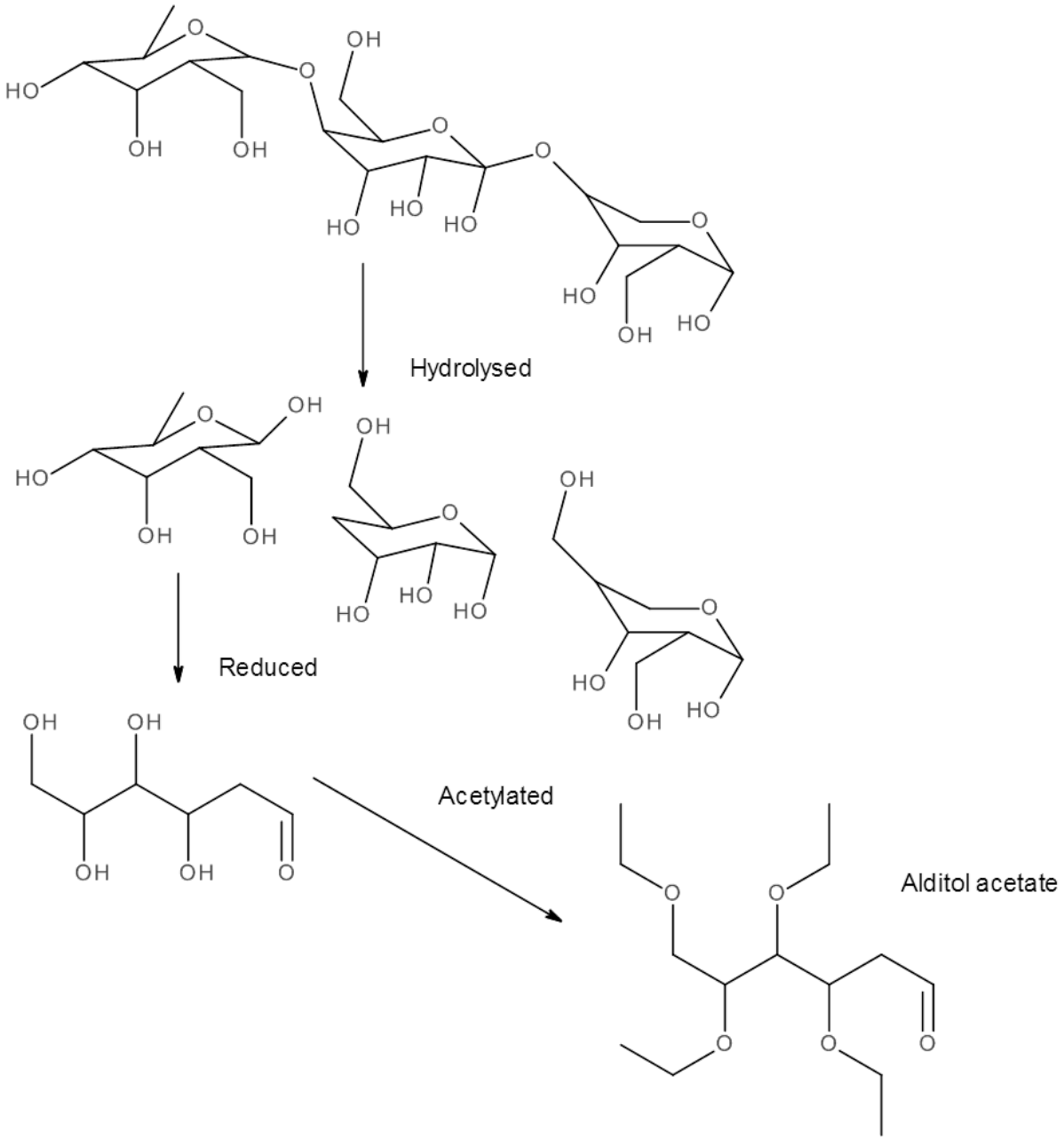

Figure 11: Schematic representation of strategy to determine the identity of sugars within the impurity via the generation of alditol acetates. All structures are drawn to show the method only and do not reflect experimental findings.

Linkage analysis was performed using the Hakomori method(90), whereby polysaccharides are first methylated by ionisation with methylsulfonylmethyl sodium and then reacted with methyl iodide, so that exposed, non bonded hydroxyl groups became methyl esters. The methylated moleculewas hydrolysedandacetylated using the Abdel method, which was stated in the

previousparagraph. Therefore acetyl groups only attach to the hydroxyl groups that were previously involved in links to other molecules and formyl ethers represent hydroxyl groups that are present in the polysaccharide.

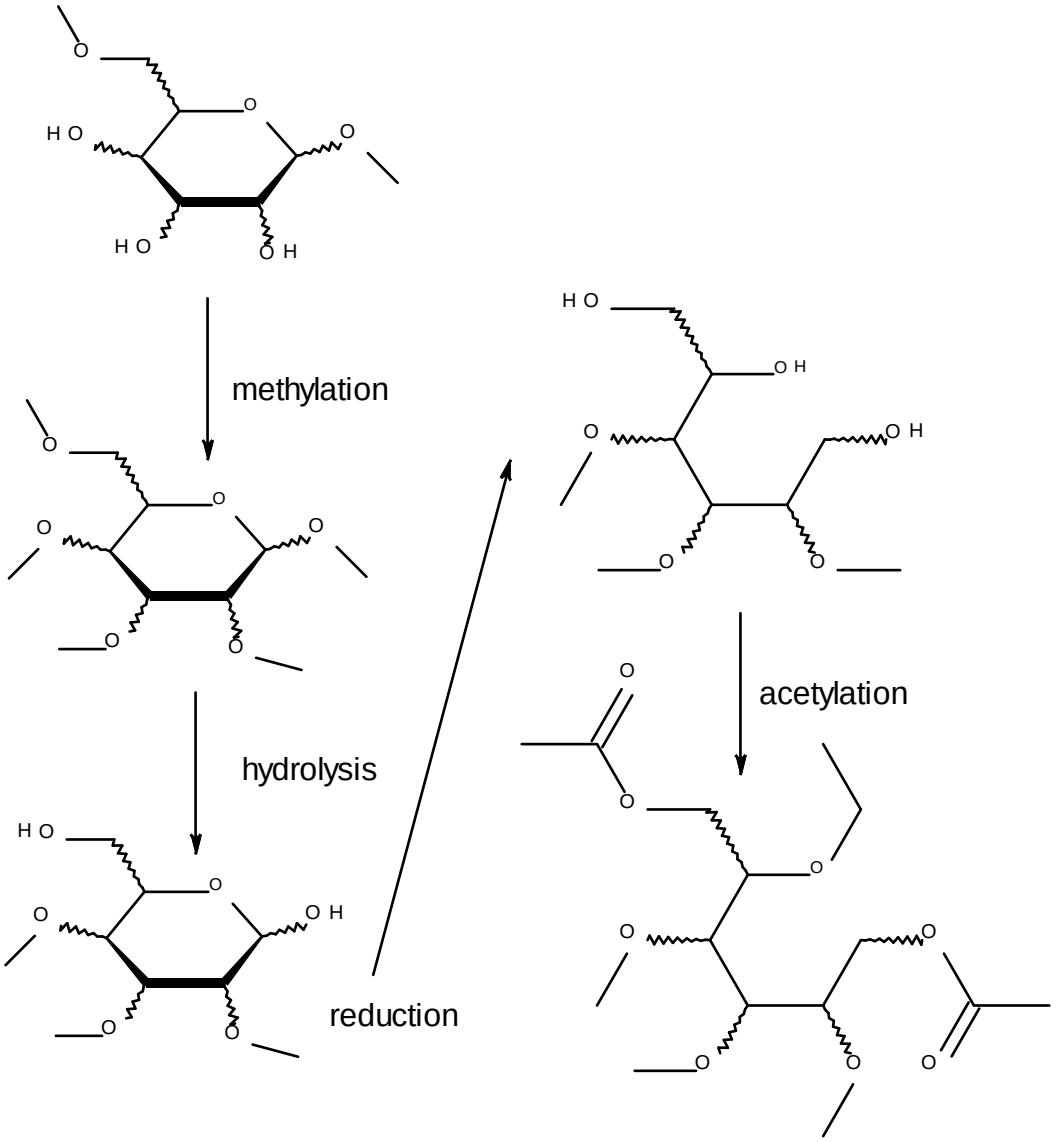

Figure 12: Simplified scheme of reactions showing the Hakomori method

Samples were then separated using gas chromatography (GC) and analysed using mass spectroscopy (MS). Molecular fragmentation occurs preferentially between carbons attached to adjacent methyl ether groups and this produces the initial molecular fragments. The mass of the

fragments then yields information regarding the overall structure of the polysaccharide, including the location of glycoside bonds.

Finally a 1 mg ml^{-1} sample in 0.1% TFA (v/v) was sent off for size analysis using matrix assisted laser desorption/ionisation (MALDI-TOF).

2.4 Analysis of chromatographically separated hydrolysate

Samples were dissolved in 0.1M borate buffer at pH 8.50 to make a concentration of 10 mg ml^{-1}. They were then centrifuged at 12,000 g for 10 minutes. The supernatant was removed, two 1:10 dilutions in borate buffer were prepared so that the concentration of lysate varied by 2 orders of magnitude. 500 µl of the sample containing the initial concentration was boiled for 30 hours using 500 µl 6M HCl to prepare a hydrolysate.

2.4.1. High Performance Liquid Chromatography analysis

100 µl of hydrolysate were added to 900 µl 2M NaOH. 20 µl was then injected into a Dionex Summit system with an 18C preparatory column using 0.1% trifluoroacetic acid (TFA) acetonitrile as a solvent. Samples were detected using UV light at 210 nm and integration of each peak was analysed using the Chromeleon® v6.8 software package. The quantity of glutamate was determined by comparing the area under the curve for a single peak with a retention time of 2.8 min, which had been determined by injecting pure monosodium glutamate and glutamate which had been treated to the same hydrolysis procedure as the sample. Sample concentration was determined by the following equation and by reference to a sample of known concentration.

$$Sample\ concentration = \frac{integration of the peak}{Peak duration \times flow rate}$$

2.4.2 Reagents used for N - terminal analysis

The other samples were mixed with 10 µl of 100 mMol 1-fluoro-2,4-dintrobenzene (FDNB) in acetone. 2 controls were used, one using sample (H1) and no FDNB, one with FDNB but no sample. These were left in the dark at 65 °C for 45 minutes. 1 µl samples were taken for visible spectroscopy using a Thermo scientific 'NanoDrop 2000' and absorbance readings were taken at 356 nm.

2.4.3 Circular dichroism to determine optical isomer excess

Samples were collected and sent off to be analysed using circular dichroism with a JASCO J-810 spectropolarimeter using a quartz cuvette with a 10 mm path length. Enantiomeric excess was determined by:

$$\frac{\left(1-\frac{A_{210}(Actual)}{A_{210}(expected)}\right)}{2}+\frac{A_{210}(Actual)}{A_{210}(expected)}$$

Negative peaks contained excess D glutamate, where no peak was present the D/L ratio was 50:50.

Chapter 3

Results

3.1 Production and purification of material

The aim of recording these yields was to determine how much PγGA could be produced and whether altering the culture conditions affected the efficiency of PγGA production. Dry weights were obtained after the initial ethanol precipitation (crude product) and after purification by reprecipitation and diafiltration (purified product). The rationale for measuring dry weights twice was in case one culturing method produced a purer product but contained less mass initially (crude product - after the first precipitation) due to fewer impurities.

3.1.1 Amount of crude product produced

The amount of crude product initially precipitated in ethanol is shown in Figure 13. A meanamount of 17.9 g dm^{-3} crude product was obtained and quantities ranged from 14.00 to 22.16 g dm^{-3}. Varying the culture conditions by addition of NaCl or Manganese did not affect the yield of the crude product (ANOVA, p = 0.058).

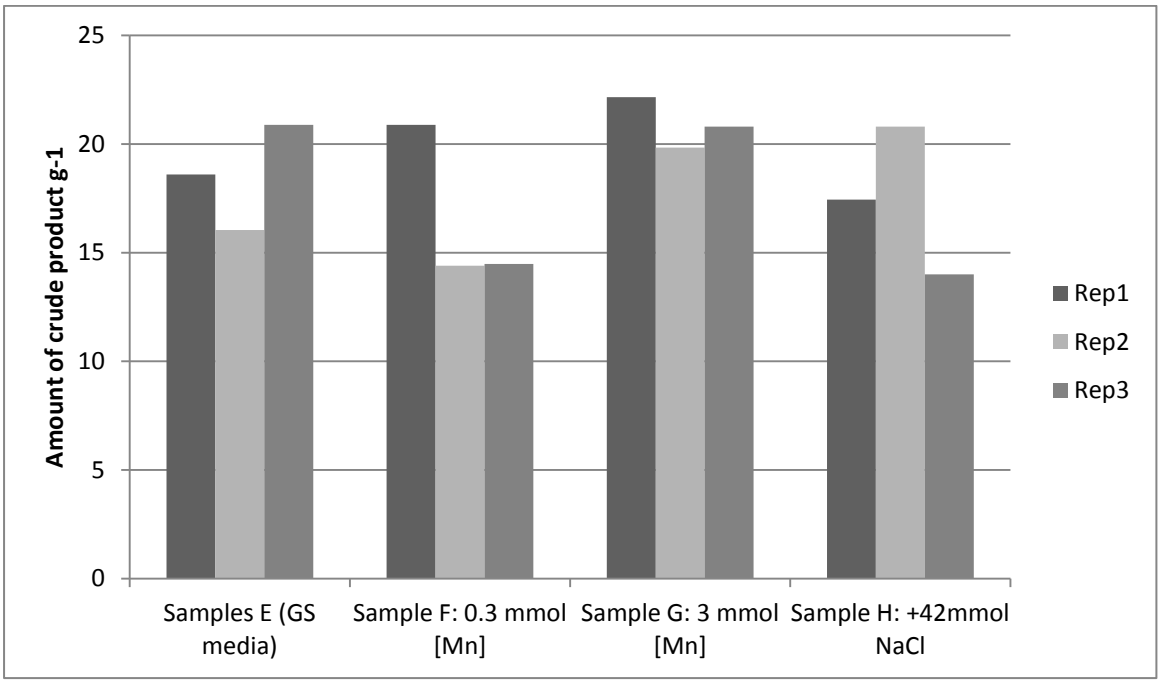

Figure 13: The amount of crude product obtained for each experiment.

Amount of purified product obtained

The quantity of sample obtained after subsequent reprecipitation and diafiltration ranged between 0.4% and 27.2%. A 2 tailed t-test showed less material was recovered when the copper precipitation method was used compared to the ethanol precipitation method ($p=6.6. \times 10^{-3}$). Figure 14 shows that out of all the samples, the mean amount of recovered sample was ~15% for the ethanol method and 8% for the copper method.

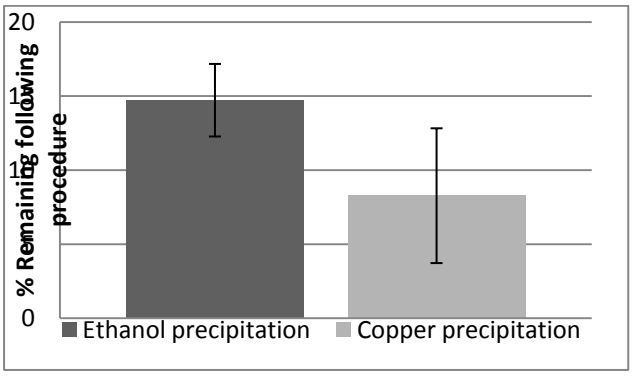

Figure 14: % Yield (w/w) following two methods of purification, stated in the text. Standard error is shown and significance was calculated with a Student's T test.

Figure 15 shows the predicted amount of product obtained from a 1 dm^{-3} culture flask after either purification method has been used. This was created by multiplying the quantity of sample obtained after the first ethanol precipitation for each biological replicate and the percentage obtained after purification. The mean for each culture condition was determined and analysed using ANOVA which showed no statistical significance between the overall yield in either of the four groups. ($F=1.338$, $p = 0.329$ for the ethanol reprecipitation method and $F= 1.09$, $p=0.407$ for the Cu^{2+} method). Therefore addition of42 mmol of NaCl or the presence/absence of Mn^{2+} does not affect the overall yield of purified or crude product when determined by dry weight.

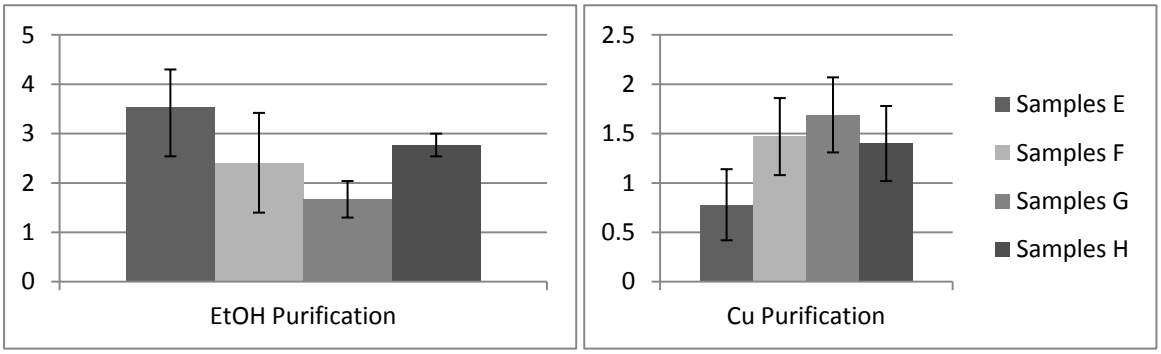

Figure 15: Mean predicted quantities of polymer obtained by multiplying the crude yield by the percentage obtained after each purification method. Error bars show standard error.

Table 4 shows the raw data for each purification attempt. No data was obtained for the quantity of commercial polymer left following the ethanol precipitation method, since the diafiltration bag split repeatedly, despite multiple attempts. This did not occur when the copper method was used. Interestingly only 14% of the mass of the commercial product was recovered. Lost mass could have been due to salts that may have been filtered out, however the company reported that the purity was >96% by mass, suggesting that most of the polymer was lost during the copper precipitation purification process. This could have been during the precipitation step, because an insufficient amount of polymer precipitated or during the diafiltration step. The filter was designed to contain proteins >20kDa and the M_w of the commercial polymer was reported to be much greater than this (quoted >100 kDa). However, due to the highly charged polymer properties and perhaps due to the lack of a globular structure, the polymer may have been able to escape into the dialysate. If the latter explanation is true, it is likely that ultrafiltration may yield more purified product if polymers are dialysed at lower concentrations.

Sample	Crude Yield $dm^3 g^{-1}$	Percentage purified by ethanol (initial weight/end weight)	Percentage purified by Cu^{2+} (initial weight/end weight)
Commercial	ND	ND	14
E1	18.60	13.17	5
E2	16.04	19.67	8.2
E3	20.88	23.96	0.4
F1	14.40	14.02	15
F2	14.48	6.20	10
F3	15.92	27.18	5.0
G1	22.16	10.63	11
G2	19.84	8.021	7.0
G3	20.8	5.14	6.0
H1	17.44	13.51	10
H2	20.80	15.19	3.1
H3	14.00	20.03	13

Table 4: Yields of product after production and after each method of purification as specified in the literature

Characterisation

The purpose of the following experiments was to determine the chemical identity of the crude product. It was also important to know if PγGA was produced by the bacterial species and if so how much of the sample was PγGA. The chemical identity of material that was not PγGA was also important to determine, since knowledge of this may lead to the development of more effective purification methods.

3.2 Fourier Transform Infrared Spectroscopy

The purpose of this experiment was to determine whether the functional groups present in our sample were the same as the sample which had been commercially supplied. After obtaining the NMR spectrum for our commercial sample (see following section) we were confident that it contained very pure PγGA. Therefore this spectrum was used as a reference. If the entire spectra of samples were different, it might indicate that the sample contained a different molecule, with perhaps very little or heavily modified PγGA. The presence of additional peaks in IR spectra of our samples may indicate properties of impurities and may help identify the functional groups of these impurities.

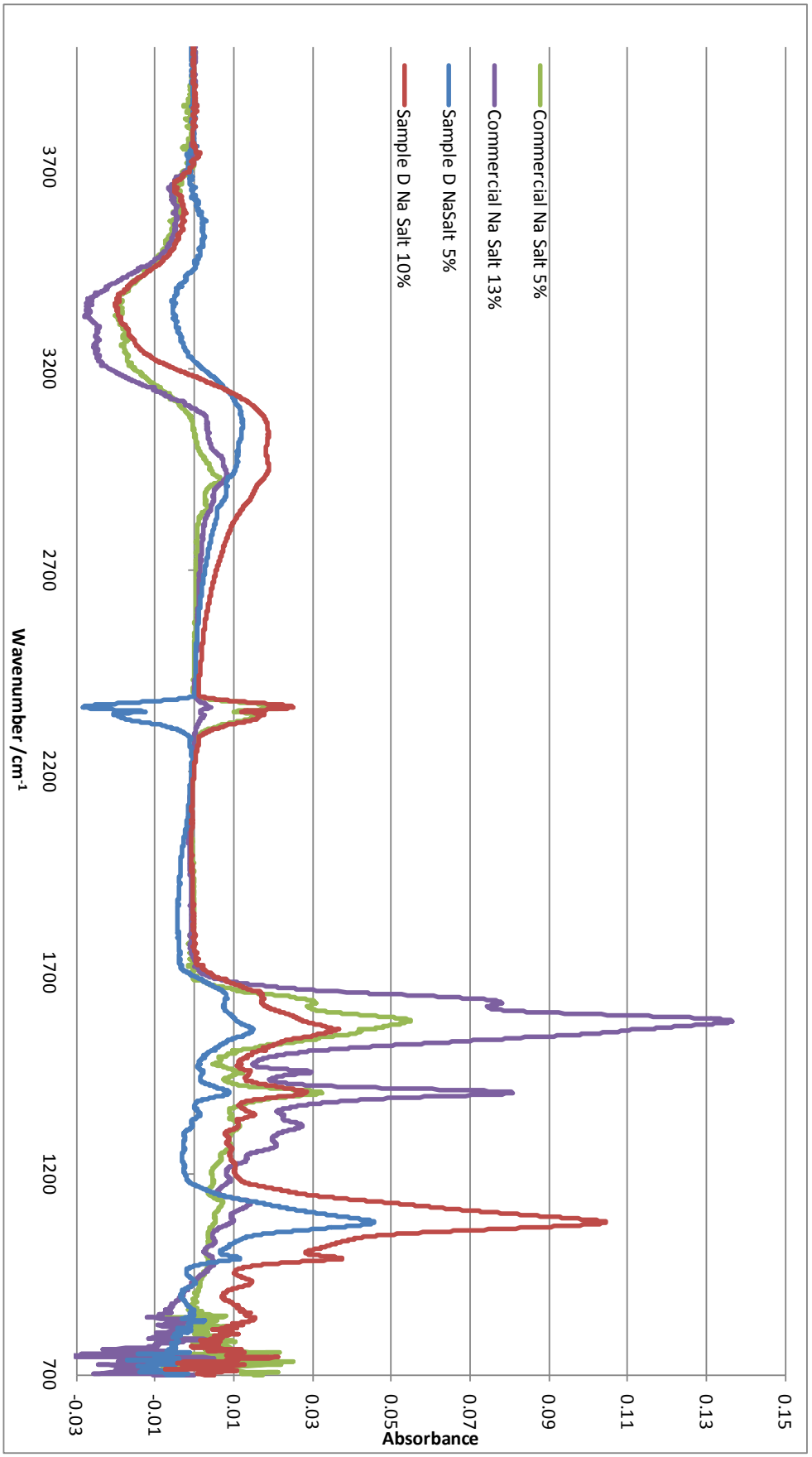

Figure 16: ATR collected FTIR spectrum of commercial PγGA and crude product from sample D. Concentrations are in wt/v

Peaks at 2400 cm^{-1}represent differences in carbon dioxide concentration (due to atmospheric conditions) and are not relevant to either sample. There are 5 main peaks in the commercial sample, which are outlined in table 5. These peaks were present in the crude product, but had shifted by up to 30 cm^{-1}. The peaks had a much greater absorbance in the commercial sample despite being of similar concentrations (compare the green – commercial 5% to purple – sample 5%).

Additional peaks from the crude product were observed at 1080 cm^{-1}.This peak is corresponds to C-O or C-N stretches in organic molecules.

Table 5: Peaks observed in ATR solution for commercial and non commercial samples.

Commercial	Sample D	
1630	1650	Amide C=O Stretch
1580	1550	Carboxylate C=O
1450	1455	Methylene
1400	1400	Alkane scissoring
1350		Carboxylic acid C=O
	1320	Carboxylic acid C=O
	1080	C-O or C-N stretch

3.3 Nuclear Magnetic Resonance

3.3.1 ^{1}H Spectra of Commercial Product

Figure 17 shows the ^{1}H spectrum for the commercial sample (sample B - sodium salt). The chemical structure of PγGA on the left is labelled with the protons α, β and γ, corresponding to the carbon atom they are attached to. The predicted ^{1}H NMR spectrum can be determined from the structure using the following rationale:

There should be three main peaks or sets of peaks. The β protons are likely to have the least chemical shift since they are furthest from electron withdrawing groups (EWGs). The α proton will have the greatest chemical shift since it is between 2 EWGs, a carboxyl and a secondary amine. The

integration trace should show that the number of βH=γH and the number of αH = βH/2 or γH/2, since there are half as many α protons as there are β and γ protons.

Hypothetically the splitting pattern should be as follows: The α proton is adjacent to 2 equivalent protons, therefore it should be split into a triplet. The β protons are adjacent to 2 equivalent γ protons and the α proton, therefore the signal should be split into a doublet of triplets. The γ proton is adjacent to 2 equivalent β protons so should be split into a triplet.

Since the secondary amine has a free pair of non-bonded electrons, the proton attached in the sample is readily exchanged with deuterium nuclei in solution and therefore may not appear in the spectrum.

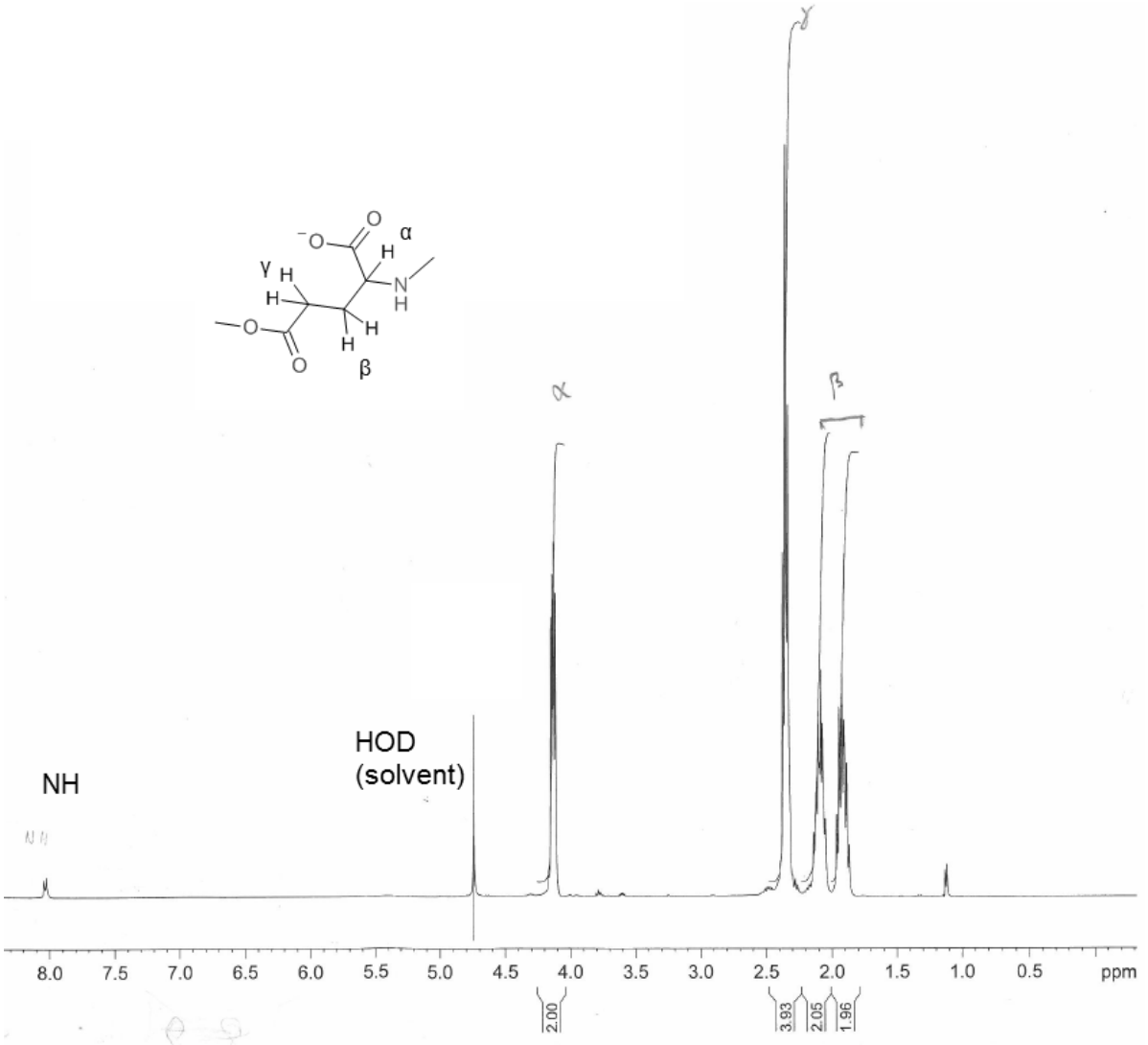

Figure 17: Obtained ^{1}H NMR spectra obtained from the commercial sample on a 400 MHz instrument. Note N-H isn't integrated as it is exchanged with deuterium in the solvent, therefore resonance at this frequency decreases with time.

Spectra of commercial product: ^{1}H NMR (400MHz, D_2O) δ 8.05 (d, J = 8 Hz), 4.13 (dt, J = 4.5 Hz, 1H), 2.35 (t, J = 8.3 Hz, 2H), 2.05 - 2.14 (m, 1H), 1.92 (sex, J = 8 Hz, 1H).

The actual spectrum obtained(summarised underneath figure 17) differs slightly from that predicted. Initially it appears there are 4 peaks. The 2 peaks with the lowest chemical shift have half the integration trace expected for 2 β protons, i.e. they have the integration trace for 1 proton each.

The implication of this is that both protons attached to the β carbon are in unique chemical environments making the position of β protons different. This can be explained by steric hindrance; there is free rotation around the Cγ-Cβ bond, but not around the Cβ-Cα bond. An example of different conformational isomer states is shown in figure 19. It is likely that the α-carboxyl or α-amide groups will be rotated away from the bulky γ-C. Since the rotation of this bond is fixed, both β-hydrogen nuclei experience the electronic effects of their neighbours. The nuclei closer to electronegative groups has a more distorted electron cloud and is observed as having a greater chemical shift on the spectra.

The ^{1}H spectra obtained here are similar to published spectra of PγGA(91). Their spectra are shown in figure 18.

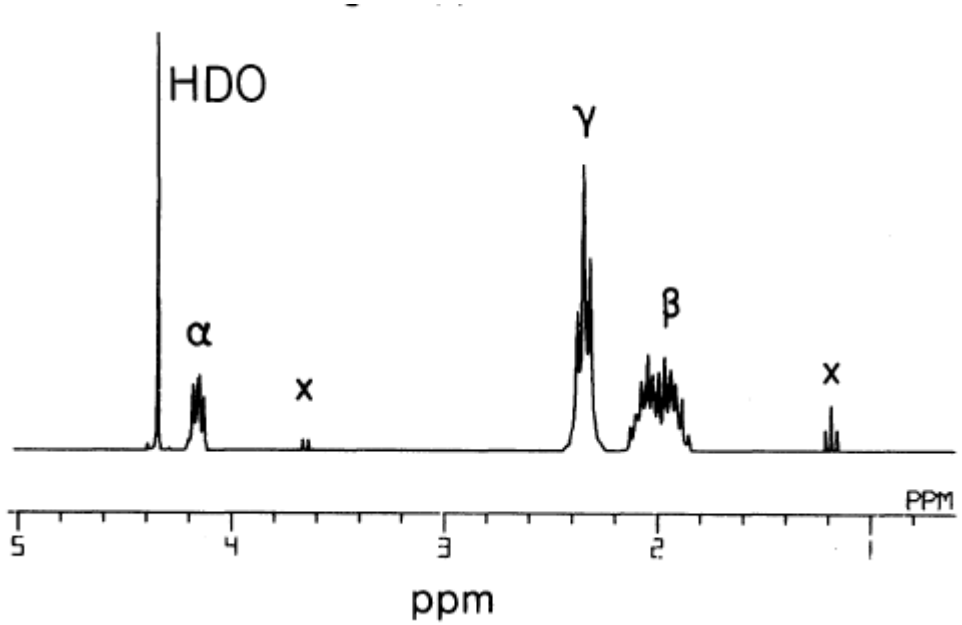

Figure 18: Published ^{1}H spectra for PγGA from Ikichi et al.(91), x denotes impurities

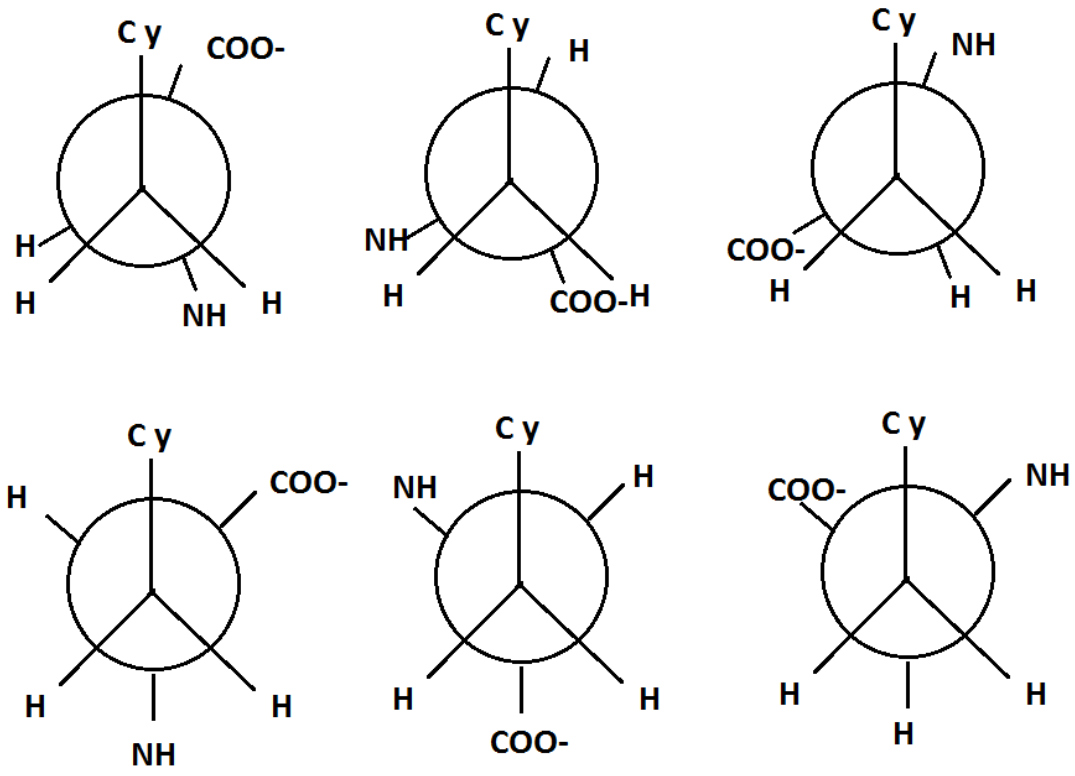

Figure 19: Conformational isomers (or rotamers) of L-PgGA. The β-carbon is in front and the α-carbon is behind.

3.3.1 ^{1}H spectra of samples before purification

Sample D

The spectrum for sample D (no additional NaCl or Mn^{2+}) is shown if figure 20. Whilst the peaks are harder to interpret in this spectra due to more overlapping peaks from impurities, particularly at chemical shifts greater than 3.0, the peaks corresponding to the β and γ protons are more clearly seen. There is a clear triplet at 2.35 ppm corresponding to the γ protons and a broad collection of peaks between 1.9 and 2.15 ppm with an equal integration trace to that of the triplet at 2.35 ppm.

Whilst some small peaks are seen peripherally to those correlating to the β and γ carbons, the smooth integration trace indicates that nearly all of the signal between 1.95 and 2.5 ppm is from the glutamyl protons. Since this signal corresponds to 4 of 5 protons per glutamyl residue and has an integration trace of 10 arbitrary units, 2 further arbitrary units of signal belong to protons in PγGA in the region of higher chemical shift. The peak of the αH is difficult to see amongst the peaks of the

impurity(ies). However this region of the spectrum has an integration trace of 19.27. Therefore the total integration trace for the whole sample is 29.27. Obtaining the fraction of the integration for H-glutamyl to the total sample, gives the proportion of protons that belong to glutamyl units.(12/29.27) or ~41% of protons in this sample are likely to be part of PγGA.

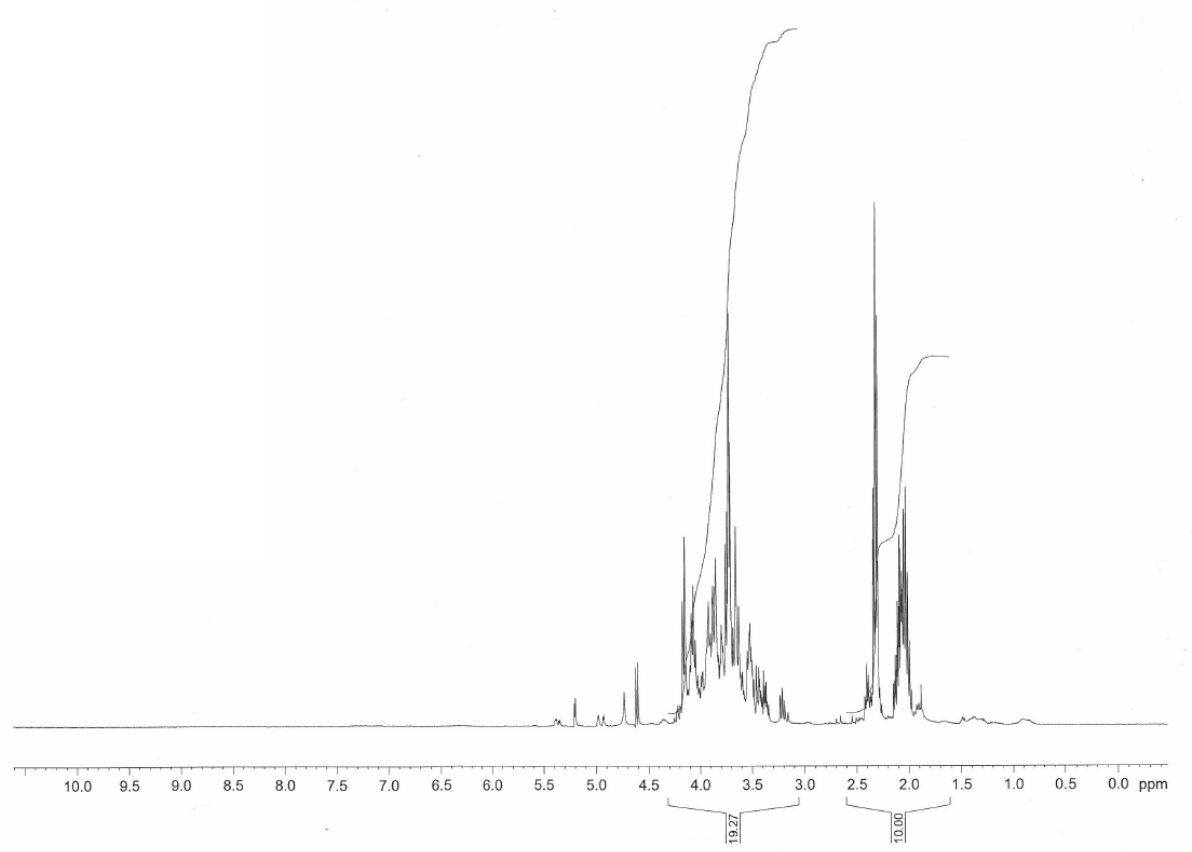

Figure 20: 1H NMR spectrum for sample D before purification.
Spectra of D: ^{1}H NMR (400 MHz, D_2O) δδ 4.36 - 3.15 (comp, 2.6H), 2.32 (t J = 7.1 Hz), 2.15 - 1.86 (m, 2H).

The remaining 59% of the protons were in the spectral region of 3.4 – 4 ppm and may belong to amines, alcohols, alkene or ether groups.

Sample E

The spectrum for sample E, which was grown under the same conditions as sample D is shown in figure 21. Using the same method as above, it appears that ~33% of protons in the spectra belong to PγGA. The other peaks are in similar areas of chemical shift as the impurities noted in sample D.

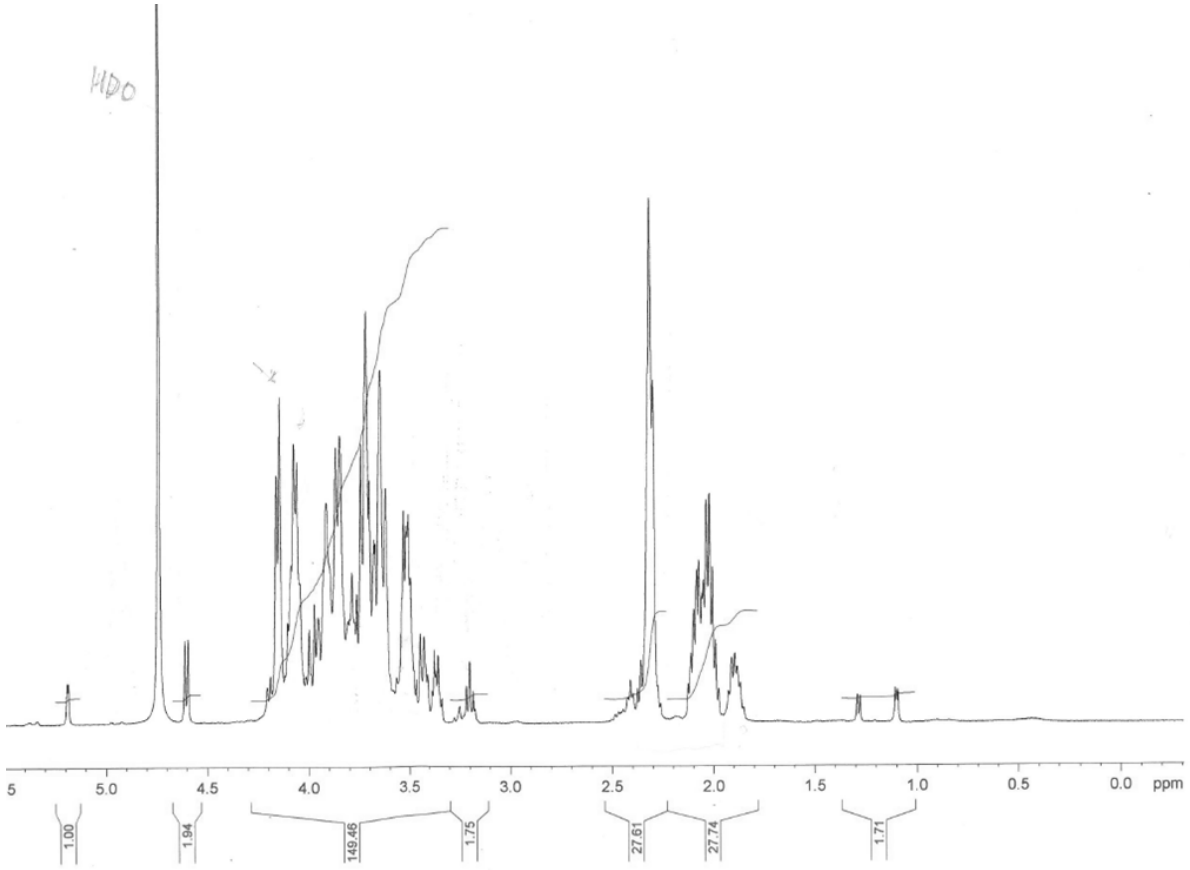

Figure 21a: 1H NMR spectra for sample E before purification, which was grown in the same conditions as sample D. Spectra of E1: ^{1}H NMR (400 MHz, D_2O) δ 5.19 (d, J = 2.0, 0.07 H), 4.61 (d, J = 6.7 0.14 H), 4.24 - 3.32 (comp 11.1 H), 2.33 (comp, 2H), 2.0 (comp, 2H)

Samples F and G

Samples F and G, which were grown with manganese were put into the NMR machine, but decent spectra were not obtained because shimming could not induce magnetic homogeneity of the sample. This was likely due to residual Mn^{n+} ions. Whilst an integration trace was not obtained for either sample, the position of the peaks appears to be with roughly the same chemical shift as the other samples. No additional peaks with greater chemical shifts were noted.

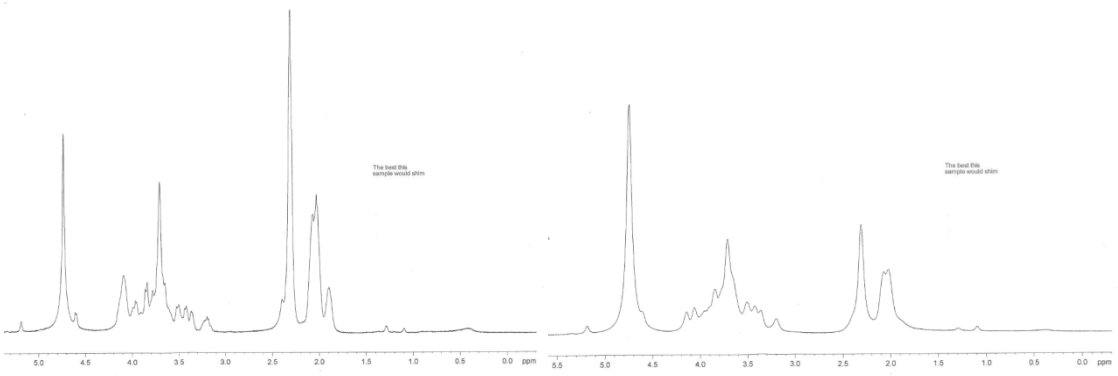

Figure 21b: Samples F (left) and G (right), where samples were grown with 0.05 and 0.5 g dm^{-3} $MnSO_4$. Spectra of F1: ^1H NMR (400 MHz, D_2O) (integration not included as sample poorly shimmed) 5.19, 4.60, 4.09, 3.97, 3.84, 3.72, 3.52, 3.43, 3.31, 2.32, 2.06, 1.89.
Spectra of G1: ^1H NMR (400 MHz, D_2O) (integration not included as sample poorly shimmed) 5.19, 4.60, 4.15, 4.09, 3.85, 3.72, 3.52, 3.46, 3.36, 3.20, 2.32, 2.09, 2.03.

Sample H

The spectrum for sample H, which was grown with a slightly higher NaCl concentration is shown in figure 22. Using the method outlined above, it shows that 48% of protons belong to PγGA.

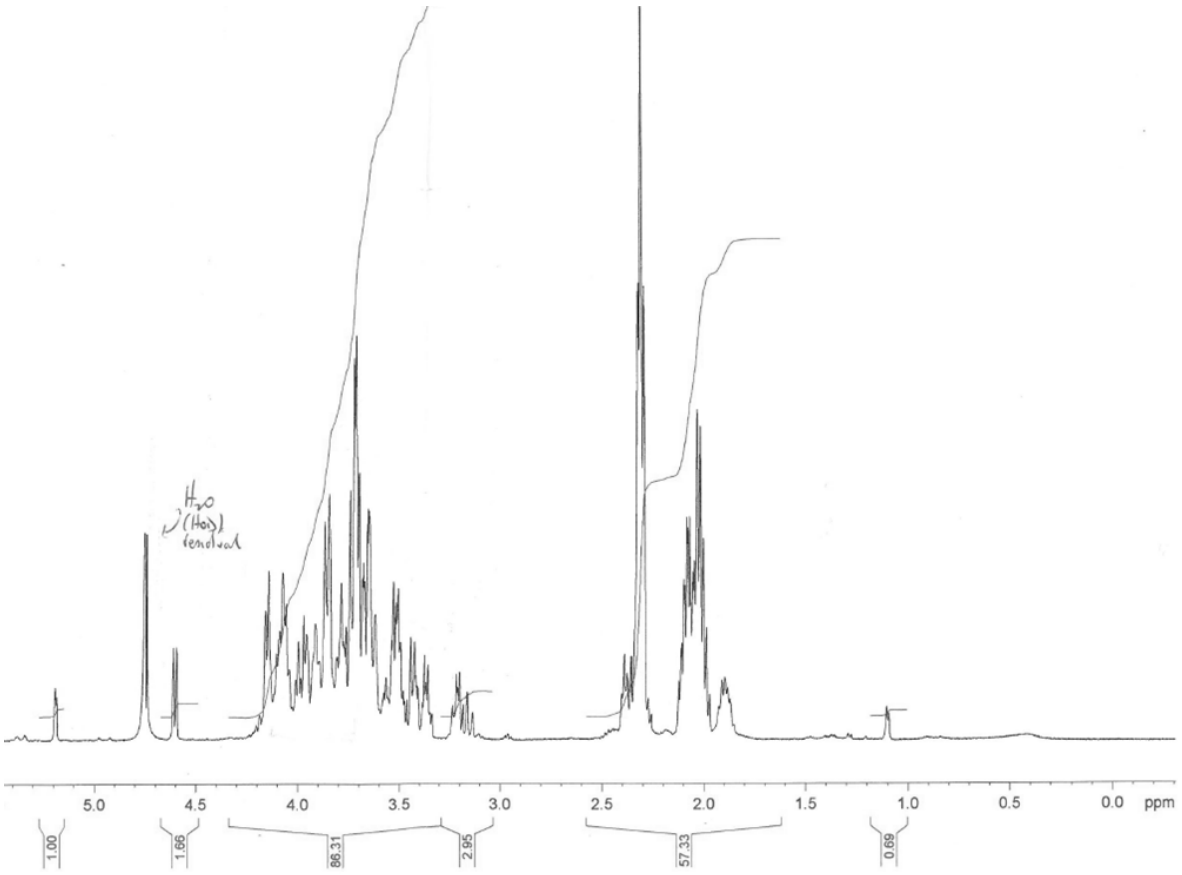

Figure 22: Spectra of H1: 1H NMR (400 MHz, D2O) δ 5.18 (d, J = 2.0, 0.07 H), 4.61 (d, J = 6.7 0.11 H), 4.21 - 3.1 (comp 6.2 H), 2.40 - 2.22 (comp, 2H), 2.14 - 1.83 (comp, 2H).

^{1}H NMR spectra for samples after purification

After purification using the ethanol method, three biological replicates for samples F, G and H were analysed using ^{1}H NMR. Purified sample E was not analysed since it was lost in transit and samples purified using the copper method were not analysed, since the samples had a blue tinge, indicating that they contained a significant amount of copper and this would have made the samples difficult to shim.

Spectra from F1, G1 and H1 are shown in figure 23 to 25. Spectra obtained from purified F and G do not show the spectra in high enough resolution to be able to see the splitting patterns for the β and γ protons. This suggests that Mn^{2+} was still present in the sample, despite washing the sample in buffered solution. It is likely that Mn^{2+} binds to the sample with high affinity due to its divalent nature.

All spectra differ from that in figure 17 (the commercial product ^{1}H NMR spectra) and therefore suggest that despite reprecipitation and dialysis pure PγGA was not obtained.

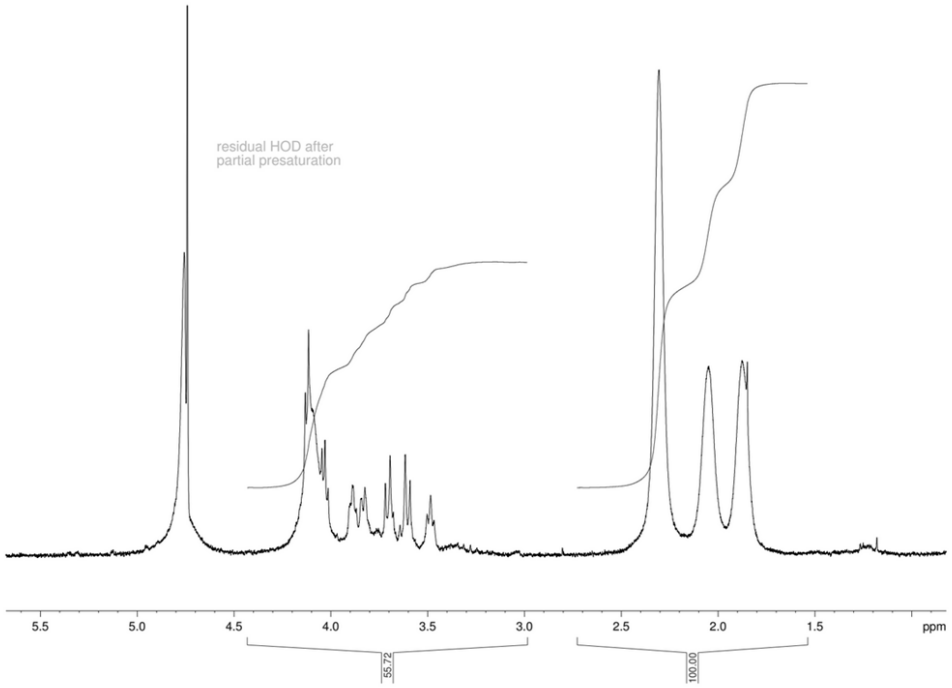

Figure 23: 1H NMR spectra for sample F1
Spectra of F1: ^{1}H NMR (400 MHz, D_2O) δ4.26 - 4.00 (comp 1.2 H), 3.95 - 3.78 (comp, 0.42 H), 3.70 (dd, $J_1$30.6, $J_2$9.8, 0.46 H), 3.49 (t, J = 8.3, 0.16 H), 2.31 (s, 2H), 2.05 (s, 1H), 1.87 (s, 1H).

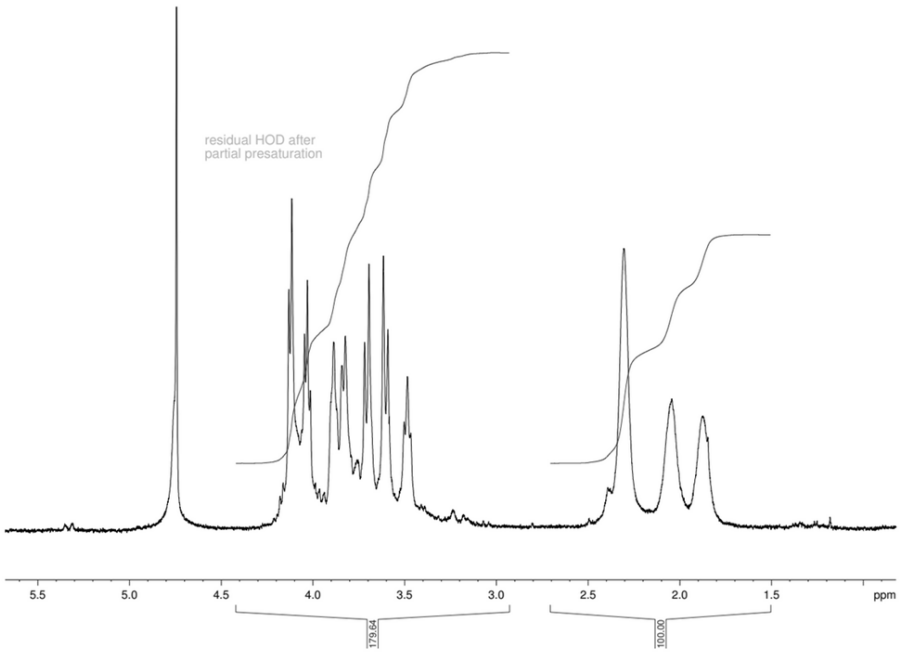

Figure 24: 1H NMR spectra for sample G1

Spectra of G1: ^{1}H NMR (400 MHz, D_2O) δ4.22 - 3.99 (comp, 2.19 H),3.93 - 3.78 (comp, 1.85 H), 3.67 (dd, J_1 = 34, J_2 = 9.0), 3.48 (t, J = 7.5, 1.01 H), 2.31 (s, 2H), 2.04 (s, 1H), 1.87 (s, 1 H)

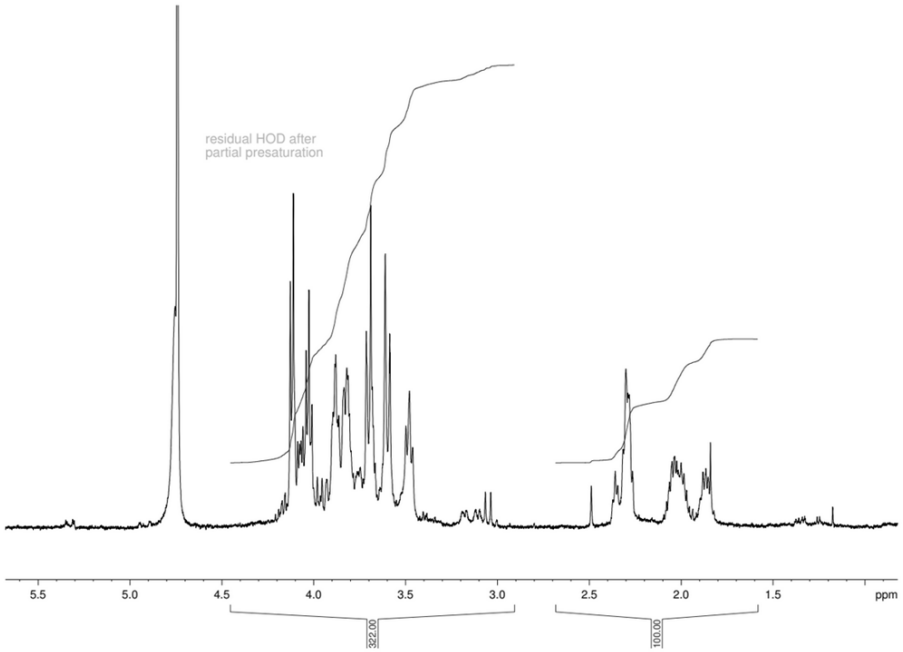

Figure 25: 1H NMR spectra for sample H1
Spectra of H1: ^{1}H NMR (400 MHz, D_2O) δ41.6 - 39.7 (comp 3.61 H), 3.92 - 3.8 (comp, 3.14 H), 3.68 (dd J_1 = 32, J_2 = 9.0, 3.91 H), 3.48 (t, J = 8, 1.38 H), 2.29 (comp, 2 H), 2.09 - 1.95 (m 1 H), 1.91 - 1.81 (m, 1H).

Using the method of calculating the percentage of protons predicted to be on PγGA via the integration traces, values of purity were obtained for each of three replicates for samples F, G and H and are displayed in table 6. The mean value of this relative measure of purity for products of each culture condition is displayed in figure 26 below. Perhaps surprisingly, it seems that the culture conditions significantly affect the γ-glutamyl proton fraction (ANOVA, p = 0.016) of samples that have been purified using the ethanol precipitation method. Purified product from samples which were prepared with 42 mmol NaCl added to the broth had a reduced proportion of PγGA compared to samples that contained no added NaCl, but a smaller molar quantity of $MnSO_4$.

Furthermore,purified samples that were prepared with less $MnSO_4$ added to the broth had a greater proportion of PγGA when compared with samples prepared with more $MnSO_4$.

Sample (Crude)	γ-glutamyl protons / total protons	Sample (Purified)	γ-glutamyl protons / total protons
A	0.4021	F1	0.7706
B	0.9940	F2	0.5687
D	0.4271	F3	0.8511
E1	0.3276	G1	0.4301
F1	ND	G2	0.5556
G1	ND	G3	0.5687
H1	0.4777	H1	0.2844
		H2	0.3647
		H3	0.4494

Table 6: Estimation of purity using integration traces from ^{1}H NMR. ND stands for no data since the samples wouldn't adequately shim.

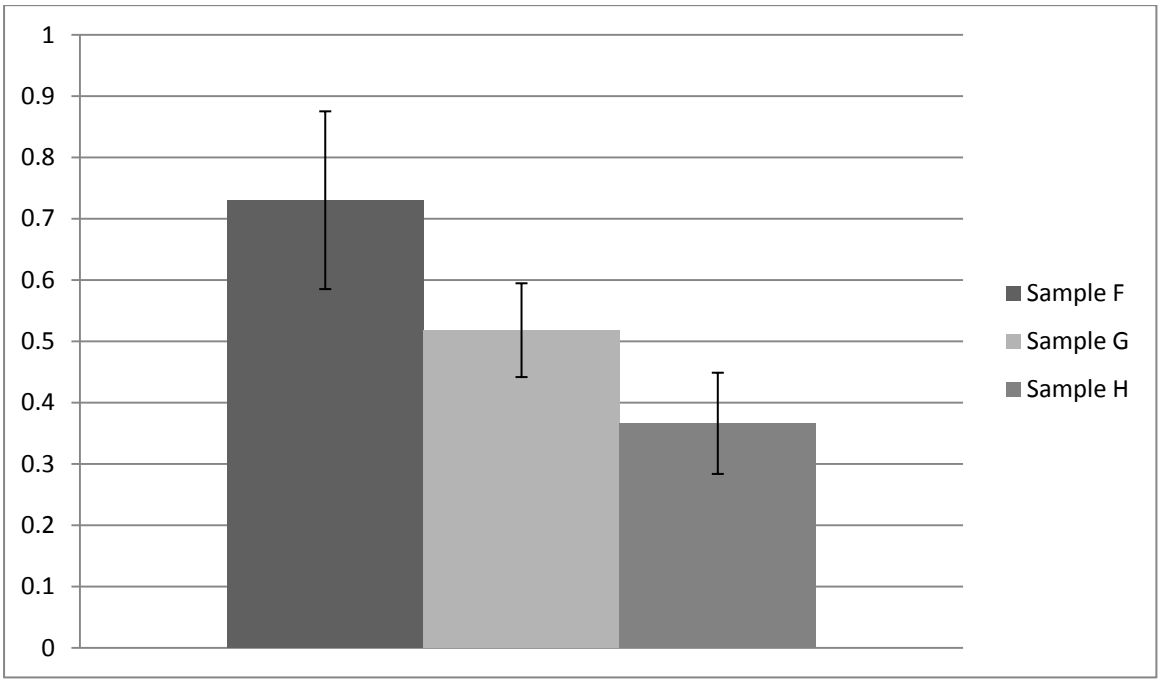

Figure 26: Effect of culture conditions on purity of ethanol purified sample. Sample F contained 300µmol dm^{-3} $MnSO_4$, sample G contained 3 mmol dm^{-3}$MnSO_4$, sample H contains 42 mmol dm^{-3} NaCl. Error bars show 1 SD.

If the impurity is a separate molecule from PγGA (i.e. it is not attached to PγGA), then a higher ionic concentration (or more NaCl) during culture may influence the properties of the impurity to precipitate more readily in ethanol, or be less permeable to dialysis tubing. This may be explained by increasing the size of the impure molecule relative to PγGA. If the impurity and PγGA are attached, then more NaCl may make the bacteria attach more of the impurity to PγGA.

Another explanation, which would support previous experiments published in the literature, would be that Mn^{2+} increases the production of PγGA in *B. subtillis* natto, as it does in *B. licheniformis.*Similarly, larger concentrations of Mn^{2+} (>615 µmol from Cromwick (23), 2mmol in sample G) in sample G are greater than the optimal Mn^{2+} concentration for optimal PγGA production. However excess Mn^{2+} concentration may be better than the absence of Mn^{2+} which is the case in sample H.

Also, addition of NaCl to sample H may have reduced the size of PγGA, therefore increasing the proportion of PγGA molecules that were less than the MWCO of the dialysis tubing. This would have meant proportionally more of sample H would have been lost during this process.

^{1}H NMR spectrum of an isolated impurity

During the first attempt of purifying PγGA from sample D (no additional NaCl or $MnSO_4$), a dialysis bag with an unknown molecular weight cut off (MWCO) was used. Instead of yielding a compound with a ^{1}H NMR spectrum similar to the commercial product, the spectrum obtained is that shown in figure 27. The peaks that correspond to protons on commercial PγGA are markedly reduced and the majority of signal is found in the region of 3.5 – 4.2 ppm, which was observed and labelled as an impurity in spectra of crude and purified products. Therefore it is believed that the method used to obtain purified PγGA actually obtained a purified form of the impurity we were trying to eradicate. Since dialysis membranes retain larger molecules,this finding may suggest that the impurity is the larger molecule. Furthermore, a purer PγGA product may be extractable from the dialysate of this experiment.

The spectrum in figure 27suggests that <6% of protons belong to PγGA.The remaining molecule(s)shows the following spectral features. The chemical shifts of the spectra are suggestive of protons connected to alcohol groups (if true protons on the hydroxyl groups are replaced with deuterium in the solvent and not seen) and therefore are likely to show the impurity is

carbohydrate, however the structure of the impurity was not determined from the spectrum. Beneath the description of the spectrum is a list of possible predicted functional groups that could cause peaks with similar splitting patterns with that chemical shift.

Since the integration trace for each peak divided by the overall integration trace between 3.2 and 4.3 ppm can be divided into similar fractions (x/14) it is likely that the impurity consists of a single molecule and not a group of separate molecules. From the table, since the total integration trace adds up to 14H, the molecule must have a multiple of 7 protons bonded to carbon in addition to any other bound to nitrogen or oxygen.

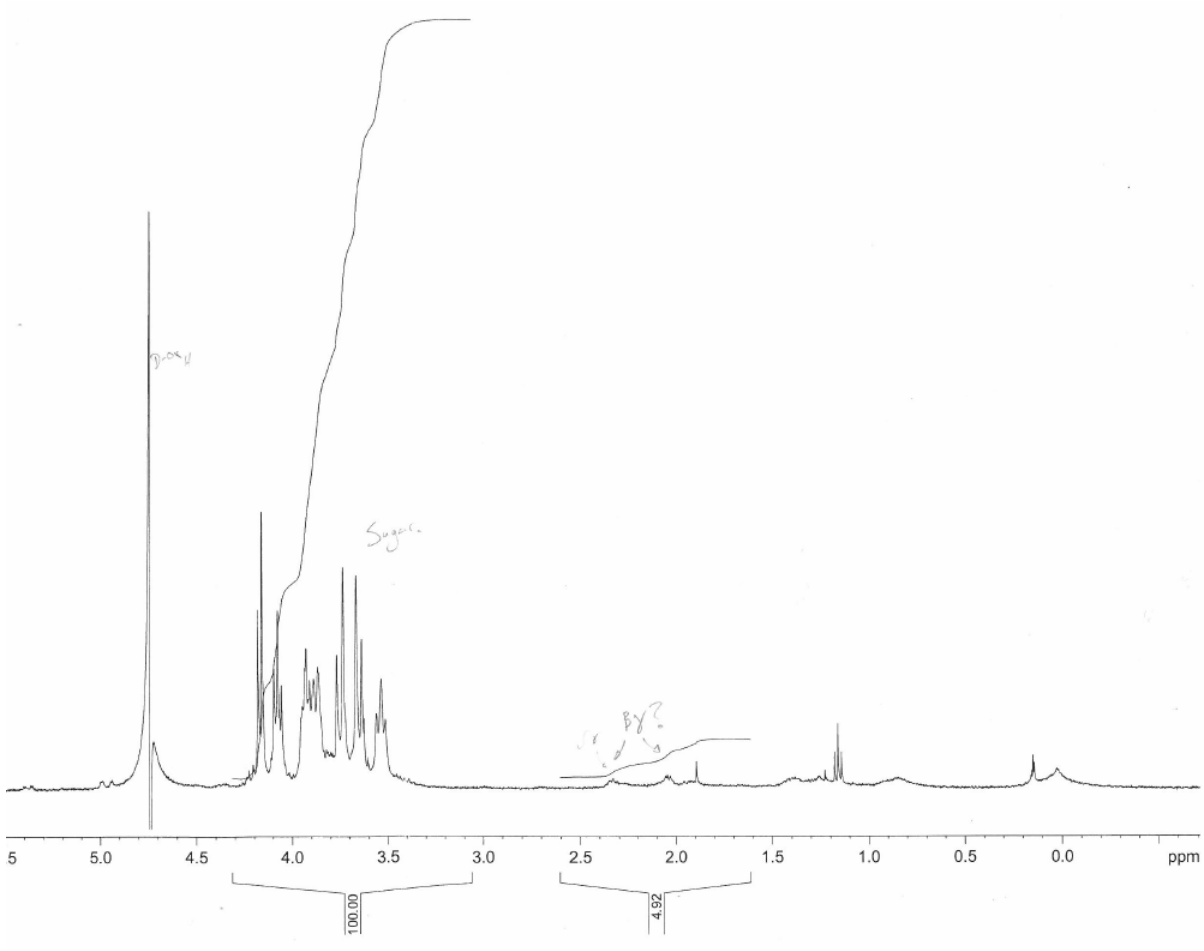

Figure 27: 1H NMR spectra of an impurity from sample D obtained by dialysis using a filter of unknown MWCO. ^{1}H NMR (400 MHz, D_2O) δ 4.18 (s, 1H), 4.16 (s, 1H), (4.08 (t, J = 17.6, 2H), 3.98 - 3.93 (comp 4H), 3.70 (dd, J_1 = 12 Hz, J_2 = 2 Hz, 4H), 3.54 (t, J = 9.6, 2H).

<table>
<tr><td>Chemical shift (δ) ppm</td><td></td><td>Splitting (J) Hz^{-1}</td><td></td><td>Integration</td><td></td><td>Possible identity of species</td><td></td></tr>
<tr><td>4.18</td><td rowspan="2">4.17</td><td>s</td><td rowspan="2">D 2</td><td>1H</td><td rowspan="2">2H</td><td> 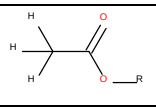 Or below</td><td rowspan="2"> 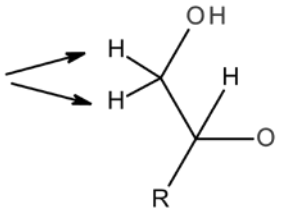
However if this is a doublet it should neighbour H δ3.7 due to the splitting pattern. Due to the splitting pattern of this peak there could only be one proton for this trace.</td></tr>
<tr><td>4.16</td><td>s</td><td>1H</td><td> 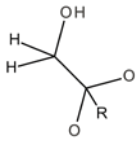 Or above</td></tr>
<tr><td colspan="2">4.08</td><td colspan="2">t
17.6</td><td colspan="2">2H</td><td colspan="2"> 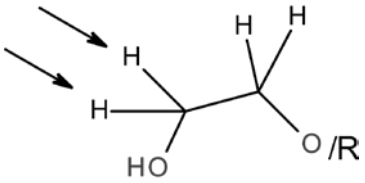 </td></tr>
<tr><td colspan="2">3.98-3.93</td><td colspan="2">Complex</td><td colspan="2">4H</td><td colspan="2">???</td></tr>
<tr><td colspan="2">3.70</td><td colspan="2">dd
J_1:12
J_2: 2</td><td colspan="2">4H</td><td colspan="2"> 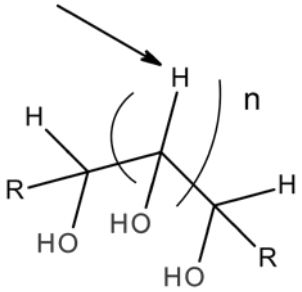 </td></tr>
<tr><td colspan="2">3.54</td><td colspan="2">t
9.6</td><td colspan="2">2H</td><td colspan="2"> 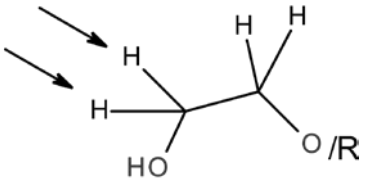 </td></tr>
</table>

3.3.5 ^{13}C NMR

^{13}C NMR spectra of a commercial sample

The predicted 13C NMR spectra should contain 5 peaks since there are 5 different chemical environments the carbons can be in. Two of the carbon atoms with 2 hydrogen atoms attached

should have a chemical shift between 15-50 ppm. The carbon with 1 attached hydrogen atom should have a shift between 20-60 ppm. The carbon that forms the amide bond should have a chemical shift of 165-175 ppm and the carbonyl carbon should have a chemical shift of 175-185 ppm. Figure 28 shows the spectra obtained for a commercial sample. There are 5 peaks which fall into the chemical shifts areas which were predicted. The spectra is similar to that shown in the literature(92), which is shown in figure 29.

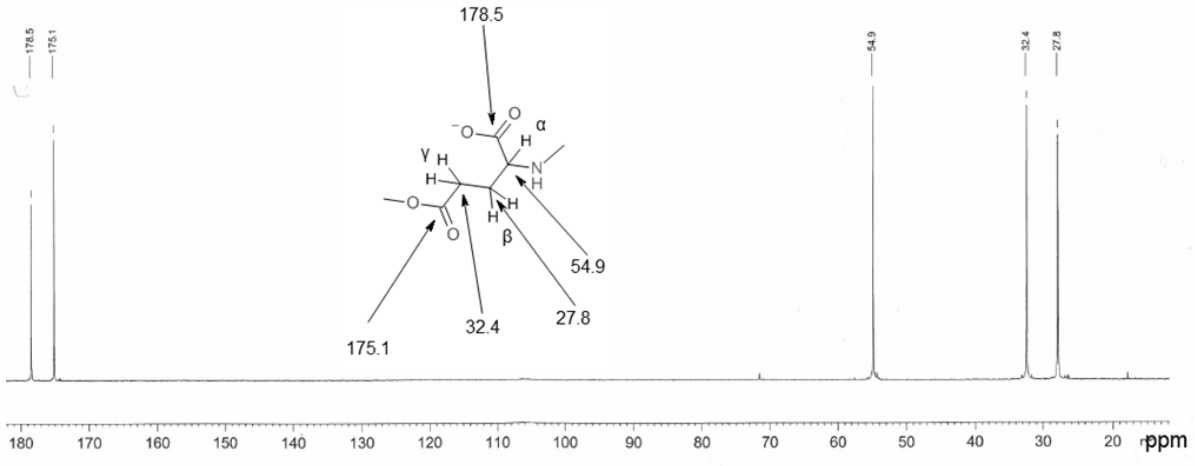

Figure 28: ^{13}C spectra obtained from commercial sample on a 400 MHz instrument. ^{13}C NMR (400MHz, D_2O) δ 178.5, 175.1, 54.9, 32.4, 27.8.

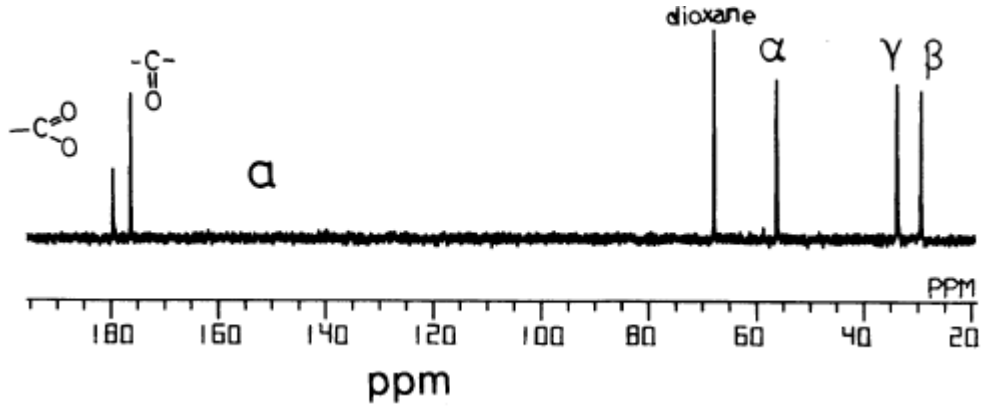

Figure 29: 13C NMR spectra published in the literature from Hikichi et al. (92)

13 C spectra of samples before purification

The decoupled ^{13}C spectrum of only one sample was obtained since it took 10 hours to run. The spectrum shows peaks where they are expected and these are labelled on the spectrum. However, there are 47 peaks and therefore 42 which do not match the spectrum of commercial PγGA and are therefore not generated by carbon in glutamyl residues. Most of these peaks (a total of 27) lie between 60 and 80 ppm, which is typical of carbons linked to oxygen atoms, such as in hydroxyl groups found in carbohydrate.^{13}C NMR spectra values for the monosaccharide glucose and its isomers are shown in figure 31 for comparison.The 5 peaks that range from 80 – 150 could also be explained by the presence of alkene groups. The 3 peaks with chemical shift greater than 170 ppm that were not on the ^{13}C spectrum of commercial product must be from carboxylic acid groups. These could be part of PγGA if the molecular structure of the polymer places these carbon atoms in different but distinct chemical environments. These environments are likely to be caused by different cationic species in the sample. Ho et al published the ^{13}C spectra for PγGA with different counter ions and found the carbonyl peaks to vary by 3 ppm when sodium or potassium was the positive ion(4).

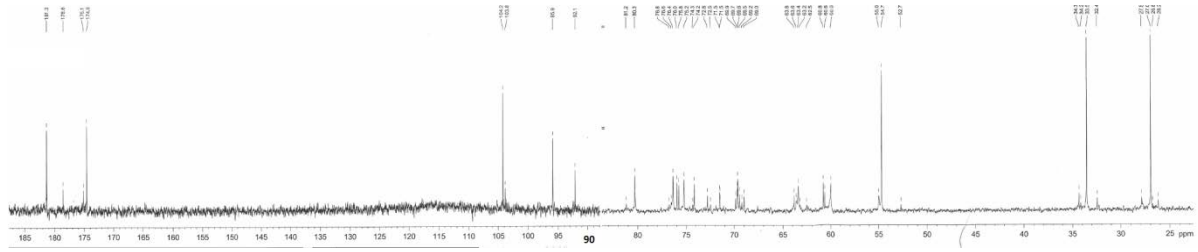

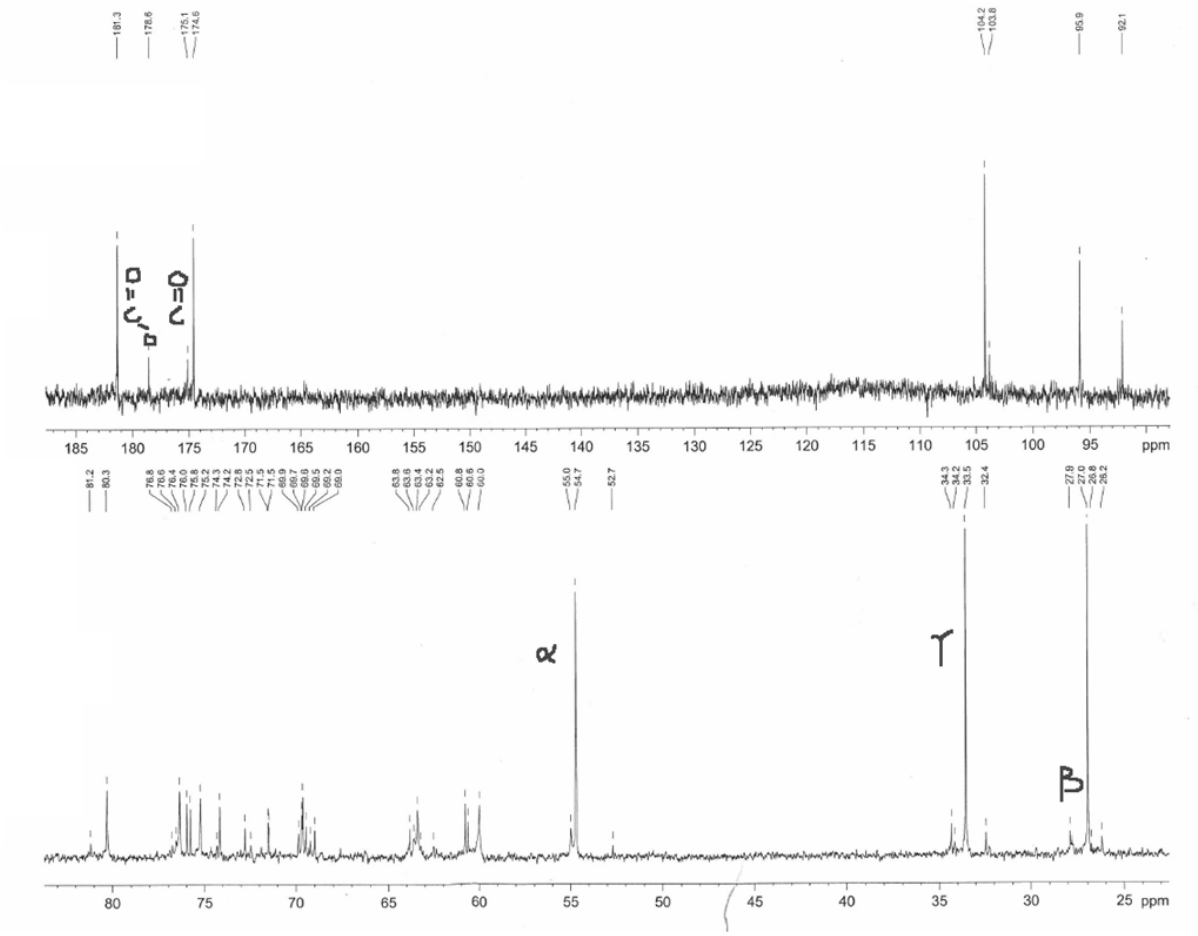

Figure 30: 13C Spectra for the crude product of sample D. Peaks which were present in the commercial sample and from the literature are labelled in red.

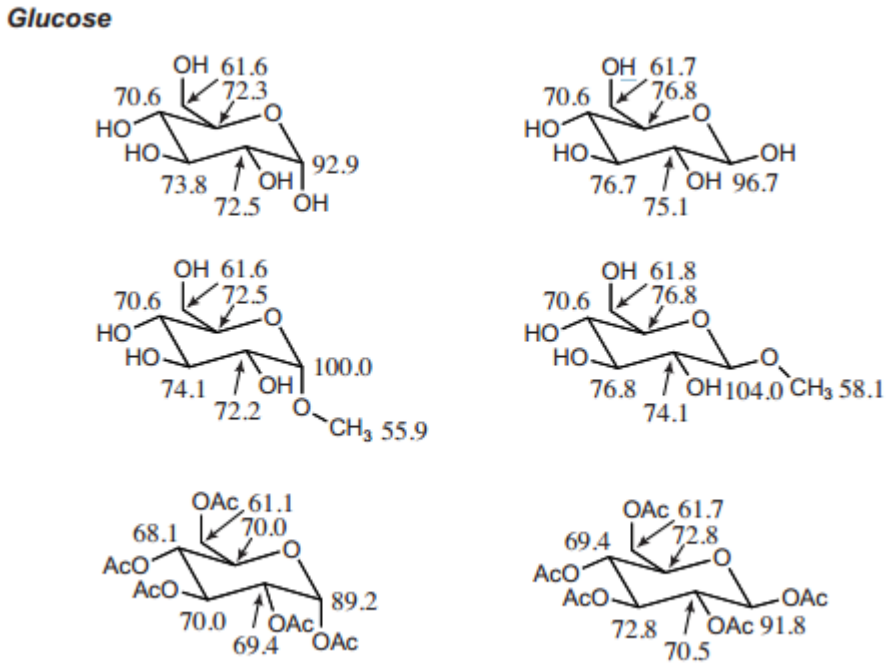

Figure 31: 13C NMR spectral peaks for glucose (top) including methylated (middle) and acetylated (bottom) derivatives. Taken from Erno et al. (89)

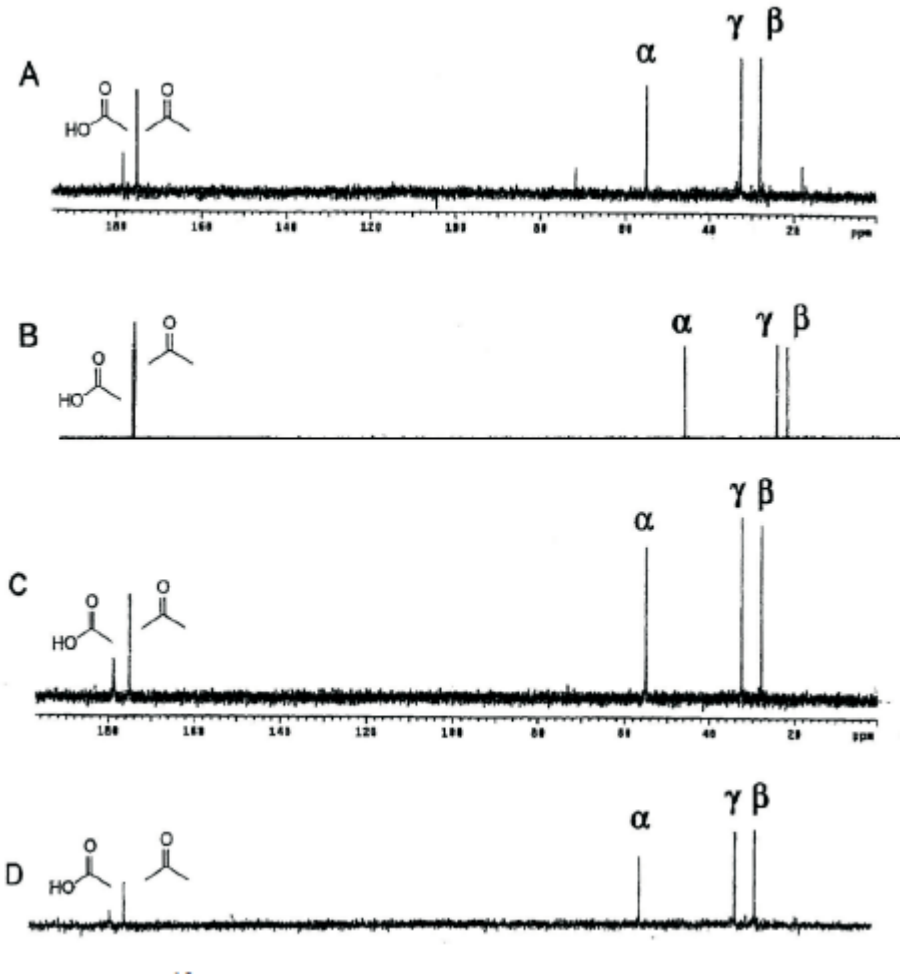

Figure 32: 13C NMR spectra for PγGA with different counter ions. A = K^+, B = Na^+, C = Ca^{2+}, D = Mg^{2+}.

3.4 Polysaccharide Analysis

The ^{1}H spectra for the molecule quoted in this section showed only protons that had a chemical shift of 3.4 - 4.3ppm (see figure 27), suggesting that all are located next to hydroxyl groups. Furthermore no peaks were observed for carbon atoms adjacent to amines or methyl groups, suggesting that amino and deoxy-sugars are not present in abundance. The purpose of the following experiments was to determine the form of carbohydrate monosaccharides and how they are linked together.

Alditol Acetate Derivative Analysis by Gas Chromatography

The gas spectra for alditol acetate derivatives of the sample are shown in figure 34, with alditol acetate derivatives of 4 known sugars (Rha = rhamnose, Ara = arabinose, Man = mannose, Gal = galactose) in the spectrum below.No peak was identified as identified as rhamnose, which is consistent with the ^{1}H NMR spectra for this material, since rhamnose is a deoxy-sugar and therefore would have produced peaks in the ^{1}H NMR spectra with a chemical shift of around 1 ppm.

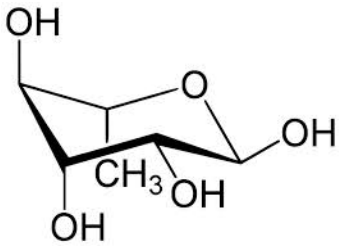

Figure 33: Chemical structure for rhamnose. If this molecule were present, the protons of the methyl group would have produced peaks with a chemical shift around 1 ppm.

Peak

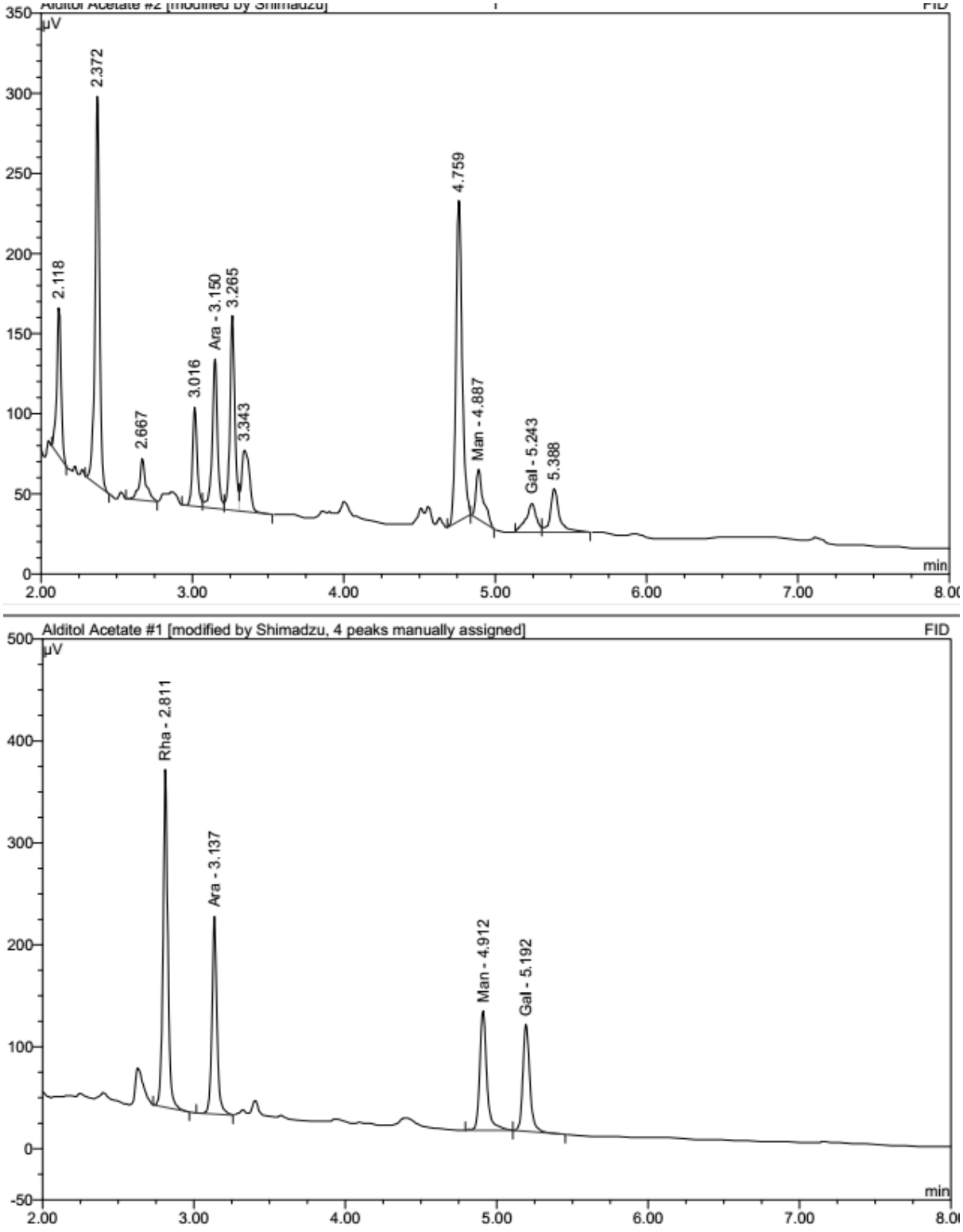

Figure 34: Chromatogram for the aliditol acetates derivatives of the experimental sample (replicate 1 - top) and prepared alidtol acetates of Rhamnose (Rha), Arabinose (Ara), Mannose (Man) and Galactose (Gal) (bottom)

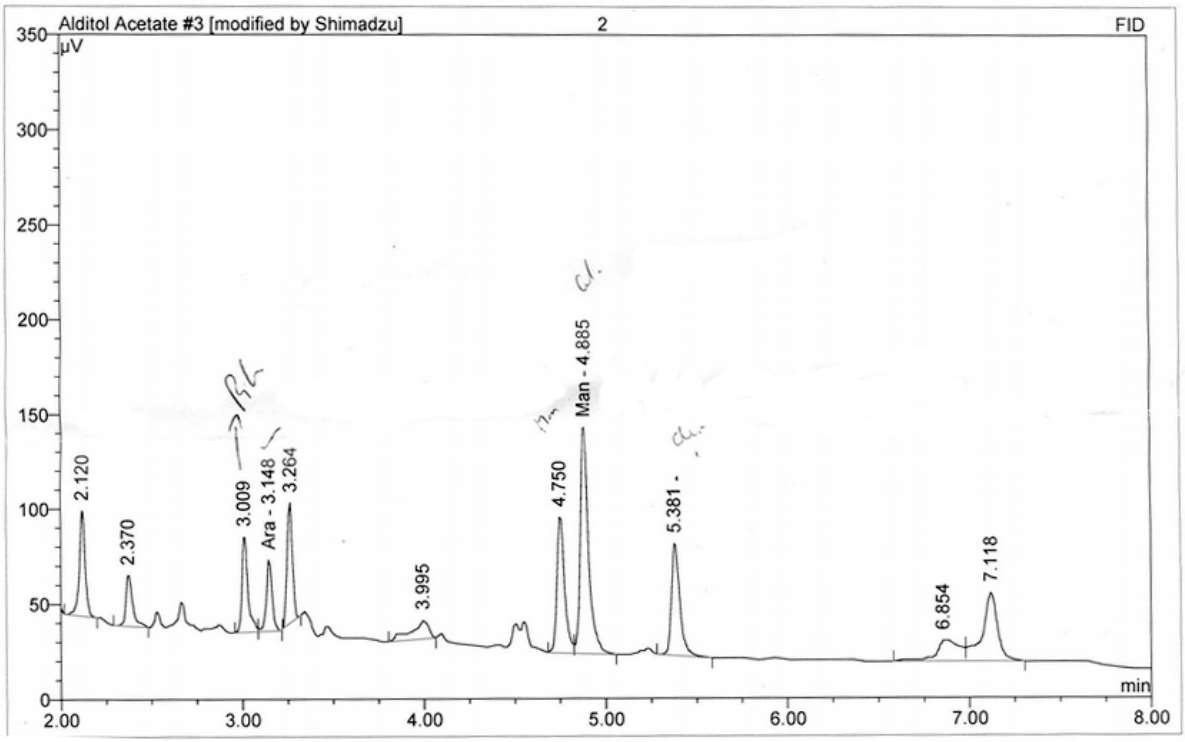

Figure 35: Replicate (2) chromatograph for the same sample.

Retention times were within 0.1 minute for galactose, mannose and arabinose. Additional peaks had retention times of 2.118 and 2.372, 3.016, 3.265, 3.343, 4.759 and 5.388. Previous work had shown that the peak at 3.016 and 4.759 may be ribose and glucose respectively.

Based on this knowledge and using the area under the curves (calculated by the GC-machine software), it is possible to predict the proportion of some of the monosacharides in the hydrolysed sample, which is shown in table 7. However, this shows that less than half of the sample was identified as monosaccharide.

Table 7: Proportion of alditol acetate derivatives in the gas chromatograph.

Sugar name	Proportion in hydrolysate 1	Proportion in hydrolysate 2	Mean
Ribose	7.0%	5.3	6.2
Arabinose	5.2%	9.4	7.3
Mannose	12.5%	23.8	18.2
Galactose	22.3%	4.5	13.4
Glucose	11.5	4.8	8.2
Unknown component	41.5%	52.2	46.9

The chromatographs are comparable, and have the same number of peaks with similar retention times. However, the relative areas under the curves vary between the two graphs, despite using the same sample and the method. On visual inspection of one product (replicate 1), the sample had developed a brown colouration after drying between subsequent additions of acetic acid. Perhaps this was caused by uneven over heating of the sample on the heating block. Therefore it is possible that some or more of this sample had oxidised. This may be why two of the peaks at 2.12 and 2.37 mins are much taller in the chromatograph for the first repeat experiment. It might also mean that the proportions of sugars obtained in the second replicate are closer to the actual composition of the sample. In light of this, if oxidation products were present in both samples then some of the peaks present in the gas chromatograph may not correspond to alditol acetate derivatives which corresponds to monosaccharides in the original sample. Therefore the actual number of monosaccharide units present in the sample may be less than the number of peaks in both chromatographs.

Whilst no papers were found for secreted exopolysaccharide of *B. Subtilliis* Natto, B subtillis species are known to produce the EPS Levan type 1 and 2. The former consists of β-2,6 linked D fructose,

whereas the latter consists of glucose – fructose chains(93). In the strain B. Subtillis FT-3 a polysaccharide composed of glucose, galactose, fucose, glucuronic acid and O-acetyl groups in a molar ratio of 2:2:1:1:1.5 has been reported(94). In retrospect it would have been wise to have included alditol acetate derivatives or fructose, glucose, fucose, galactose and glucuronic acid to the reference sample to determine whether they were present in the derived sample.

Linkage analysis using GC-MS

Gas chromatography separated the sample that had been prepared using the Hakomori method. The sample was believed to be hydrolysed carbohydrate, converted into methyl, acetyl alditol acetates. The GC spectra is shown in figure 36 and demonstrates that nearly all of the observed sample were eluted in the first 2 large peaks, which represent retention times of 14.90 min and 15.14 min.

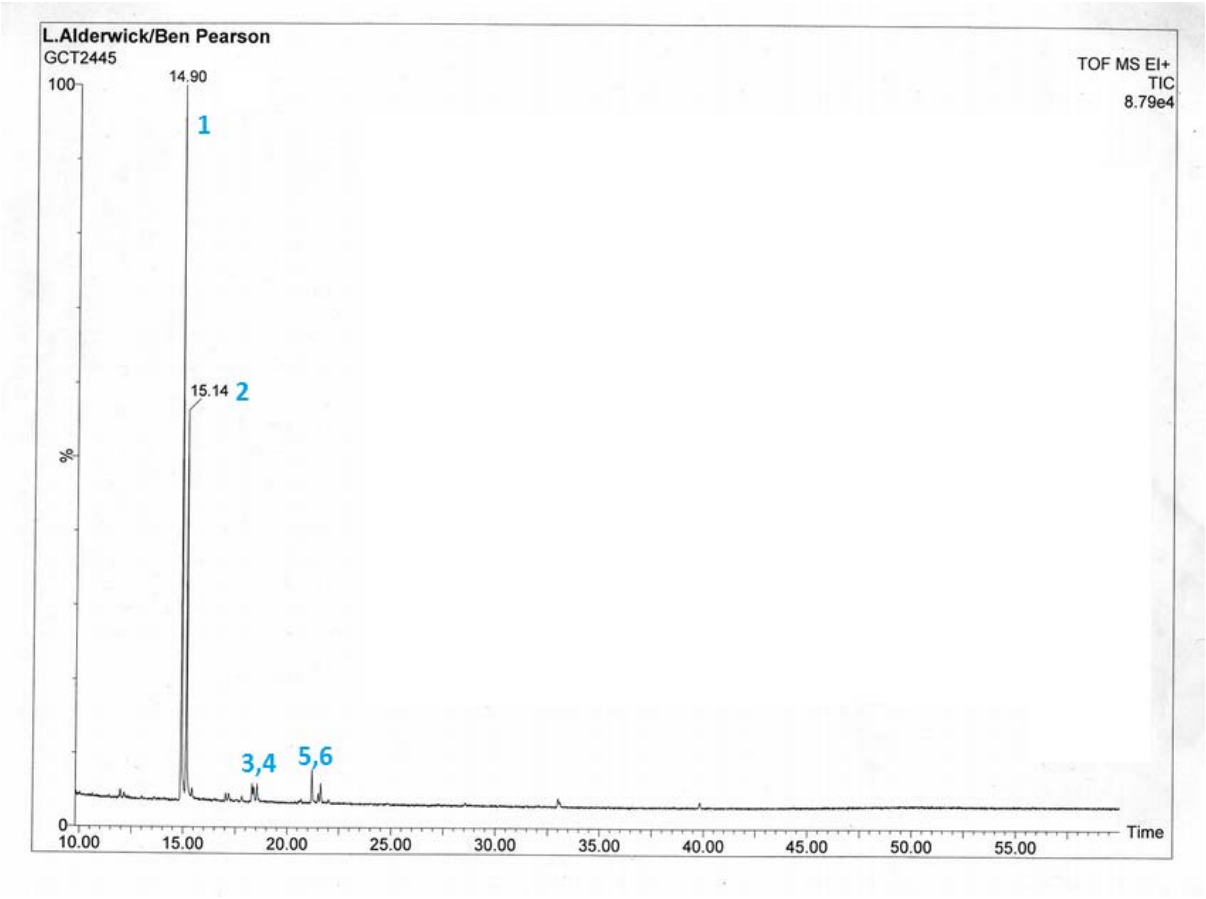

Figure 36: Gas chromatogram for the sample treated by the Hakomori method. Blue numbers show where a mass spectrum was taken.

A total of 6 mass spectra were obtained after separation by gas chromatography. The retention times for these mass spectra are 14.9 min, 15.1 min, 18.3 min, 18.5 min, 21.2 min and 21.7 min and are labelled 1 to 6 on the chromatograph in blue.

Fortunately, interpretation of the mass spectra is made easier by the following rules(95):

1) The lowest peak should have a m/z value of 43 or more. Species with a mass of 43 represents the ion $CH_3C\text{-}O^+$.
2) Fission primarily occurs between adjacent carbons atoms in the sugar chain (i.e. not between carbons atoms on acetyl groups).
3) The fission occurs preferentially between carbons that areboth attached to adjacent methyl ethers, then between carbons which are attached to one methyl ether and one acetyl group. Finally carbon-carbon bonds, where both carbons are bonded to acetyl groups are broken.

4) When a bond breaks between carbon atoms where one is attached to a methoxyl group and the other an acetyl group, the positive charge is taken by the carbon attached to the methoxyl group. Therefore the other fragment (attached to the acetyl) will not be seen.
5) Secondary fragments are then formed by the loss of acetic acid (m/z 60), ketene (m/z 42), methanol (m/z 32), formaldehyde (m/z 30)

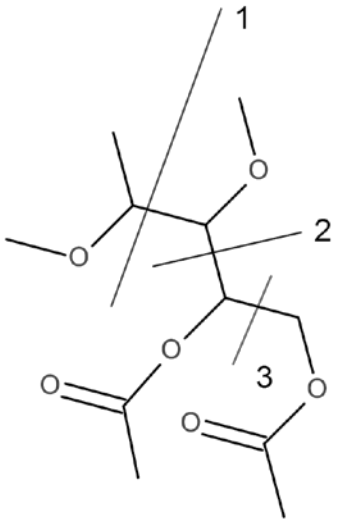

Figure 37: diagrammatic illustration showing the preference of splitting of carbon-carbon bonds in methylated alditol acetates. At the split (2), the positive charge is only taken by the carbon linked to the methoxyl group (on top), so the lower fragment does not produce a signal.

Figure 38 shows the spectra of the sample separated by gas chromatography which had a retention time of 14.9 minutes. A fragment with a m/z ratio of 189 can only be from a fragment containing 3 carbons from the sugar, 2 acetyl groups and 1 methoxy group. The next fragment has a m/z of 162/3, which is only 27 less than our first fragment. This peak could only be a secondary fragment of the first if it had a m/z ratio of 159 or less (see rule 5), therefore this isa primary fragment. The only fragment that has a mass of 162 would be a 3 carbon backbone species with 2 methoxyl groups and

1 acetyl group.

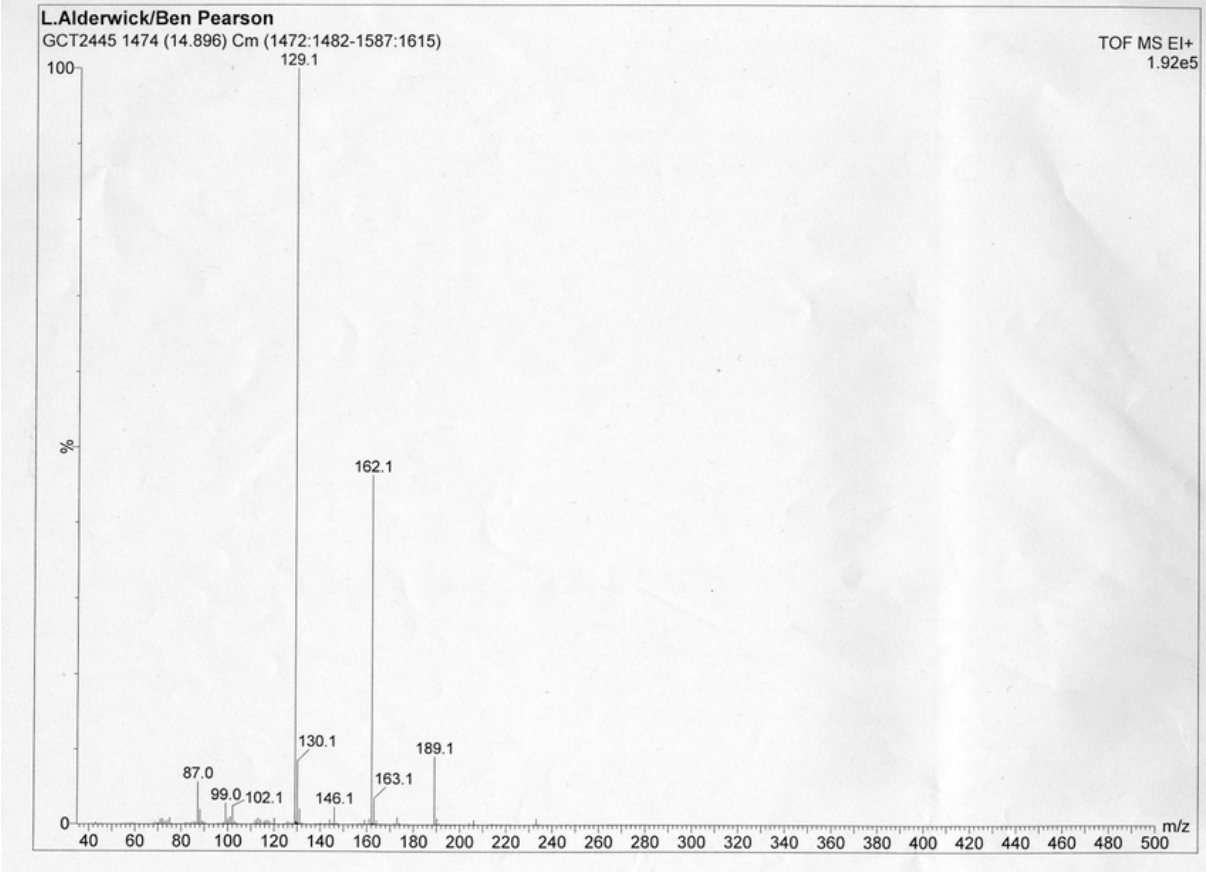

Figure 38: First mass spectra obtained from the sample separated by gas chromatography

Due to rule 3, the split bond must have occurred between 2 carbons attached to methoxyl groups.From these 2 primary fragments there can be 2 possible molecules; either the alditol acetate derived from 3,4, 6 or 2,3,4-tri-O-methyl hexose.The primary and secondary fragments are shown in figures 39 and 40. Note however, that due to the nature of the fission, protons can be missing or added and species may have a slightly altered m/z ratio by a few units.

The 3,4,6-tri-O-methyl hexose (see figure 39a) has adjacent methoxyl groups in only one location, therefore it will only produce 2 primary fragments with masses of 161.2 and 189.2. The lighter primary fragment (left) can split between adjacent acetyl and methoxyl groups, producing a fragment H_2C^+-O-CH_3 with a mass of 45.1 and also another fragment with an acetyl and methoxy group which is invisible due to rule 4. The larger species with 189.2 m/z can form other secondary

products by losing acetyl or methoxyl group producing the species on the far right of the diagram. If the carbon backbone breaks between the methoxyl and the acetyl group another invisible primary species forms, but this can produce secondary species with an m/z ratio of 87.1. Comparison of the below diagram to the MS shows that 3,4,6-*O*-methyl alditol acetate derivative of a hexose is consistent with mass spectrum.

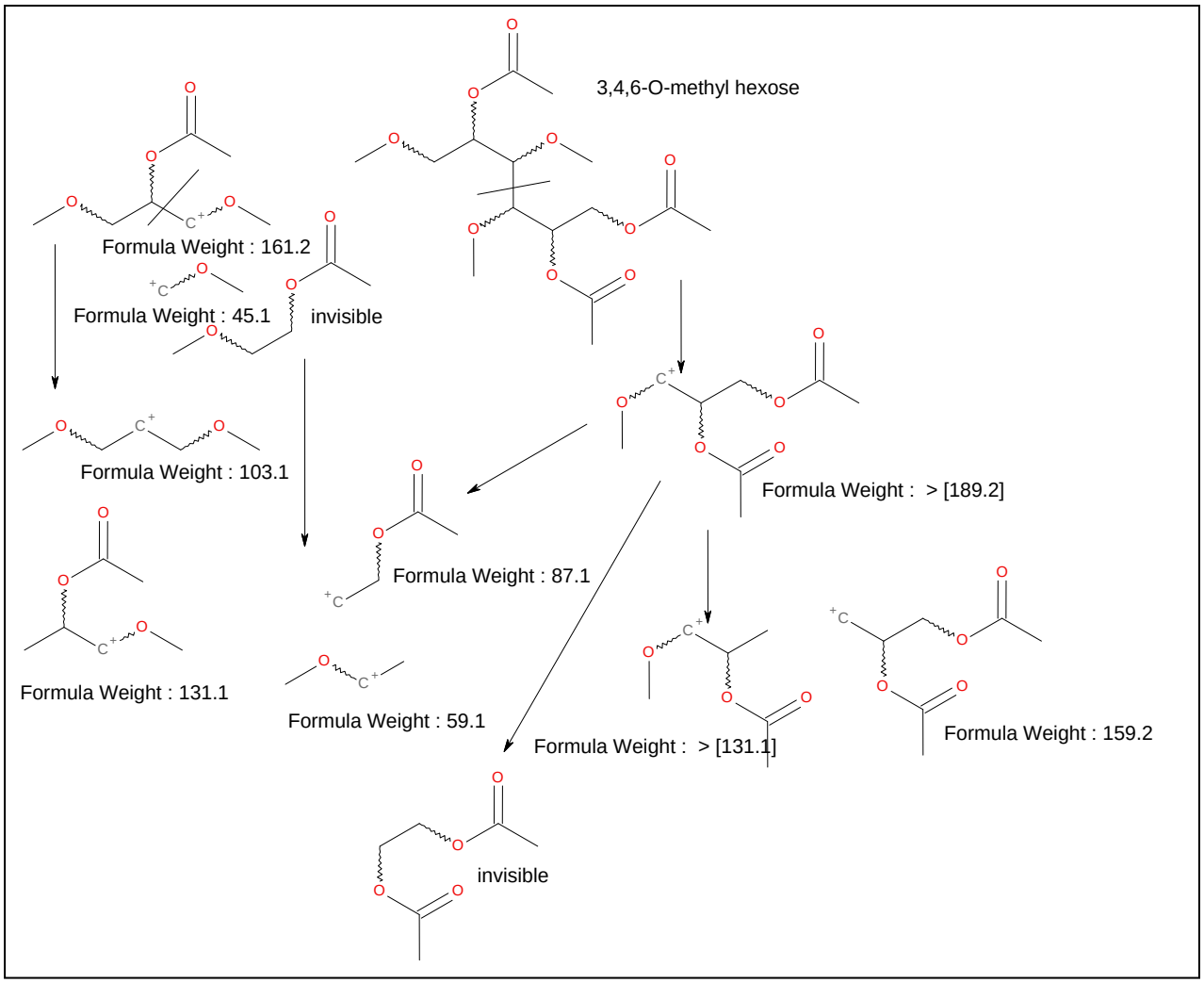

Figure 39a: Further splitting to give additional species that would be seen in the spectra

Figure 39b shows the possible fragmentation patterns of 2,3,4-*O*-methyl alditol acetate of a hexose. Initially there are 2 places the molecule can split (between the 2nd and 3rd, or the 3rd and 4thcarbon). This produces primary fragments with m/z ratios of 104.1, 233.2, 161.2 and 189.2. The largest possible fragment 233.2 can produce further secondary species by loss of acetyl groups (-

60)/methoxyl groups (-42) forming species with masses of 173.2, and 191.2 These peaks will be unique to the 2,3,4-*O*-methylated hexose alditol acetate and not present in the3,4,6 methylated isomer.

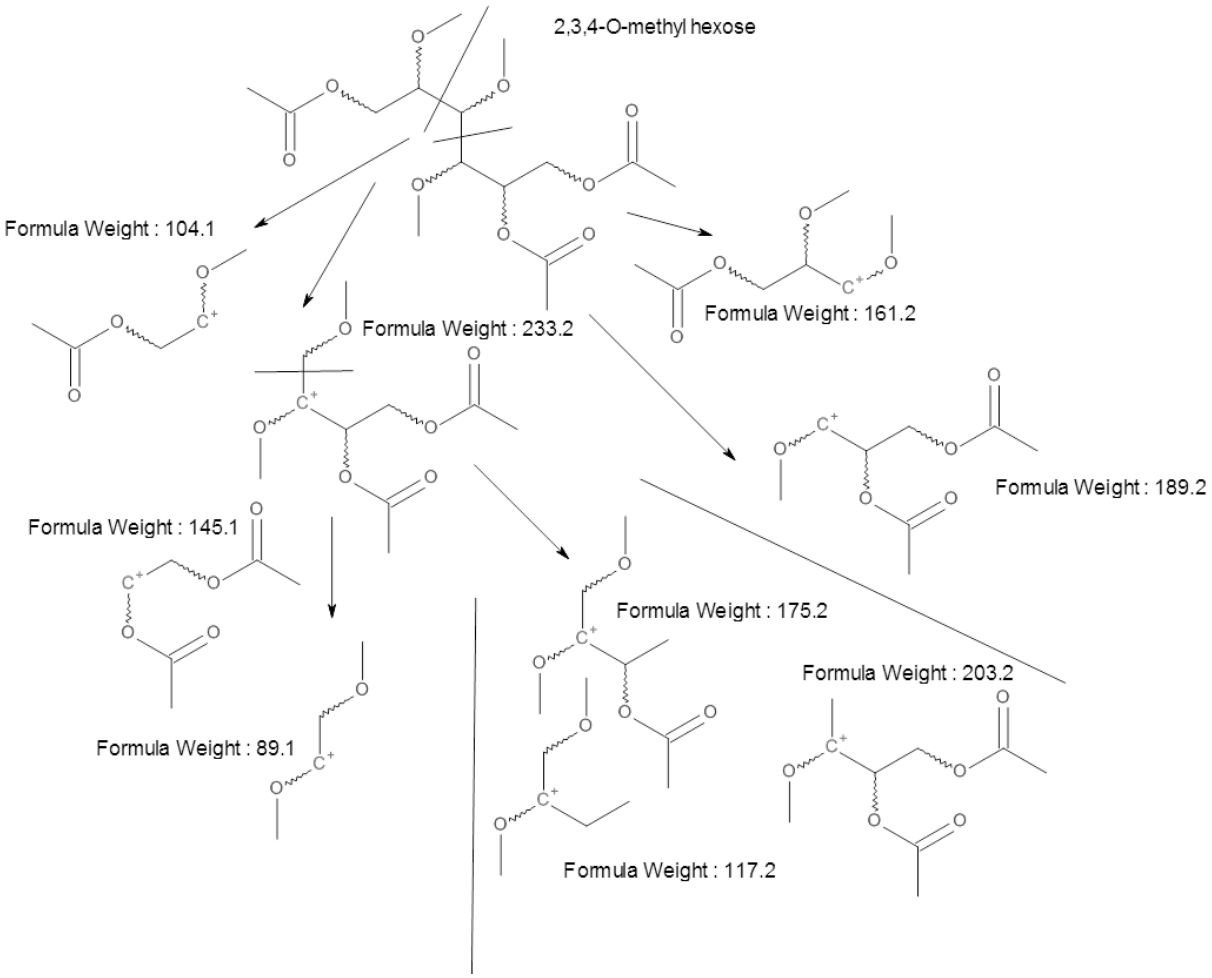

Figure 39b: Fragmentation pattern of a 2,3,4-*O*-methyl alditol acetate derivative of a hexose

The mass spectra in figure 38 does not show peaks at 233 or 104 and does not have peaks representing the secondary fragments unique to the 2,3,4-O-methylated isomer. Therefore the species responsible for producing the first spectra is likely to be the 3,4,6-O-methylated isomer.

The second mass spectra (figure 40) has a collection of peakswhich makes it almost identical to the first and likely represents a different hexose species or set of species, with a similar methylation pattern. However since the GC trace is smaller this species is not as abundant as the first.

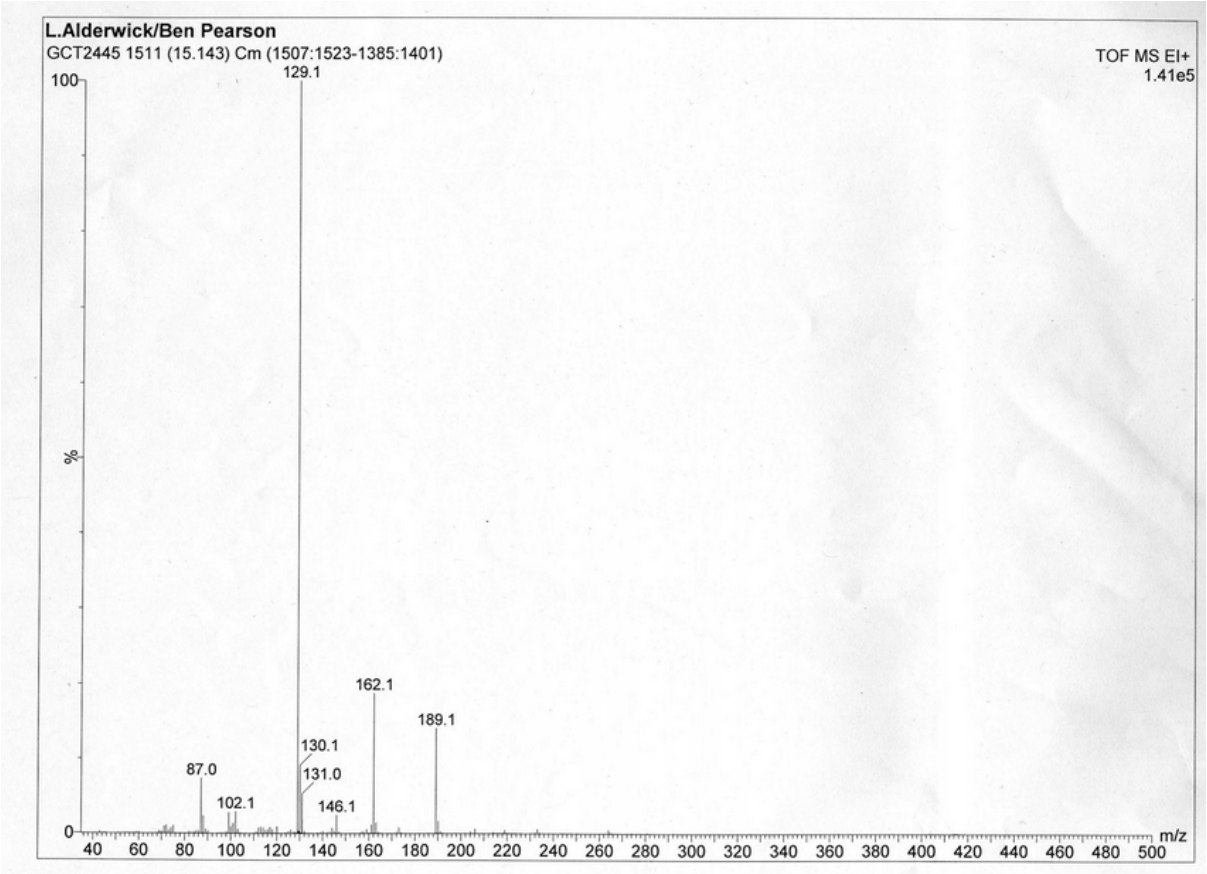

Figure 40: Mass spectrum for the second peak in the gas chromatogram, with a retention time of 15.1 min.

Figure 36(the gas chromatograph) shows that the first 2 molecules discussed makes up the majority of the sugars in the compound. Due to the NMR spectra obtained, these common units are unlikely to contain nitrogen or methyl groups. The species with greater retention times made up a much smaller proportion of the overall sample and therefore signals from these species may not have been noted on the ^{1}H spectrum for this sample. Therefore aminated and deoxy sugars could be present in the species with longer retention times.

The third spectrum (figure 41), which has a retention time of 18.3 min has a spectrum which is also similar to the first two, but it also shows an additional species with a m/z ratio of 173.2, 191.2, 100,

233, which suggests it is likely to consist of a 2,3,4-O-trimethyl alditol acetate (hexose) derivative due to the reasons discussed above.

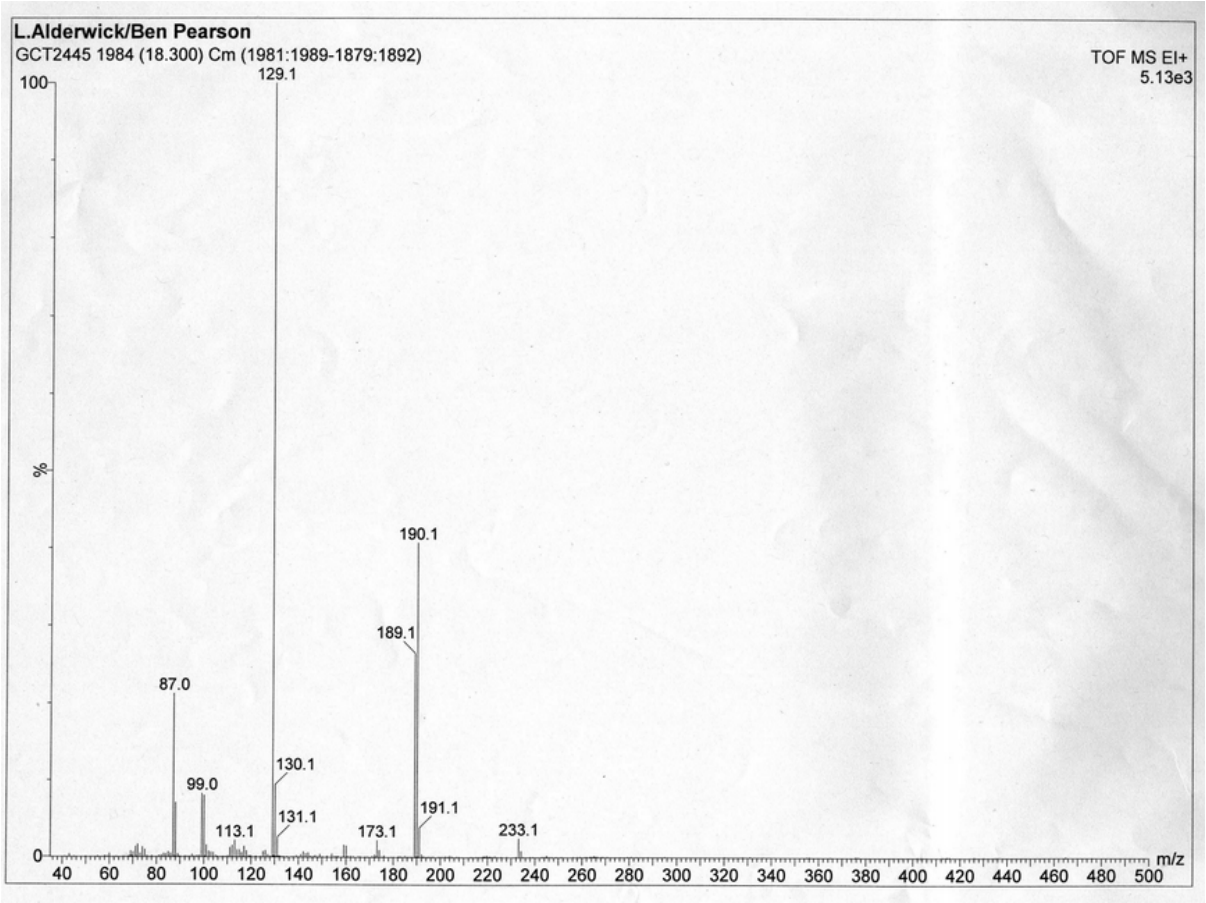

Figure 41: Mass spectrum for the third peak in the gas chromatogram, with a retention time of 18.3 min

The 4th spectrum which had a retention time of 18.5 minutes is very different to the first three and has a very large species with a m/z of 362.1. This must be a 5 carbon sugar with 5 acetyl groups attached. If the sugar is a hexose (and heptoses are extremely rare), the remaining carbon not included in this 5 carbon species cannot be methylated, as this would invalidate rule 4, or the 5C species would be non-charged and therefore not seen on MS. Furthermore, the other fragment cannot be a simple methyl group, since this would not produce a molecular splitting with a 5-C acetyl fragment. The other carbon could be attached to an acetyl or an acetamido group (see figure 43). Both would give similar spectra, since N-H weighs only 1 atomic mass unit less than oxygen.

Table 8: Shows the m/z for primary and secondary fragments. No acetoamido group is used in this table for simplicity.

		Secondary species				
Primary species	Mass	-1 Acetyl	-2 acetyl	-3 acetyl	-4 acetyl	-5 acetyl
Primary molecule	434	374	314	254	194	134
5C	361.2	301	241	181	121	61
4C	289.2	229	169	109	49	
3C	217.2	257	197	137		
2C	145.1	85	25			
1C	73.1	13				

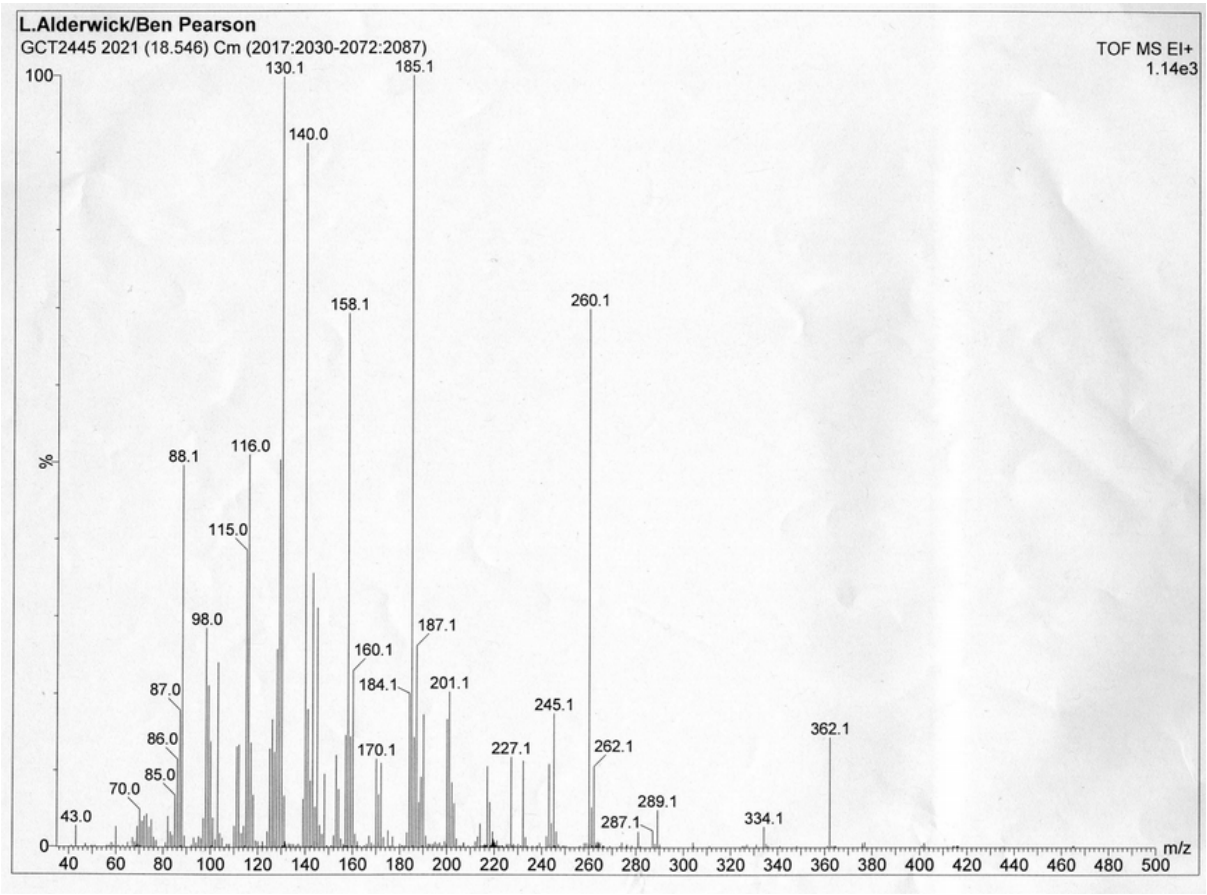

Figure 42: Mass spectrum for the fourth peak in the gas chromatogram, with a retention time of 18.5 min

Figure 43: splitting pattern of a non-methylated hexose.

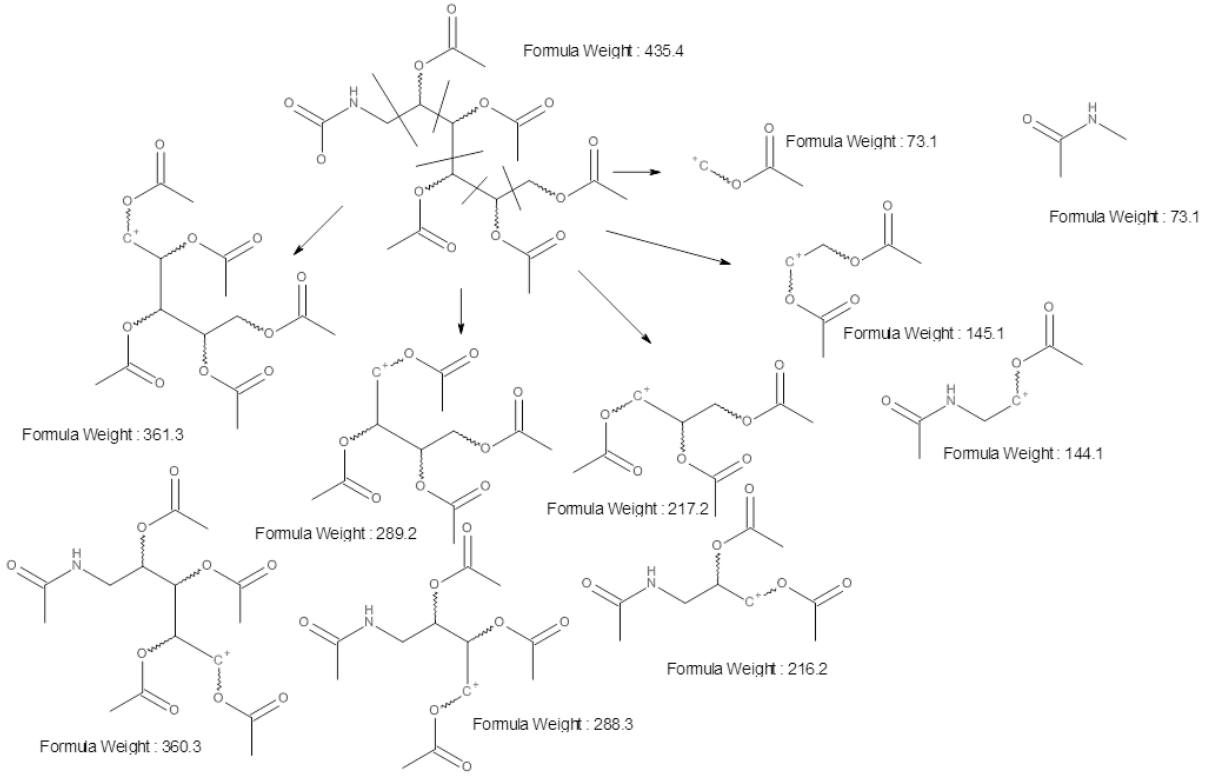

Whilst the mass spectrum shows the presence of species with similar mass to the primary fragments proposed in table 6, there are additional peaks which cannot be accounted for by their secondary fragments. This may be because there are two species being analysed by the mass spectrometer. By eliminating the spectral peaks caused by primary and secondary fragments of a non-methylated pentose derivative, there are 2 large peaks remaining at 260 and 116. Only the presence of 2-O-methyl pentose explains these peaks. The remaining peaks in the spectrum are accounted for by the secondary fragments of this molecule (see figure 44). Figure 45 shows the spectrum again, but with the peaks circled in different colours representing which molecules caused which peaks in the spectrum.

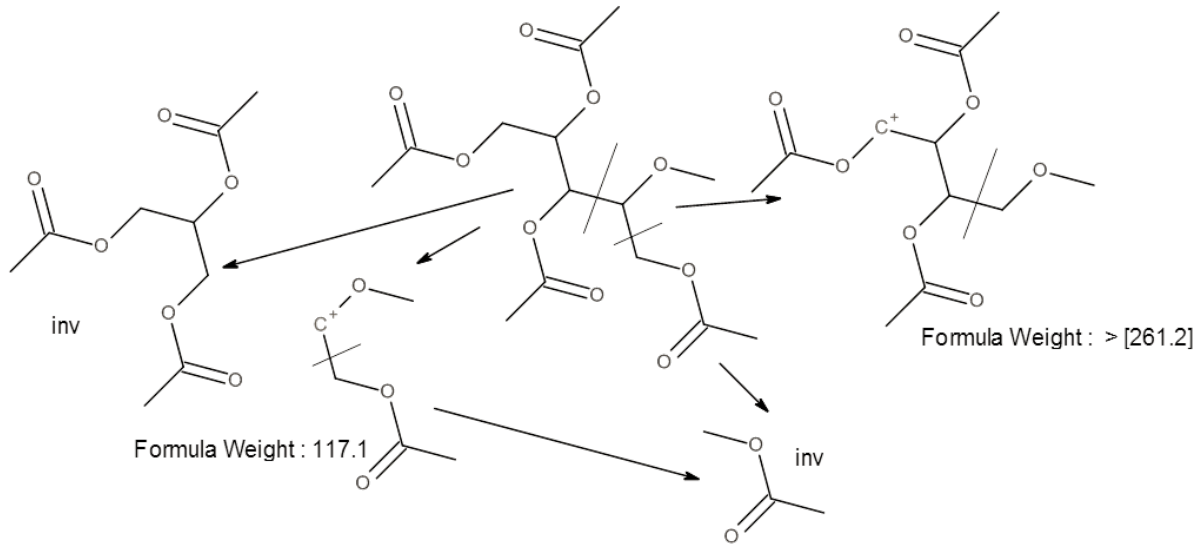

Figure 44: Splitting of 2-O-methyl pentose. Masses of visible spectra are displayed.

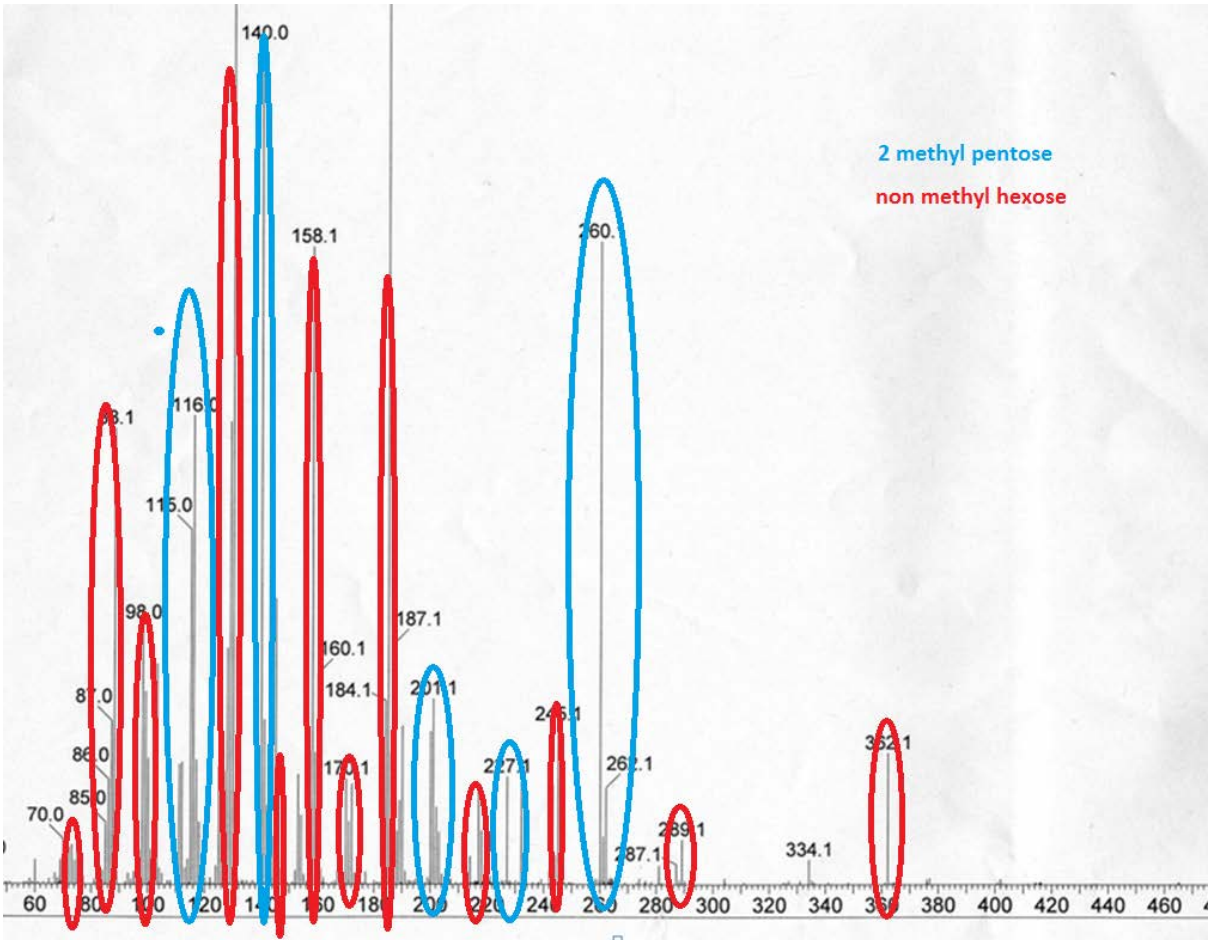

Figure 45: Spectra accounted for by 2 molecules forming separate primary and secondary fragments.

The fifth spectrum contains a peak which is less than 43 atomic mass units per charge, which breaks rule 1. It also contains ionic species which have large masses that do not correlate with typical masses of primary fragments of monosaccharides or related molecules. Therefore the spectrum is likely to represent a non-monosaccharide related molecule. This cannot be glutamate, since a fully methylated glutamate derivative would be 1,5-dimethoxy-N methyl-pentan-2-amine, which would have a maximum mass of 161.2.

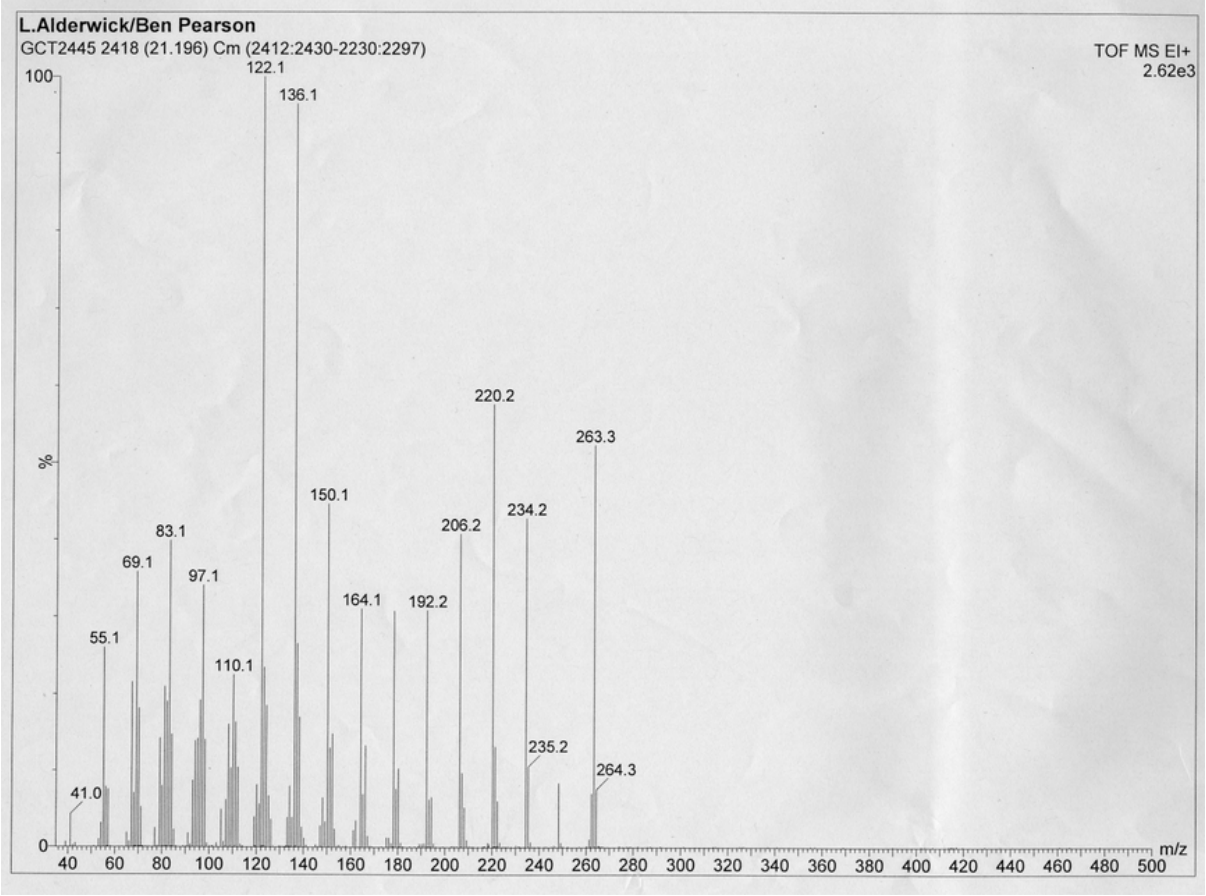

Figure 46: Mass spectrum for the fifth peak in the gas chromatogram, with a retention time of 21.2 min

The sixth spectrum (figure 47), which has a retention time of 21.6 minutes, is similar to the fourth spectrum, but with fewer total peaks. All peaks can be accounted for by a non methylated alditol acetate derivative of a hexose or amino sugar. Amino sugar derivatives are known to have longer

retention times in GC than their non aminated counterparts. This may suggest that the original molecule was an amino sugar.

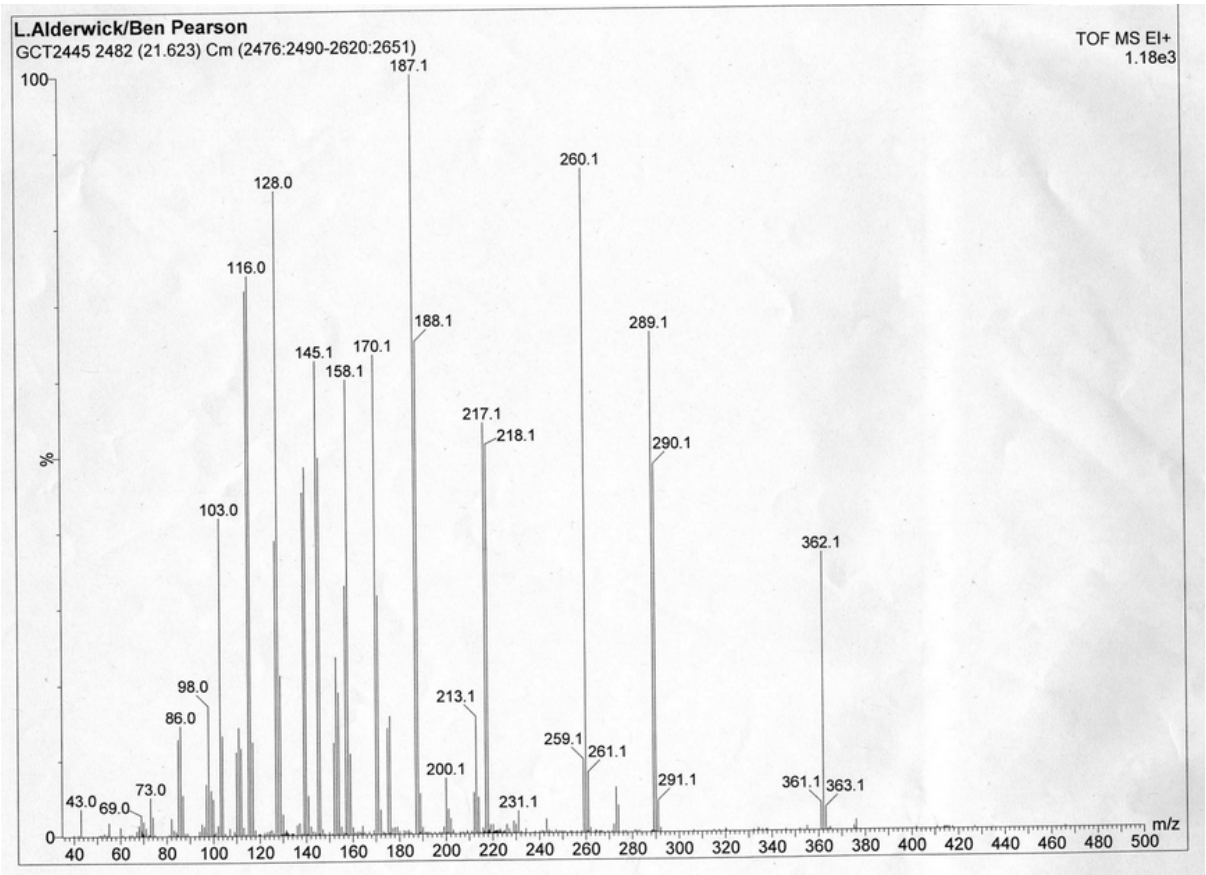

Figure 47: Mass spectrum for the sixth peak in the gas chromatogram, with a retention time of 21.6 min

Unfortunately the sample sent for MALDI-TOF analysis did not produce any useful data regarding the molecular size of the sample.

3.4.3 Conclusions from both experiments.

The chromatogram of alditol acetates suggests that the mixture of sugar residues is quite complex, with a possibility of up to 12 different sugar isomers. Out of these 12, a possible 6 were potentially identified, making up the majority of the carbohydrate. This included both hexoses and the pentose ribose.

Hakomori methylation identified 5 different variations of methylation of monosaccharide hexoses and pentoses in 6 mass spectra separated by gas chromatography. These species are summarised in

table 9. The most abundant variant was the 3,4,6-O-trimethyl-hexose, which represents a sugar where the Hakomori method was unable to add methyoxyl groups to carbons 1, 2 and 5. In many hexose molecules such as glucose, galactose and mannose the hydroxyl group of the 5thcarbon is bonded to the 1st carbon and therefore will not be methylated by the Hakomori methylation (see figure 48). The same is also true of pentoses, but the 4th carbon is unavailable to participate in methylation. Therefore the polysaccharide is likely to be composed of mostly 1 ➔ 2 glycosidic bonds between hexoses.

Table 9: A summary of species determined by the Hakomori method and the corresponding species they represent in the sample.

Alditol acetate derivative on MS	Sugar molecule in sample	Glycosidic bond	Mass spectra
3,4,6-O-methyl hexose	1,2,5 substituted hexose	1➔ 2	1, 2
2,3,4,-O-methyl hexose	1,5,6 substituted hexose	1➔6	3
Non methylated hexose/aminohexose	Fully substituted hexose	Branching from 1,2,3,4,6?	4, 6
2-O-methyl pentose	1,3,4 substituted pentose	1➔ 3	4

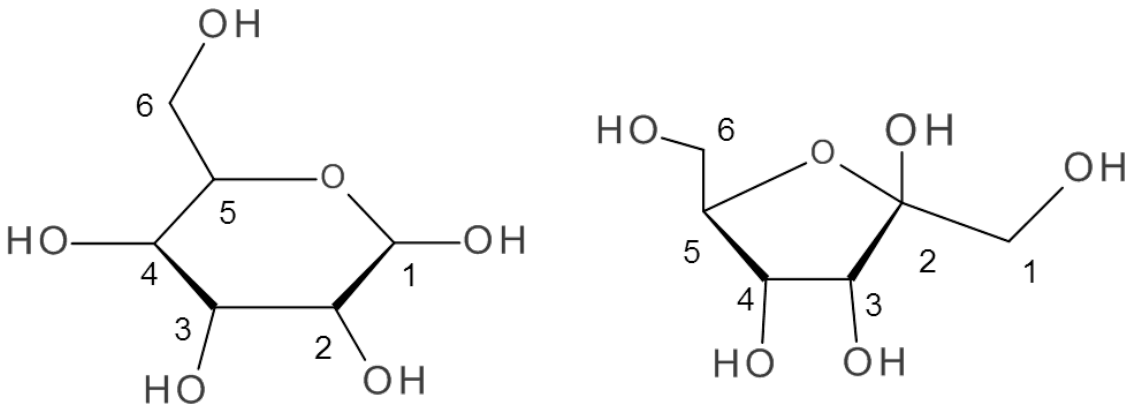

Figure 48: The structure of many hexoses implies that methylation cannot occur on the 5th carbon by the Hakomori method.

3.5 HPLC separation,determination of M_n and D/L excess.

3.5.1 Purpose of the separation

The purpose of this experiment was to determine a purity of the crude product as a percentage per mass. Treating samples with FDNB was used in conjunction with HPLC to determine the molecular number (M_n) of the sample. The circular dichroism experiment performed on hydrolysed sample was used to determine the ratio of D and L glutamate monomers present in polymerised PγGA.

3.5.2 Determination of purity of mass in crude samples by chromatography

Neutralised hydrolysed sample and 2 controls, pure PγGAand water was injected into the HPLC equipment. The chromeleon software package then produced a report with a chromatograph which reported the number of peaks for different retention times and also the area under the peaks. An example of the report produced is shown in figure 49. This area was compared to a sample that had been prepared using 100% pure monosodium glutamate. This sample had an equal weight/volume concentration as the other samples. Peaks at 2.8 minutes were assumed to be caused by glutamate, since this was the only peak produced by pure glutamate. Areas under the curve for each sample were divided by the area under the curve for pure glutamate to give the purity as a percentage of the control sample (wt/v). Table 10 shows the area under the curve for each sample and the

predicted concentration. This is shown graphically in figure 50. Surprisingly the table and figure shows that there was much greater concentrations of glutamate in samples grown with additional NaCl.

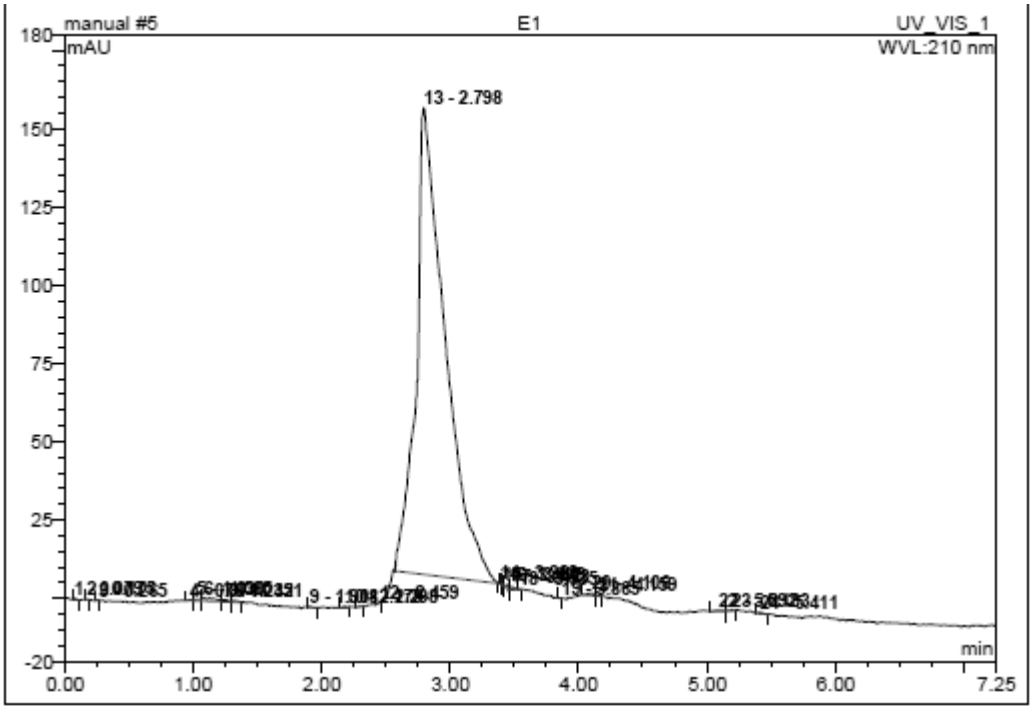

No.	Ret.Time min	Peak Name	Height mAU	Area mAU*min	Rel.Area %	Amount n.a.	Type
1	0.08	n.a.	0.423	0.010	0.02	n.a.	BMB
2	0.18	n.a.	0.131	0.002	0.01	n.a.	BMB
3	0.26	n.a.	0.204	0.003	0.01	n.a.	BMB
4	0.97	n.a.	0.330	0.010	0.03	n.a.	BM
5	1.03	n.a.	0.614	0.027	0.07	n.a.	M
6	1.09	n.a.	1.071	0.122	0.31	n.a.	M
7	1.24	n.a.	0.633	0.040	0.10	n.a.	M
8	1.32	n.a.	0.535	0.029	0.07	n.a.	MB
9	1.91	n.a.	0.242	0.007	0.02	n.a.	BMB
10	2.18	n.a.	0.249	0.009	0.02	n.a.	BMB
11	2.30	n.a.	0.239	0.006	0.02	n.a.	BMB
12	2.46	n.a.	0.254	0.009	0.02	n.a.	BMB
13	2.80	n.a.	148.860	39.087	98.84	n.a.	BMB
14	3.39	n.a.	0.336	0.005	0.01	n.a.	BMB
15	3.41	n.a.	0.310	0.004	0.01	n.a.	bMB

Figure 49: Chromatograph for sample E with the computer generated report underneath

Table 10: Integration values for areas under the curve at 210 nm obtained from the Chromeleon software package.

Sample	Area under curve	Fraction of glutamate (x/Glu)
E1	39.1	0.229
E2	30.7	0.190
E3	No Data	
F1	30.6	0.180
F2	28.6	0.156
F3	34.2	0.201
G1	40.1	0.235
G2	31.7	0.186
G3	90.7	0.532
H1	110.1	0.646
H2	99.6	0.584
H3	76.8	0.450
L Glu	170.5	0.229

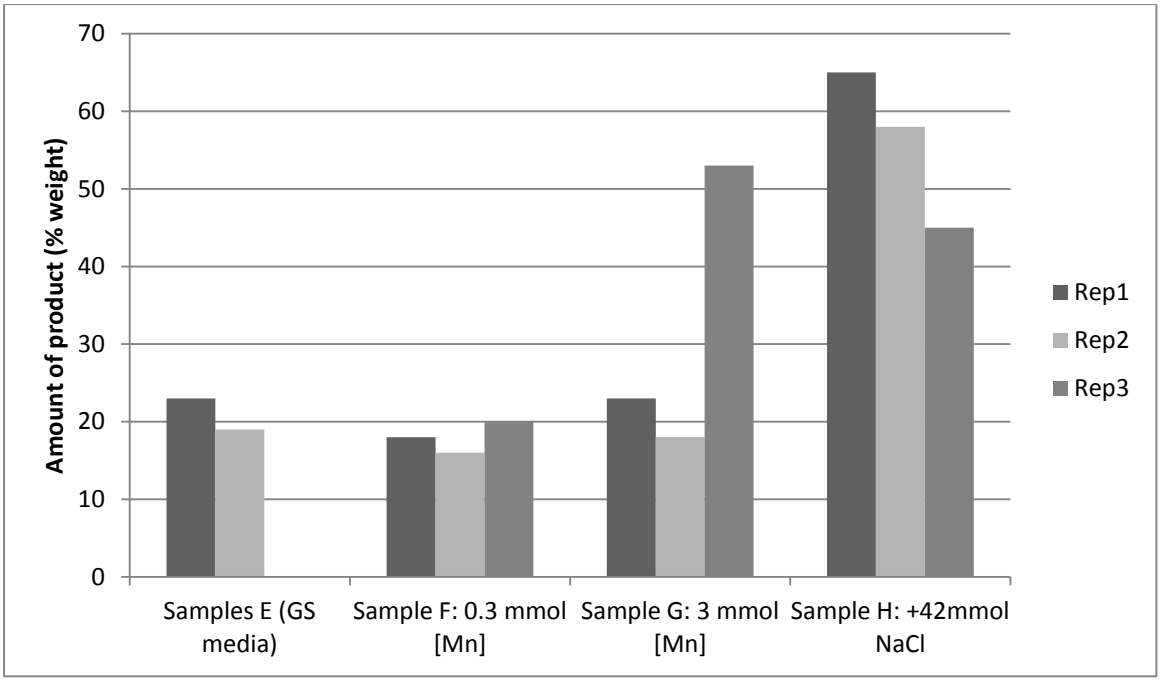

Figure 50: % concentration of glutamate found through chromatography.

Sample eluted from the chromatography machine was collected. The amount of glutamate was calculated from the area under the curve and the volume of liquid was determined by the time taken to collect the sample divided by the flow rate of the machine. The concentration of the collected sample was determined by the mass of glutamate predicted divided by the total volume of the solution.

3.5.3 Molecular number of PγGA

An FDNB assay was performed by adding non hydrolysed sample of known mass concentration 10 µg ml^{-1} crude product to an excess of FDNB. Absorbance was measured at 356 nm and values obtained from the literature were used to determine the molar concentration of FDNB-PγGA. Figure 51 shows the graph obtained for the literature(1), which shows the relationship A_{365} = Concentration (µM) x 0.009.

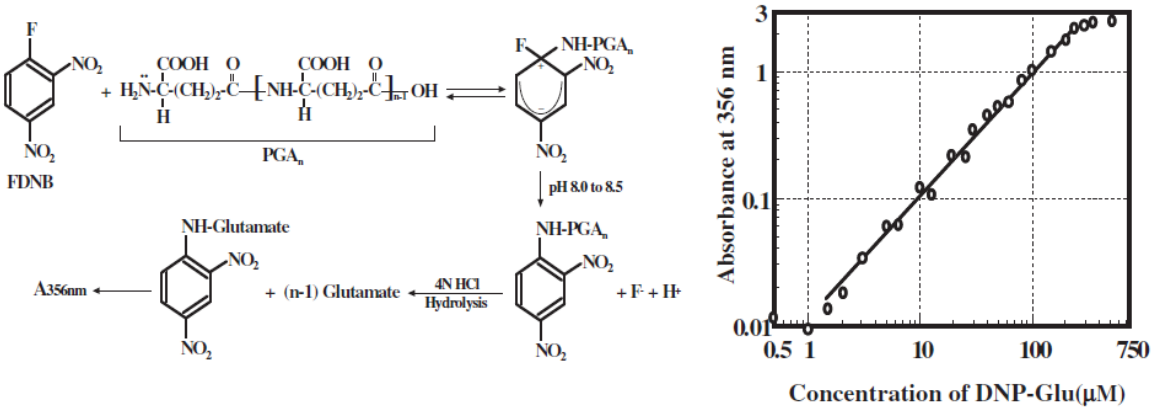

Figure 51: Diagram showing the correlation between absorbance at 356 nm and concentration of DNP – Glu.

The molar quantity of glutamate was determined by the equation:

$$\frac{Concentration of sample(w/v) \times \%\ glutamate}{Mass of glutamyl\ (127)} = Molar\ quantity\ of\ glutamate$$

Using the values obtained in the previous section for the molar concentration of glutamate in hydrolysed samples we determined M_n for each sample by the following equation:

$$\frac{Molar quantity of glutamate}{Molar quantity of FDNB} = M_n$$

The molecular number for each sample is given in table 11 and shown graphically in figure 52. This appears to show that sample H has a greater molecular number compared to other samples.

Table 11: Molecular number M_n obtained from the molar concentration and absorbance of FDNB-Glu at 365.

Sample (crude) 1 mg ml^{-1}	%glutamate	Molar quantity μmol ml^{-1}	A_{365}	M_n
E1	0.229	1.81	0.015	108.3
E2	0.190	1.50	0.013	103.6
E3	0.000			
F1	0.180	1.41	0.015	84.8
F2	0.156	1.23	0.014	79.1
F3	0.201	1.58	0.013	109.4
G1	0.235	1.85	0.013	128.1
G2	0.186	1.47	0.012	110.1
G3	0.532	4.19	0.016	235.6

H1	0.646	5.08	0.025	183.0
H2	0.584	4.60	0.026	159.2
H3	0.450	3.55	0.018	177.3
Commercial				108.3

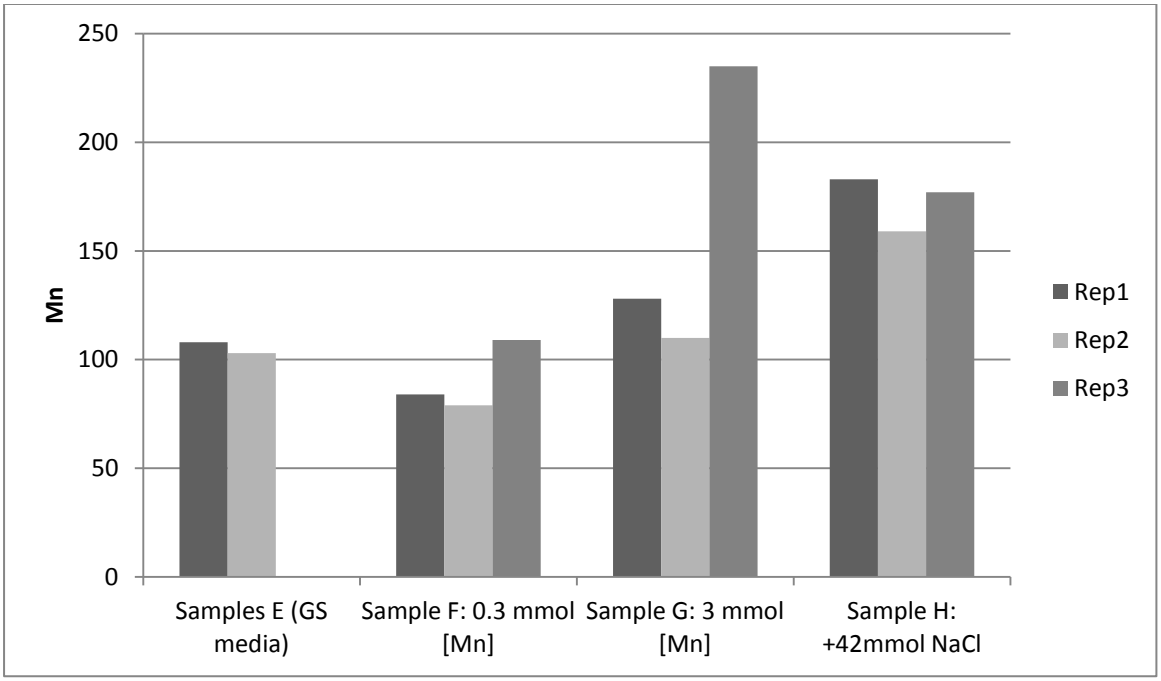

Figure 52: M_n for each sample.

3.5.4 Circular dichroism

The aim of this experiment was to determine the D/L ratio of the samples.Samples taken from the chromatography machine had a 2.8 minutes retention time. The time taken to collect the sample (between 14 and 45 seconds) was multiplied by the flow rate to determine the volume. The mass of sample was calculated using the percentage glutamate value obtained in the previous section multiplied by 200 µl, which was injected into the chromatography machine. Predicted maximum absorbance at 210 was calculated using the equation:

$$A_{210}(\max) = 34.5 \times concentration\ (mg\ ml^{-1})$$

And the minimum was the 0 – A_{210}(max). The equation in the method section was used to calculate the D/L ratio.

Circular dichroism data was only recorded for 5 samples as the rest were lost, the spectra was obtained from 800 to 190 nm and the voltage showed that the results were reliable over 200 nm for all samples recorded. These are shown in figure 53. Spectra showed a peak at 206 nm, but A_{210} was used. All samples measured appeared to have a slightly concentration of D glutamate (see table 13), but sample G2 was found to have a much higher D glutamate content than the other samples measured.

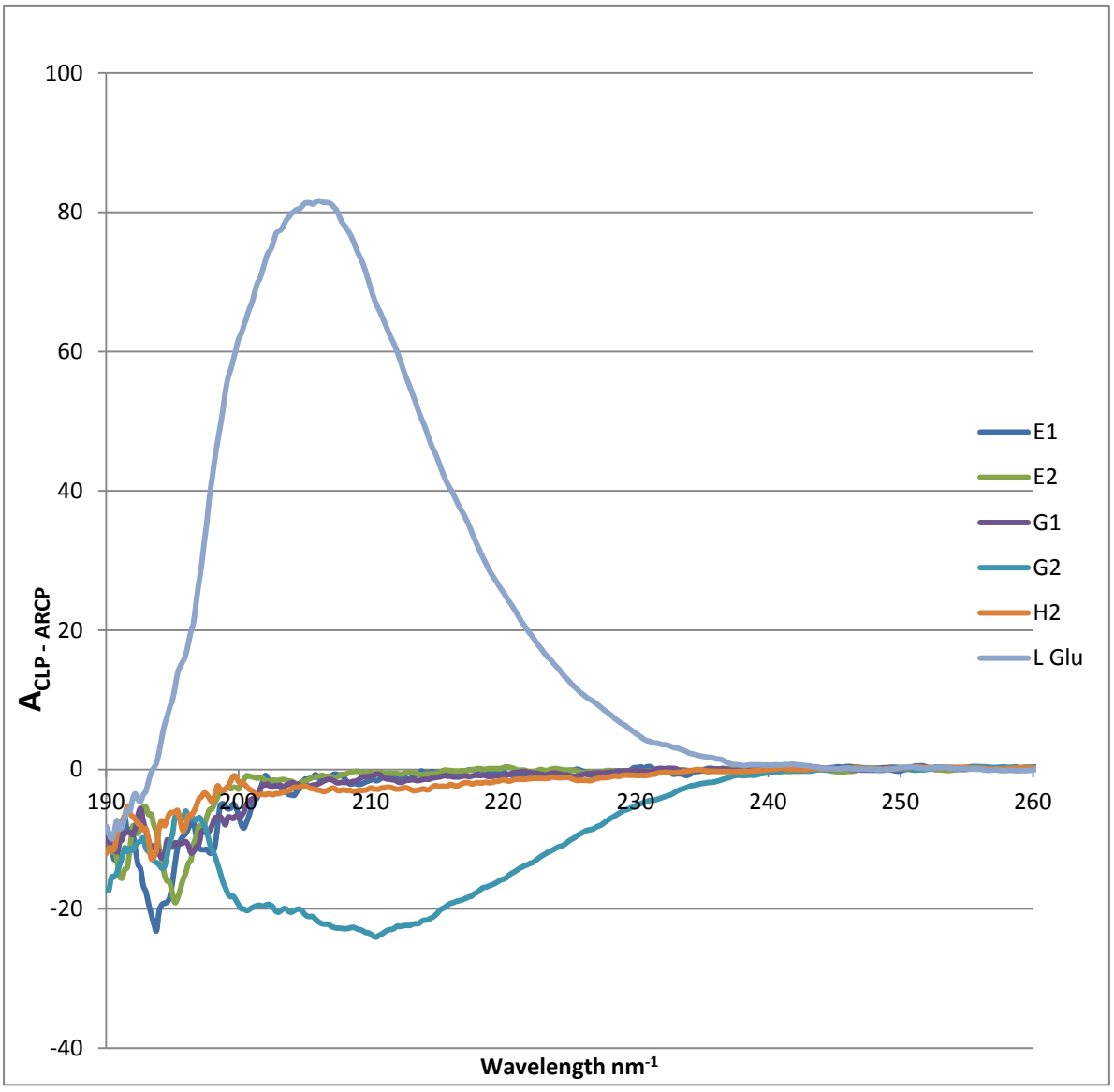

Figure 53: CD spectra obtained for samples A_{LCP} is absorbance of left circularly polarised light and A_{RCP} is absorbance of right polarised light.

D %	L %	Sample	D/L
55.8	44.2	E1	1.262443
50.5	49.5	E2	1.020202
52.2	47.8	G1	1.09205
73.5	26.5	G2	2.773585
51.3	48.7	H2	1.053388

Table 12: % of D and L glutamate identifiedusing CD

3.5.5 Predicting purity by mass from ^{1}H purity

Since we found the crude product consisted of polysaccharide and glutamate, we could calculate the purity of the sample by weight from the percentage of protons that belonged to glutamyl residues which was determined from the NMR spectrum of each sample. To calculate the molar fraction of glutamyl, the following equation was used:

$$\frac{^1H_{purity}}{nH_{glutamyl}} / (\frac{^1H_{purity}}{nH_{glutamyl}}) + \frac{1 - {}^1H_{purity}}{nH_{sugar}})$$

Or the mass fraction of PγGA using the adapted equation:

$$\frac{^1H_{purity} \times mass_{glutamyl}}{nH_{glutamyl}} / (\frac{^1H_{purity} \times mass_{glutamyl}}{nH_{glutamyl}}) + \frac{1 - {}^1H_{purity} \times mass_{sugar}}{nH_{sugar}})$$

Where: $^1H_{purity}$ referred to the percentage of protons determined by the integration trace of the NMR spectra, $nH_{glutamyl}$ and nH_{sugar} referred to the number of protons per glutamyl and sugar unit visible on the NMR spectrum, which was 7 and 6 respectively. $Mass_{glutamyl}$ and $Mass_{sugar}$ referred tothe mass of each monomer unit, which was calculated as 128 and 162 respectively.

This made the following assumptions:

1) That the only impurity in the sample was carbohydrates

2) That the sugar and glutamyl chains were large enough to mean the mass contributed by terminal residues was insignificant compared to polymerised units
3) That all glutamyl chains were deprotonated and that the only counter ion was sodium

3.5.6 Correlation between ^{1}H and chromatography derived mass purity

This allows a second method to calculate the %mass of PγGA. Therefore both the chromatography method and the ^{1}H method can be compared (see table 13). Only 2 samples were measured by both techniques and there is a discrepancy between the values obtained. When determined chromatographically sample E appears slightly less pure and sample H is appears more pure compared to purity values calculated using NMR. ^{1}H measurements could be due to the incorrect assumptions outlined in the previous section. Furthermore NMR measurement shows the relative ratios of organic hydrogen and measurements do not take into the amount of precipitated inorganic ions. However in all these experiments the total ions varied by only 2.5%, therefore the salt proportion of the samples is unlikely to vary extensively.

Table 13: Comparison of methods used to calculate purity of PγGA by mass.

Sample	$\%purity_{^{1}H\ NMR}$	$\%purity_{chromatography}$
Crude E1	24.7	22.9
Crude H1	38.1	64.6

Chapter 4

Discussion

4.1 Chemical Identity of Crude Precipitates

IR absorption experiments showed that samples contained similar functional groups to commercial obtained PγGA, but samples also demonstrated other functional groups not present in commercial PγGA. These groups either contained carbon oxygen or carbon nitrogen bonds. Using ATR with samples of similar weight/volume concentration illustrated that samples had reduced absorption of light at wavelengths typical of PγGA absorption. This was further evidence that the sample contained an impurity.

^{1}H, and ^{13}C NMR confirmed that our commercial sample was mostly PγGA. It also showed that our sample contained atoms which were in similar electrochemical environments to the commercial sample and therefore provided further evidence that our samples contained PγGA. These spectra also showed that the additional functional groups were either hydroxyl groups or alkene groups. With IR absorbance data we could conclude that these were hydroxyl groups. Whilst a structure wasn't determined from NMR of the impurity, from these two experiments we were able to rule out the presence of many other functional groups and the impurity was highly suspected to be carbohydrate. Furthermore we were able quantify relative proportions of PγGA in both crude samples and purified samples.

GC-MS analysis of an unexpectedly obtained isolated impurity was shown to consist mostly of hexoses, which were linked through their 1^{st} and 2^{nd} carbon atoms. However other sugar residues and linking patterns were found in lesser abundance. No reference of this carbohydrate was referred to in the literature.

Other investigations found that PγGA within the samples had the greatest number of chains that were between around 80 and 240 units long. For the few samples that were measured these units contained slightly more of the D isomer. This is consistent with experiments reported in the literature for PγGA produced by *B. subtillis natto.*

4.2 Yields of crude products and PγGA from *B. subtillis natto*

From 12 experiments, we managed to obtain a mean quantity of 17.9 g dm^{-3} of crude product using *B. subtillis natto*. Ogawa et al using the same subspecies claimed to produce 35 g dm^{-3} PγGA by using different media consisting of 60 g dm^{-3} maltose, 70 g dm^{-3} soy sauce and 30 g dm^{-3} sodium glutamate(86). Their yield was nearly double the mean yield we obtained; this may be because they used 50% more glutamate or 20% more sugar. Since the composition of their soy sauce is unknown, it is impossible to say whether it was of benefit for PγGA production.

4.2.1 Effect of NaCl and Mn^{2+} on samples

Analysing the quantities of products showed that addition of NaCl or Mn^{2+} did not affect the amount of crude or purified product obtained. It was only when purified samples were analysed using ^{1}H NMR spectroscopy that the relative fraction of protons on PγGA/impurities were significantly greater. These values reflected what was expected to be found based on experiments using *B. licheniformis* – that concentrations of Mn^{2+} between 60 and 600 µmol would increase the yield of PγGA more than concentrations greater than 600 µmol. We found that 200 µmol of $MnSO_4$ resulted in a greater proportion of purified PγGA compared with 2 mmol. 2 mmol $MnSO_4$ resulted in a greater proportion of PγGA compared to no $MnSO_{4,}$. Table 14 converts the ^{1}H purity to % weight purity using the formula discussed in section 3.5.5. This ratio of mass increase is similar to that reported by Cromwick et al (see figure 9) (23).

Table 14: Purity of purified samples determined by ^{1}H integration tracing.

Sample	^{1}H purity (mean)	% weight purity (mean)	Ratio by weight
F (200 µmol $MnSO_4$)	0.73	0.64	2.21
G (2 mmol $MnSO_4$)	0.52	0.42	1.45
H (no $MnSO_4$)	0.37	0.29	1

Cromwick et al. determined PγGA concentration in broth aliquots by gel permeation chromatography, which involved a rapid (although non preparatory) purification step. This suggested that the concentration of pure PγGA increased in samples grown with 61.5 to 615 µmol of $MnSO_4$. Our spectra show only the ratio of PγGA/impurity after purification and no useful spectra for samples F and G were obtained before purification, since Mn^{2+} reduced the ability of the NMR machine to shim the sample (see figure 21b). Therefore we cannot specify whether Mn^{2+}has effected the overall yield, or made the purification method more efficient, by a mechanism such as reducing the relative size of the carbohydrate impurity.

The HPLC experiment observed the amount of glutamate present in hydrolysate of crude product and used this prerequisite information to determine the molecular mass and D/L ratio. The results suggest that addition of 42 mmol NaCl double to triple the glutamate fraction in crude samples and also increase the size of PγGA. This is this opposite finding to studies using the similar organism B. subtillis chungkookjang, which found addition of NaCl reduces the size of PγGA(1).

If Mn^{2+} concentrations increase the PγGA fraction of purified sample, but NaCl increased size and the fraction of PγGA in crude sample then it follows that the purification procedure favoured small, less concentrated PγGA in crude samples. This seems to contradict the mechanism of diafiltration, which acts like a sieve and allows diffusion of small molecules into the dialysate. However the authors of the purification method also reported that the molecular weight of their samples decreased following purification (84), which is consistent with our findings. In these experiments the molecular size of the purified product was never determined; therefore this possibility cannot be refuted.

An alternative interpretation of the HPLC results based on experimental error.

It is possible that an experimental error was made. The first 5 experiments run (H1 -3, L-Gul and G3) had significantly higher quantities measured compared to the rest of the samples. One possibility that might explain this would be if a 25 µl was accidentally replaced with a 10 µl syringe after injecting the first 5 samples. This would imply that crude product in samples G3 – H3 contain less

glutamate and it would account for the discrepancy between the % mass calculated by NMR and chromatography in sample H1. Figure 54 shows the adjusted values of % glutamate fraction if the error had been made. It indicates that crude samples contained a similar glutamate fraction and therefore low $MnSO_4$ concentrations do not increase the overall glutamate fraction before purification.

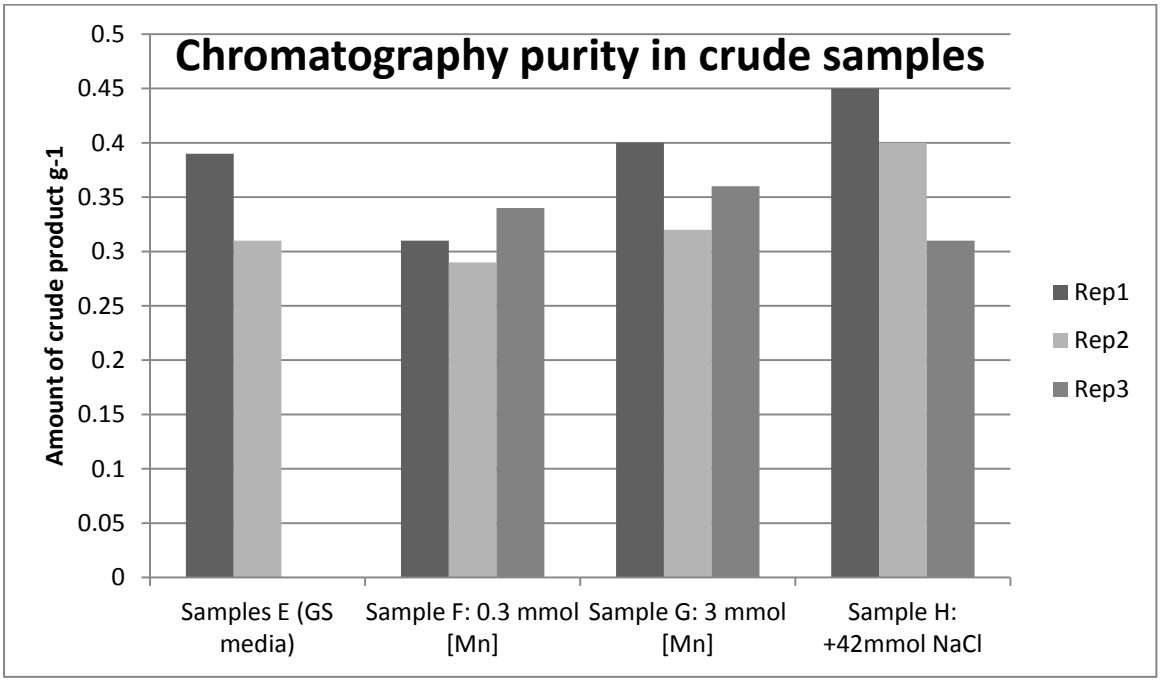

Figure 54: Adjusted values of glutamate concentration by percentage mass. (1st 5 samples divided by a factor of 2.5 to account for possible experimental error).

Furthermore this experimental error would have implications for the molecular number of the crude samples. Figure 55 shows the adjusted M_n if the experimental mistake had been made. It clearly shows that the size of samples grown with additional NaCl would have been smaller. This would then explain why a greater fraction of PγGA would have been lost during the purification process (through the dialysis tubing). Finally, this would be consistant with published findings – that additional NaCl decreases the molecular size of PγGA produced by *B. subtillis natto.*

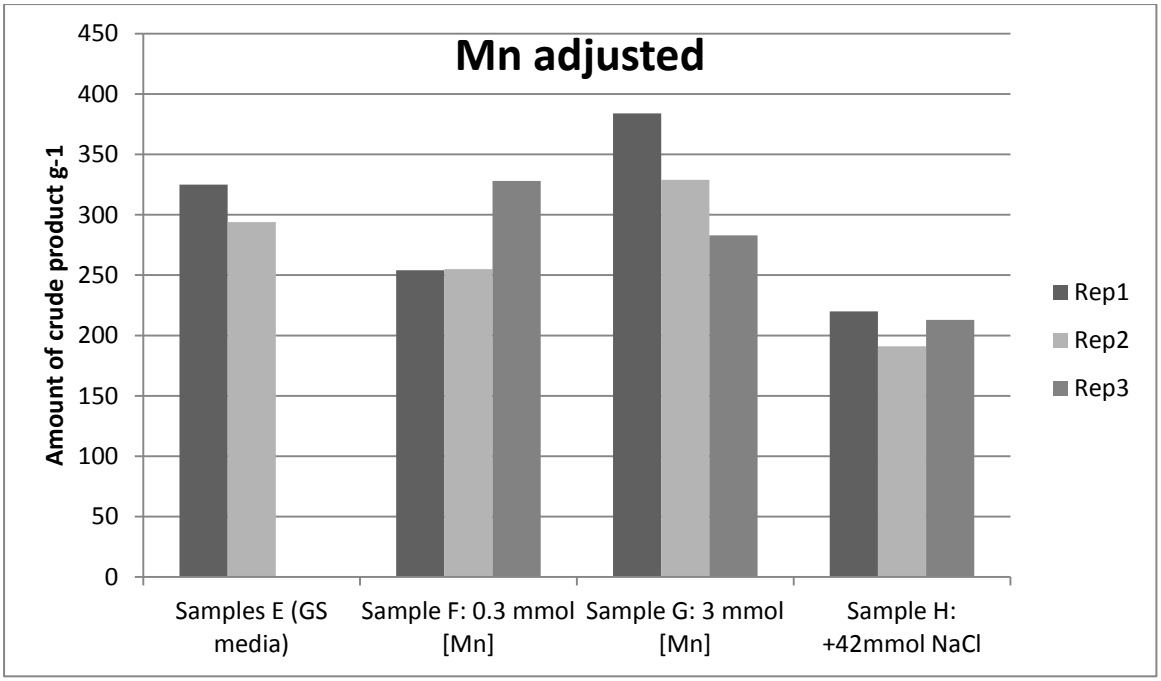

Figure 55: Adjusted values for M_n based on the potential experimental error mentioned in the text.

4.3 Why Purification of PγGA may not have been achieved

In this study we were unable to purify PγGA to the same standard obtained by the producer of commercial PγGA. Despite following a published purification(84)protocol ^{1}H NMR still showed the presence of what was believed to be carbohydrates in the sample. Since the authors of this method used a different bacillus species - *B. licheniformis* (ATCC 9945A) it is possible that their organism did not produce the same carbohydrate and therefore the authors were able to obtain a pure (or purer) form of PγGA.However, the authors did not perform ^{1}H NMR spectroscopy on their samples and instead used a variety of other methods (see below) to determine that their level of purity was “very pure (>95%)”.Whilst they did not refer to the presence of polysaccharide in their purified samples, the infrared spectrum of their purified sample shows peaks which were present in our unpurified

sample (at 1080 cm^{-1}), which are believed to be caused by the carbohydrate.

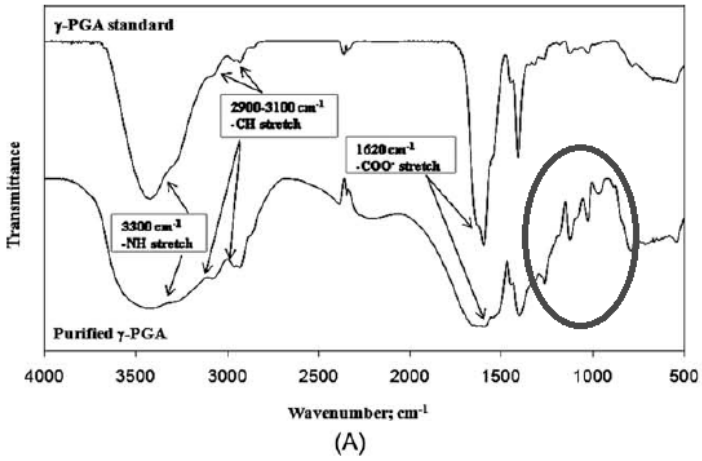

Figure 56: IR spectra for the authors PγGA standard (top) and Cu^{2+} purified samples (bottom). Additional absorbance peaks at lower wavenumbers present in their sample, but not in their standard are circled.

Furthermore the authors claim to have recovered 85% mass using the copper method and 82% using the ethanol precipitation method. This is an order of magnitude greater than the amount obtained in this study (8% for copper and 15% for ethanol extractions). One possible explanation other than the use of a different species is that the authors used dialysis bags with a MWCO of 10kDa. However they claimed that the molecular weight of PγGA in the broth was ~220 kDa, therefore it is unlikely that a MWCO this low was required.Although the molecular weight of samples was not determined, the molecular number suggested that the size of our samples was significantly smaller than theirs. Perhaps the size of the polymer used in this study meant that the method of purification published by Manocha et al. was inefficient for our purpose.

Oddly, after purification the authors found that the $M_w$of their sample decreased, suggesting that larger molecules were lost following dialysis. Measurement of M_w was done with the gold standard of PγGA size determination(96)-gel permeation chromatography. This is a form of size exclusion chromatography and monitors eluted sample by absorbance at 210 nm. However no analysis is ever performed to ensure the eluant contains PγGA and no other molecules and since our results indicate the impurity may be a large molecule further proof may be required to ensure the M_w of PγGA is

being measured.

From the literature, it is difficult to assess how universally problematic PγGA purification is. A patented method of producing medically pure PγGA links purity to the whiteness of the sample, or whether it produces an immune response in rats (85). Goto and Kunioka published a different method of purifying PγGA using centrifugation, methanol precipitation, further centrifugation and desalting. They determined the purity of their samples using an amino acid autoanalyser (Hitach 835) on hydrolysates(83). This may have only shown the relative proportions of amino acids, indicating protein impurities and not polysaccharide. Similarly, the authors who wrote the protocol that was followed in this study only measured purity by the precipitation of proteins using a Bradford assay (84). It was reported using these methods that their samples were 86->95% pure, but the findings presented here conflict with these findings. Our findings suggest that ^{1}H NMR is a useful tool for observing impurities and may be helpful in proving the organic purity of a PγGA sample. Also, linearity was observed in the ATR FTIR spectra at 1630 cm^{-1}. This may be used as an estimate of purity in conjunction with the assays mentioned by the literature if no other proteins are believed to be present.

4.4 Possible directions for future research into the purification of PγGA.

Our experiments suggested that PγGA was difficult to extract from ethanol precipitated broth because samples contained two large molecules. An experiment with a dialysis bag of unknown MWCO suggested that at least in some circumstances, the carbohydrate may be larger than PγGA. Since the polysaccharide analysis suggested the presence of 1,2 substitued hexoses, these could be a potential target for enzymatic degradation prior to dialysis and purification. Further research could attempt using a range of glycoside hydrolases to digest the carbohydrate. A more sophisticated approach might try to identify which sugars linked before selecting an enzyme. Further experiments using alditol acetate separation, with more monosaccharide derivatives references and more

complex 2D NMR experiments may identify specific enzymes that may aid PγGA purification. A simpler method might be to simply extract PγGA from dialysate using tubing with a larger MWCO.

1. Sung MH, Park C, Kim CJ, Poo H, Soda K, Ashiuchi M. Natural and edible biopolymer poly-gamma-glutamic acid: Synthesis, production, and applications. Chem Rec. 2005;5(6):352-66.
2. Zanuy D, Aleman C, Munoz-Guerra S. A microscopic view of a helical poly(gamma-peptide): Molecular dynamics simulations of a 20-residue unionized poly(gamma-D-glutamic acid) in water. Macromol Theory Simul. 2000;9(8):543-9.
3. Ashiuchi M, Misono H. Biochemistry and molecular genetics of poly-gamma-glutamate synthesis. Appl Microbiol Biot. 2002;59(1):9-14.
4. Ho GH, Ho TI, Hsieh KH, Su YC, Lin PY, Yang J, et al. gamma-polyglutamic acid produced by Bacillus subtilis (natto): Structural characteristics, chemical properties and biological functionalities. J Chin Chem Soc-Taip. 2006;53(6):1363-84.
5. Margaritis A, Buescher JM. Microbial biosynthesis of polyglutamic acid biopolymer and applications in the biopharmaceutical, biomedical and food industries. Crit Rev Biotechnol. 2007;27(1):1-19.
6. Shih IL, Van YT, Shen MH. Biomedical applications of chemically and microbiologically synthesized poly(glutamic acid) and poly(lysine). Mini-Rev Med Chem. 2004;4(2):179-88.
7. Zanuy D, Nussinov R, Aleman C. From peptide-based material science to protein fibrils: discipline convergence in nanobiology. Phys Biol. 2006;3(1):S80-S90.
8. Zanuy D, Aleman C, Munoz-Guerra S. On the helical conformation of un-ionized poly(gamma-D-glutamic acid). Int J Biol Macromol. 1998;23(3):175-84.
9. Zanuy D, Aleman C. Poly(gamma-glutamic acid) in aqueous solution: molecular dynamics simulations of 10- and 20-residue chains at different temperatures. Biomacromolecules. 2001;2(3):651-7.
10. Zanuy D, Aleman C. Molecular dynamics study of complexes of poly(glutamate) and dodecyltrimethylammonium. Biomacromolecules. 2007;8(2):663-71.
11. Ivanovics G, Horvath S. On the Chemical Structure of the Capsule of B. Anthracis and B. Megatherium. Acta Physiologica Academiae Scientiarum Hungaricae. 1953;4(3-4):400-8.
12. Rhie GE, Jang J, Cho M, Chun JH, Cho MH, Park J, et al. The Poly-gamma-D-Glutamic Acid Capsule of Bacillus anthracis Enhances Lethal Toxin Activity. Infect Immun. 2011;79(9):3846-54.
13. Leppla SH, Robbins JB, Schneerson R, Shiloach J. Development of an improved vaccine for anthrax. The Journal of Clinical Investigation. 2002;110(2):141-4.
14. Scorpio A, Chabot DJ, Day WA, O'Brien DK, Vietri NJ, Itoh Y, et al. Poly-gamma-glutamate capsule-degrading enzyme treatment enhances phagocytosis and killing of encapsulated Bacillus anthracis. Antimicrob Agents Ch. 2007;51(1):215-22.
15. Kocianova S, Vuong C, Yao Y, Voyich JM, Fischer ER, DeLeo FR, et al. Key role of poly-gamma-DL-glutamic acid in immune evasion and virulence of Staphylococcus epidermidis. J Clin Invest. 2005;115(3):688-94.
16. Shih IL, Van YT. The production of poly-(gamma-glutamic acid) from microorganisms and its various applications. Bioresource Technol. 2001;79(3):207-25.
17. Chambers M. Chemical Information Specialized Information Service Bethesda, USA: US National library of Medicine; 2013 [cited 2013 18/09/2013]. Available from: http://chem.sis.nlm.nih.gov/chemidplus/cas/25513-46-6.

18. Bovarnick M. The Formation of Extracellular d(-)-Glutamic Acid Polypeptide by Bacillus Subtilis. J Biol Chem. 1942;145:9.
19. Park C, Choi JC, Choi YH, Nakamura H, Shimanouchi K, Horiuchi T, et al. Synthesis of super-high-molecular-weight poly-gamma-glutamic acid by Bacillus subtilis subsp chungkookjang. J Mol Catal B-Enzym. 2005;35(4-6):128-33.
20. Park C, Choi YH, Shin HJ, Poo H, Song JJ, Kim CJ, et al. Effect of high-molecular-weight poly-gamma-glutamic acid from Bacillus subtilis (chungkookjang) on Ca solubility and intestinal absorption. J Microbiol Biotechn. 2005;15(4):855-8.
21. Gardner JM, Troy FA. Chemistry and biosynthesis of the poly(gamma-D-glutamyl) capsule in Bacillus licheniformis. Activation, racemization, and polymerization of glutamic acid by a membranous polyglutamyl synthetase complex. J Biol Chem. 1979;254(14):6262-9.
22. Gardner JM, Troy FA. Chemistry and Biosynthesis of the Poly(Gamma-D-Glutamyl) Capsule in Bacillus-Licheniformis - Activation, Racemization, and Polymerization of Glutamic-Acid by a Membranous Polyglutamyl Synthetase Complex. J Biol Chem. 1979;254(14):6262-9.
23. Cromwick AM, Birrer GA, Gross RA. The Effects of Manganese on the Biosynthesis of Gamma-Poly(Glutamic Acid) by Bacillus-Licheniformis Atcc-9945a. Abstr Pap Am Chem S. 1994;207:165-IEC.
24. Birrer GA, Cromwick AM, Gross RA. Gamma-Poly(Glutamic Acid) Formation by Bacillus-Licheniformis 9945a - Physiological and Biochemical-Studies. Int J Biol Macromol. 1994;16(5):265-75.
25. Bajaj I, Singhal R. Poly (glutamic acid) - An emerging biopolymer of commercial interest. Bioresource Technol. 2011;102(10):5551-61.
26. Ren S-X, Fu G, Jiang X-G, Zeng R, Miao Y-G, Xu H, et al. Unique physiological and pathogenic features of Leptospira interrogans revealed by whole-genome sequencing. Nature. 2003;422(6934):888.
27. Kapatral V, Anderson I, Ivanova N, Reznik G, Los T, Lykidis A, et al. Genome sequence and analysis of the oral bacterium Fusobacterium nucleatum strain ATCC 25586. J Bacteriol. 2002;184(7):2005-18.
28. Weber J. Poly(gamma-glutamic acid)s are the major constituents of nematocysts in Hydra (Hydrozoa, Cnidaria). J Biol Chem. 1990;265(17):9664-9.
29. Hezayen FF, Rehm BHA, Eberhardt R, Steinbuchel A. Polymer production by two newly isolated extremely halophilic archaea: application of a novel corrosion-resistant bioreactor. Appl Microbiol Biot. 2000;54(3):319-25.
30. Niemetz R, Kärcher U, Kandler O, Tindall BJ, König H. The Cell Wall Polymer of the Extremely Halophilic Archaeon Natronococcus occultus. Eur J Biochem. 1997;249(3):905-11.
31. Inomata N, Chin K, Nagashima M, Ikezawa Z. Late-Onset Anaphylaxis Due to Poly (gamma-glutamic acid) in the Soup of Commercial Cold Chinese Noodles in a Patient with Allergy to Fermented Soybeans (Natto). Allergol Int. 2011;60(3):393-6.
32. Duncan R. Polymer conjugates as anticancer nanomedicines. Nature Reviews Cancer. 2006;6(9):688-701.
33. Fante C, Eldar-Boock A, Satchi-Fainaro R, Osborn HMI, Greco F. Synthesis and Biological Evaluation of a Polyglutamic Acid–Dopamine Conjugate: A New Antiangiogenic Agent. J Med Chem. 2011;54(14):5255-9.
34. Akagi T, Baba M, Akashi M. Development of vaccine adjuvants using polymeric nanoparticles and their potential applications for anti-HIV vaccine. Yakugaku Zasshi. 2007;127(2):307-17.
35. Dekie L, Toncheva V, Dubruel P, Schacht EH, Barrett L, Seymour LW. Poly-L-glutamic acid derivatives as vectors for gene therapy. J Control Release. 2000;65(1-2):187-202.
36. Chen L, Tian HY, Chen J, Chen XS, Huang YB, Jing XB. Multi-armed poly(L-glutamic acid)-graft-oligoethylenimine copolymers as efficient nonviral gene delivery vectors. Journal of Gene Medicine. 2010;12(1):64-76.
37. Poo H, Park C, Kwak MS, Choi DY, Hong SP, Lee IH, et al. New biological functions and applications of high-molecular-mass poly-gamma-glutamic acid. Chem Biodivers. 2010;7(6):1555-62.

38. Cady CT, Lahn M, Vollmer M, Tsuji M, Seo SJ, Reardon CL, et al. Response of murine gamma delta T cells to the synthetic polypeptide Poly-Glu(50)Tyr(50). J Immunol. 2000;165(4):1790-8.
39. Uto T, Akagi T, Yoshinaga K, Toyama M, Akashi M, Baba M. The induction of innate and adaptive immunity by biodegradable poly(gamma-glutamic acid) nanoparticles via a TLR4 and MyD88 signaling pathway. Biomaterials. 2011;32(22):5206-12.
40. Kim TW, Lee TY, Bae FC, Hahm JH, Kim YH, Park C, et al. Oral administration of high molecular mass poly-gamma-glutamate induces NK cell-mediated antitumor immunity. J Immunol. 2007;179(2):775-80.
41. Health NIo. ClinicalTrials.gov US: NIH; 2013 [cited 2013 20/09/2013]. Available from: http://clinicaltrials.gov/ct2/show/results/NCT01826045.
42. Bae SR, Park C, Choi JC, Poo H, Kim CJ, Sung MH. Effects of ultra high molecular weight poly-gamma-glutamic acid from Bacillus subtilis (chungkookjang) on corneal wound healing. J Microbiol Biotechnol. 2010;20(4):803-8.
43. Tanimoto H, Mori M, Motoki M, Torii K, Kadowaki M, Noguchi T. Natto mucilage containing poly-gamma-glutamic acid increases soluble calcium in the rat small intestine. Biosci Biotechnol Biochem. 2001;65(3):516-21.
44. Tanimoto H, Fox T, Eagles J, Satoh H, Nozawa H, Okiyama A, et al. Acute effect of poly-gamma-glutamic acid on calcium absorption in post-menopausal women. J Am Coll Nutr. 2007;26(6):645-9.
45. Wang TL, Kao TH, Inbaraj BS, Su YT, Chen BH. Inhibition Effect of Poly(gamma-glutamic acid) on Lead-Induced Toxicity in Mice. J Agric Food Chem. 2010.
46. Karmaker S, Saha TK. Chelation of vanadium(IV) by a natural and edible biopolymer poly(gamma-glutamic acid) in aqueous solution: Structure and binding constant of complex. Macromolecular bioscience. 2008;8(2):171-6.
47. Yoshida H, Klinkhammer K, Matsusaki M, Moller M, Klee D, Akashi M. Disulfide-Crosslinked Electrospun Poly(gamma-glutamic acid) Nonwovens as Reduction-Responsive Scaffolds. Macromolecular bioscience. 2009;9(6):568-74.
48. Matsusaki M, Yoshida H, Akashi M. The construction of 3D-engineered tissues composed of cells and extracellular matrices by hydrogel template approach. Biomaterials. 2007;28(17):2729-37.
49. Rodriguez DE, Romero-Garcia J, Ramirez-Vargas E, Ledezma-Perez AS, Arias-Marin E. Synthesis and swelling characteristics of semi-interpenetrating polymer network hydrogels composed of poly(acrylamide) and poly(gamma-glutamic acid). Mater Lett. 2006;60(11):1390-3.
50. Gonzales D, Fan K, Sevoian M. Synthesis and swelling characterizations of a poly(gamma-glutamic acid) hydrogel. Journal of Polymer Science, Part A: Polymer Chemistry. 1996;34(Compendex):2019-27.
51. Hsu SH, Lin CH. The properties of gelatin-poly (gamma-glutamic acid) hydrogels as biological glues. Biorheology. 2007;44(1):17-28.
52. Huang MH, Yang MC. Swelling and biocompatibility of sodium alginate/poly(gamma-glutamic acid) hydrogels. Polym Advan Technol. 2010;21(8):561-7.
53. Choi HJ, Kunioka M. Preparation Conditions and Swelling Equilibria of Hydrogel Prepared by Gamma-Irradiation from Microbial Poly(Gamma-Glutamic Acid). Radiat Phys Chem. 1995;46(2):175-9.
54. Poologasundarampillai G, Ionescu C, Tsigkou O, Murugesan M, Hill RG, Stevens MM, et al. Synthesis of bioactive class II poly([gamma]-glutamic acid)/silica hybrids for bone regeneration. J Mater Chem. 2010;20(40):8952-61.
55. Hsu FY, Cheng YY, Tsai SW, Tsai WB. Fabrication and evaluation of a biodegradable cohesive plug based on reconstituted collagen/gamma-polyglutamic acid. J Biomed Mater Res B. 2010;95B(1):29-35.
56. Ge Y, Ning W, Chao Z. Flocculating properties of the novel bioflocculant Poly(gamma-glutamic acid) and its use in jean dyeing wastewater treatment. In: Shi YG, Zuo JL, editors. Adv Mater

Res-Switz. Advanced Materials Research. 183-185. Stafa-Zurich: Trans Tech Publications Ltd; 2011. p. 125-9.
57. Yu X, Wang M, Wang QH, Wang XM. Biosynthesis of polyglutamic acid and its application on agriculture. In: Shi YG, Zuo JL, editors. Adv Mater Res-Switz. Advanced Materials Research. 183-185. Stafa-Zurich: Trans Tech Publications Ltd; 2011. p. 1219-23.
58. Shih IL, Van YT, Sau YY. Antifreeze activities of poly(gamma-glutamic acid) produced by Bacillus licheniformis. Biotechnol Lett. 2003;25(20):1709-12.
59. Berekaa MM, El Aassar SA, El-Sayed SM, El Borai AM. PRODUCTION OF POLY-gamma-GLUTAMATE (PGA) BIOPOLYMER BY BATCH AND SEMICONTINUOUS CULTURES OF IMMOBILIZED BACILLUS LICHENIFORMIS STRAIN-R. Braz J Microbiol. 2009;40(4):715-24.
60. Chen X, Chen S, Sun M, Yu Z. High yield of poly-gamma-glutamic acid from Bacillus subtilis by solid-state fermentation using swine manure as the basis of a solid substrate. Bioresour Technol. 2005;96(17):1872-9.
61. Chen X, Chen SW, Sun M, Yu ZN. Medium optimization by response surface methodology for poly-gamma-glutamic acid production using dairy manure as the basis of a solid substrate. Appl Microbiol Biot. 2005;69(4):390-6.
62. Hoppensack A, Oppermann-Sanio FB, Steinbuchel A. Conversion of the nitrogen content in liquid manure into biomass and polyglutamic acid by a newly isolated strain of Bacillus licheniformis. Fems Microbiol Lett. 2003;218(1):39-45.
63. Potter M, Oppermann-Sanio FB, Steinbuchel A. Cultivation of bacteria producing polyamino acids with liquid manure as carbon and nitrogen source. Appl Environ Microb. 2001;67(2):617-22.
64. Waley SG. The Structure of Bacterial Poly Glutamic Acid. J Chem Soc. 1955:517-22.
65. Bruckner V, Szekerke M, Kovacs J. [Synthesis of alpha,gamma-poly-L-glutamic acid and alpha,gamma-poly-D-glutamic acid]. Hoppe Seylers Z Physiol Chem. 1957;309(1-3):25-42.
66. Kajtar M, Bruckner V. Improved Synthesis of Stereoisomeric Poly-Gamma-Glutamic Acids, I. Synthesis via polymethyl Esters. Acta Chimica Academiae Scientarium Hungaricae. 1969;62(2):191-&.
67. Hollosi M, Kajtar M, Bruckner V. Improved Synthesis of Stereoisomeric Poly-Gamma-Glutamic Acids .2 Syntheses via Polybenzyl and Poly-T-Butyl Esters. Acta Chimica Academiae Scientarium Hungaricae. 1969;62(3):305-&.
68. Sanda F, Fujiyama T, Endo T. Chemical synthesis of poly-gamma-glutamic acid by polycondensation of gamma-glutamic acid dimer: Synthesis and reaction of poly-gamma-glutamic acid methyl ester. J Polym Sci Pol Chem. 2001;39(5):732-41.
69. Sanda F, Fujiyama T, Endo T. Stepwise synthesis of gamma-glutamic acid 16-mer. Macromol Chem Phys. 2002;203(4):727-34.
70. Ashiuchi M, Soda K, Misono H. A poly-gamma-glutamate synthetic system of Bacillus subtilis IFO 3336: Gene cloning and biochemical analysis of poly-gamma-glutamate produced by Escherichia coli clone cells. Biochemical and Biophysical Research Communications. 1999;263(1):6-12.
71. Ashiuchi M, Nakamura H, Yamamoto T, Kamei T, Soda K, Park C, et al. Poly-gamma-glutamate depolymerase of Bacillus subtilis: production, simple purification and substrate selectivity. J Mol Catal B-Enzym. 2003;23(2-6):249-55.
72. Ashiuchi M, Nawa C, Kamei T, Song JJ, Hong SP, Sung MH, et al. Physiological and biochemical characteristics of poly gamma-glutamate synthetase complex of Bacillus subtilis. Eur J Biochem. 2001;268(20):5321-8.
73. Ashiuchi M, Shimanouchi K, Nakamura H, Kamei T, Soda K, Park C, et al. Enzymatic synthesis of high-molecular-mass poly-gamma-glutamate and regulation of its stereochemistry. Appl Environ Microb. 2004;70(7):4249-55.
74. Ashiuchi M, Tani K, Soda K, Misono H. Properties of glutamate racemase from Bacillus subtilis IFO3336 producing poly-gamma-glutamate. J Biochem. 1998;123(6):1156-63.
75. Tarui Y, Iida H, Ono E, Miki W, Hirasawa E, Fujita K, et al. Biosynthesis of poly-gamma-glutamic acid in plants: transient expression of poly-gamma-glutamate synthetase complex in tobacco leaves. J Biosci Bioeng. 2005;100(4):443-8.

76. Urushibata Y, Tokuyama S, Tahara Y. Characterization of the Bacillus subtilis ywsC gene, involved in gamma-polyglutamic acid production. J Bacteriol. 2002;184(2):337-43.
77. Fouet A, Candela T. Poly-gamma-glutamate in bacteria. Mol Microbiol. 2006;60(5):1091-8.
78. Troy FA. Chemistry and Biosynthesis of the Poly(gamma-D-glutamyl) Capsule in *Bacillus Licheniformis*. The Journal of Biological Chemistry. 1973;248(1):10.
79. Horinouchi S, Kada S, Nanamiya H, Kawamura F. Glr, a glutamate racemase, supplies D-glutamate to both peptidoglycan synthesis and poly-gamma-glutamate production in gamma-PGA-producing Bacillus subtilis. Fems Microbiol Lett. 2004;236(1):13-20.
80. Ashiuchi M, Nishikawa Y, Matsunaga K, Yamamoto M, Shimanouchi K, Misono H. Genetic design of conditional D-glutamate auxotrophy for Bacillus subtilis: Use of a vector-borne poly-gamma-glutamate synthetic system. Biochem Bioph Res Co. 2007;362(3):646-50.
81. Ashiuchi M, Yamashiro D, Minouchi Y. Moonlighting Role of a Poly-gamma-Glutamate Synthetase Component from Bacillus subtilis: Insight into Novel Extrachromosomal DNA Maintenance. Appl Environ Microb. 2011;77(8):2796-8.
82. Bajaj IB, Singhal RS. Enhanced Production of Poly (gamma-glutamic acid) from Bacillus licheniformis NCIM 2324 by Using Metabolic Precursors. Appl Biochem Biotech. 2009;159(1):133-41.
83. Goto A, Kunioka M. Biosynthesis and Hydrolysis of Poly(Gamma-Glutamic Acid) from Bacillus-Subtilis Ifo3335. Biosci Biotech Bioch. 1992;56(7):1031-5.
84. Margaritis A, Manocha B. A Novel Method for the Selective Recovery and Purification of gamma-Polyglutamic Acid from Bacillus licheniformis Fermentation Broth. Biotechnol Progr. 2010;26(3):734-42.
85. Prescott AL, Stock., inventor; Cresent Innovations, Inc., assignee. Method for producing medical and commercial grade poly-gamma-glutamic acid of high molecular weight. United States2008.
86. Ogawa Y, Yamaguchi F, Yuasa K, Tahara Y. Efficient production of gamma-polyglutamic acid by Bacillus subtilis (natto) in jar fermenters. Biosci Biotech Bioch. 1997;61(10):1684-7.
87. Iza Radecka DH, Terence Bartlett, Aditya Bhat, Gopal Kedia, inventor; University of Wolverhamton, assignee. Improved viability of probiotic microorganisms using poly - gamm - glutamic acid. United Kingdom patent WO2013030596 A1. 2013.
88. Richardson J. IR Spectroscopy. IR Spectroscopy. [Educational]. In press 2011.
89. Erno Pretsch PB, Martin Badertscher. Structure Determination of Organic Compounds: Tables of Spectral Data. Berlin: Springer; 2009.
90. Björndal H, Hellerqvist CG, Lindberg B, Svensson S. Gas-Liquid Chromatography and Mass Spectrometry in Methylation Analysis of Polysaccharides. Angewandte Chemie International Edition in English. 1970;9(8):610-9.
91. Hikichi K, Tanaka H, Konno A. Nuclear-Magnetic-Resonance Study of Poly(Gamma-Glutamic Acid)-Cu(Ii) and Mn(Ii) Complexes. Polym J. 1990;22(2):103-9.
92. Hayakawa I, Hayashi C, Sasaki N, Hikichi K. Elongational flow studies of hinged rodlike molecules. Journal of Applied Polymer Science. 1996;61(10):1731-5.
93. Marvasi M, Visscher PT, Casillas Martinez L. Exopolymeric substances (EPS) from Bacillus subtilis: polymers and genes encoding their synthesis. Fems Microbiol Lett. 2010;313(1):1-9.
94. Morita N, Takagi M, Murao S. A New Gel-Forming Polysaccharide Produced by Bacillus subtilis FT-3 Its Structure and its Physical and Chemical Characteristics. Bulletin of the University of Osaka Prefecture Ser B, Agriculture and biology. 1979;31:27-41.
95. Björndal H, Hellerqvist CG, Lindberg B, Svensson S. Gas-Liquid Chromatography and Mass Spectrometry in Methylation Analysis of Polysaccharides. Angewandte Chemie International Edition in English. 1970;9(8):610-9.
96. Ashiuchi M. Analytical approaches to poly-gamma-glutamate: quantification, molecular size determination, and stereochemistry investigation. Journal of chromatography B, Analytical technologies in the biomedical and life sciences. 2011;879(29):3096-101.